

Optimizing Geothermal Heat Mining and Methane Control to Address Climate Change

Dissertation

Presented in Partial Fulfillment of the Requirements for the Degree Doctor of Philosophy
in the Graduate School of The Ohio State University

By

Qingrun Yang

Graduate Program in Civil Engineering

The Ohio State University

2024

Dissertation Committee

Jeffrey M. Bielicki, Ph.D., Advisor

Gil Bohrer, Ph.D.

Jordan D. Clark, Ph.D.

Daniel B. Gingerich, Ph.D.

Copyrighted by

Qingrun Yang

2024

Abstract

The human-induced increase in greenhouse gas (GHG) concentrations is the primary driver of recent global warming, leading to a series of climate changes, including sea level rise, ocean acidification, and more frequent and severe weather extremes. These changes have profound impacts on global ecosystems and human societies.

The world has recognized the necessity for countries to cooperate in combating climate change, resulting in international treaties such as the Kyoto Protocol and the Paris Agreement. The success of international cooperation depends on a portfolio of various approaches to eliminate, reduce, substitute, and compensate for GHG emissions.

The transition from fossil fuels to renewable energy can effectively mitigate GHG emissions. Wind and solar energy have experienced substantial growth over the past decade, yet the development of geothermal energy remains stagnant despite its immense potential. Considering its additional advantages, such as the dual benefits of generating both electricity and heat, the stability of energy generation, and the synthesis with carbon capture and storage, more focus should be placed on geothermal energy. Meanwhile, most efforts to address climate change have focused on mitigating carbon dioxide (CO₂) emissions and removing their accumulation from the atmosphere. While there is ~210x more CO₂ than methane (CH₄) in the atmosphere, the atmospheric concentration of CH₄ has increased faster and alone contributes an amount of radiative forcing that is about

30% of the contribution from CO₂. With positive temperature-driven feedbacks that release CH₄ to the atmosphere as temperatures rise, a shorter atmospheric lifetime than CO₂, and continued reliance on natural gas, a portfolio approach is urgently needed to slow, stop, and reverse the accumulation of CH₄ in the atmosphere. To provide insights to address the above issues, this dissertation focuses on optimizing strategies for geothermal heat mining and CH₄ control.

Chapter 2 explored the optimal geothermal heat mining (OGHM) problem at the facility level, which aims at maximizing profit within a time horizon for a site. The problem is formulated as an optimal control model, which is solved by a proposed analytical algorithm. Solutions to the OGHM problem can be categorized into four situations: 1) the mass flow rate keeps the maximum; 2) the mass flow rate keeps as 0; 3) the mass flow rate starts as the maximum, decreases to a constant value, and finally recovers to the maximum; and 4) the mass flow rate starts as 0, and changes to the maximum. Further based on analysis from an economic view, for the cases that have positive optimal profits, the solutions of finite-time OGHM problems can be considered as a combination of the solution of the infinite-time problem and one final stage with a maximum mass flow rate. Results show that surrounding media temperature, efficiency, and compression cost have significant influences on the optimal profit, and CO₂ geothermal systems perform better for shallow, low-grade heat sources when compared to water geothermal systems.

Chapter 3 investigates pathways for CH₄ control in a top-down system view, including mitigation to avoid CH₄ emissions and removal of CH₄ that is in the atmosphere. We develop and implement the *Model for Optimization of Methane Emissions and removal*

with Negative Technologies Under climate Mitigation (MOMENTUM) that determines cost-effective pathways for CH₄ emissions mitigation in energy, agriculture, and waste sectors, and atmospheric CH₄ removal amid trajectories for mitigation and removal of CO₂. Results indicate that relying solely on mitigating CH₄ emissions is not feasible to meet climate goals, and it is imperative that CH₄ removal technologies are developed and deployed at a substantial scale. Initial CH₄ removal cost and CH₄ removal learning rate have more impact on the total cost of CH₄ control than the maximum CH₄ removal potential or the maximum CH₄ removal growth rate, and when CH₄ removal needs to begin is influenced by scale-related parameters much more than by cost-related parameters. In addition, if societal influences are considered, the avoided social cost always outweighs the optimal CH₄ control cost, which indicates a net benefit to controlling CH₄ emissions.

Chapter 4 establishes an agent-based model in a bottom-up system view to simulate the interactions among the government, suppliers, and consumers, which considers the introduction of a CH₄ emission market to initial commodity/service markets. Three sectors are analyzed, including agriculture, energy, and waste sectors, accounting for ~90% of CH₄ emissions in the US. The suppliers and consumers in each sector are modeled with heterogeneity, local interactions, and adaptations. Case studies on Ohio, US indicate that the emission cap is the main factor influencing CH₄ control, which should be established in the most efficient way (reduced by 3% per year). The emission market penalty price has a minimal effect on the amount of CH₄ reduction. Moreover, CH₄ control always leads to a net benefit, and the government should implement more

incentives to encourage earlier deployments of negative-cost CH₄ mitigation techniques. Meanwhile, the government should pay more attention to the waste sector, especially the landfill source, which is faced with the most difficulties in mitigating CH₄ emissions.

Dedication

I dedicate this dissertation to my parents and my girlfriend, Zhixin. Thank you all for your constant love and support.

Acknowledgments

I would like to express my deepest gratitude to my advisor, Prof. Jeff Bielicki. Your guidance, support, and wisdom have been invaluable throughout my PhD journey. Your belief in my abilities and your constant encouragement have inspired me to push my boundaries and achieve my goals.

I am also extremely grateful to the members of my committee, Prof. Gil Bohrer, Prof. Jordan Clark, and Prof. Daniel Gingerich. Your insightful feedback, constructive criticism, and valuable suggestions have significantly shaped this work. Thank you for your time, patience, and commitment to my research.

I would like to extend my appreciation to my colleagues and friends: Dr. Yang Ju, Dr. Martina Leveni, Dr. Marcos Miranda, Dr. Kay Sung, Dr. Theresia Yazbeck, Sam Copeland, Jacob Gardner, Cassidy Jenney, Diego Hincapie Ossa, Shannay Rawal, Teagen Reasch, and Han Wang. Your assistance and shared knowledge have made the lab a stimulating and enjoyable place to work, and your friendship and the countless moments of laughter have kept me grounded and motivated.

My heartfelt thanks go to my parents. Mom and Dad, your unconditional love and belief in me have been my greatest source of strength. Your sacrifices and encouragement have motivated me to reach this milestone. I am forever indebted to you.

Lastly, I would like to express my love and appreciation to my girlfriend, Zhixin He.

Your constant support, understanding, and patience have meant the world to me. Thank you for standing by my side through all the ups and downs. Your presence has been a constant source of comfort and inspiration.

The four years at The Ohio State University flew by, and the first year of remote learning from China due to the COVID-19 pandemic made the entire PhD journey seem even shorter. I would like to acknowledge everyone else who has contributed to this journey in any way. Thank you all.

Vita

2017..... B.Eng., Electrical Engineering, Xi'an Jiaotong University
2020..... M.Eng., Electrical Engineering, Xi'an Jiaotong University
2022 to 2024 Graduate Teaching Associate, The Ohio State University
2022 to present Graduate Research Associate, The Ohio State University

Fields of Study

Major Field: Civil Engineering with a Specialization in Environmental Engineering

Table of Contents

Abstract.....	ii
Dedication.....	vi
Acknowledgments.....	vii
Vita.....	ix
List of Tables	xii
List of Figures.....	xiii
Chapter 1. Introduction.....	1
1.1. Background.....	1
1.2. Motivation.....	4
1.3. Dissertation Overview	7
Chapter 2. An Analytic Approach to Optimal Geothermal Heat Mining.....	8
2.1. Introduction.....	8
2.2. Methods.....	11
2.2.1. Model	11
2.2.2. Algorithm.....	15
2.3. Economic Interpretation.....	20
2.3.1. Stationary Rate of Return on Reservoir Stored Heat	20
2.3.2. Solutions to Infinite-Time OGHM Problems	22
2.3.3. Relationship Between Finite-Time and Infinite-Time OGHM problems.....	25
2.4. Results.....	29
2.5. Conclusions.....	36
Chapter 3. Pathways of Methane Control to Address Climate Change.....	38
3.1. Introduction.....	38
3.2. The <i>MOMENTUM</i> for Optimal CH ₄ Control	41
3.2.1. <i>MOMENTUM</i> : The Global Climate Component.....	42
3.2.2. Technology Model	45

3.2.3. Optimization Model	50
3.2.4. Scenarios	50
3.3. Results	52
3.3.1. Optimal CH ₄ Control Costs and Pathways for Several Shared Socioeconomic Pathways	52
3.3.2. Sensitivity of Climate Goals in 2100 by Shared Socioeconomic Pathway	55
3.3.3. Dependence of Total Cost of CH ₄ Control on Several Key Parameters	58
3.3.4. Dependence of the Year CH ₄ Removal Begins on Key Parameters	61
3.4. Discussion and Conclusions	63
Chapter 4. Agent-Based Analysis for Methane Emission Control	67
4.1. Introduction	67
4.2. Methods	70
4.2.1. System Boundary and Settings	71
4.2.2. Government	72
4.2.3. Emission market: Trading Scheme	73
4.2.4. Suppliers	75
4.2.5. Consumers	78
4.2.6. Commodity/service market	81
4.2.7. Simulation process	85
4.2.8. Scenarios	87
4.3. Results	88
4.4. Discussion and Conclusions	97
Chapter 5. Conclusions	100
5.1. Geothermal Heat Mining	100
5.2. Methane Control	102
Bibliography	104
Appendix A	128
Appendix B	134

List of Tables

Table 2-1: Baseline Parameters	29
Table 3-1: Baseline Parameters for CH ₄ Removal Approaches	51
Table 3-2: Summary of Shared Socioeconomic Pathway (SSP) Scenarios Used in This Study	51
Table 3-3: Summary of Results for Start Year for CH ₄ Removal Depending on Several Key Parameters.	62
Table 4-1. Algorithm for Determining Clearing Price in the Emission Market	75
Table 4-2. Base-case Parameters for CH ₄ Emission Control Agent-Based Model	87
Table 4-3. Final Total Emissions as Percentages of the Initial Emission (Average of All Simulation Seeds)	90
Table 4-4. All-Time Costs and Percents of Penalty Receivers (Average of All Simulation Seeds)	94

List of Figures

Figure 2-1. Geothermal Heat Mining and Energy Conversion.....	11
Figure 2-2. Situations of Mass Flow Rate Solutions for the OGHM Problem	17
Figure 2-3. Flow Chart of Algorithm on Solving the Mass Flow Rate	18
Figure 2-4. Solutions to Infinite OHM Problem Under Different Situations.	23
Figure 2-5. Relationship Between Finite-Time and Infinite-Time OGHM problems	26
Figure 2-6: Numerical results from discretized models with different discretization numbers and analytical results from the continuous model.....	29
Figure 2-7: Sensitivity analysis of different techno-economic parameters on the optimal solution of mass flow rate	31
Figure 2-8: Sensitivity analysis of different techno-economic parameters on the optimal profit.....	34
Figure 2-9: Profits of Using CO ₂ and Water as the Working Fluid Under Different Depths and Thermal Gradients (Thermosiphon effect is not considered)	35
Figure 2-10: Minimum Required Thermosiphon Effect (J/g) for CO ₂ to Be Same Profitable as Water.....	35
Figure 3-1: The Model for Optimization of Methane Emissions and removal with Negative Technologies Under Climate Mitigation (MOMENTUM) for Methane Pathways	42
Figure 3-2: Example Alignment from the Energy Sector.....	47
Figure 3-3: Optimal CH ₄ Control Costs and Pathways for Several Shared Socioeconomic Pathways (SSPs) and Global Mean Surface Temperature Goals in 2100.	54
Figure 3-4: Sensitivity Analysis of Climate Goals in 2100 for Five Representative SSPs	56
Figure 3-5: Sensitivity of Total Cost of CH ₄ Control to Important Parameters.	59
Figure 4-1. A Schematic Diagram of the Agent-Based Model for Methane Emission Control	70
Figure 4-2. System Boundary and Settings of the Agent-Based Model for Methane Emission Control	71
Figure 4-3: Simulation Process of the Agent-Based Model for Methane Emission Control	86
Figure 4-4. Dynamics of Emissions Under Different Emission Cap Reduction Rates. ...	89
Figure 4-5. Dynamics of Emission Market Clearing Price Under Different Emission Market Settings.	92
Figure 4-6. Dynamics of Emission Allowance Clearing Quantity Under Different Emission Cap Reduction Rates.....	93

Figure 4-7. Dynamics of Price Change (Average of All Simulation Seeds) Under Different Emission Cap Reduction Rates.	97
Figure A-1: Climate Model Calibration Results for Five Representative SSPs.	129
Figure A-2: Fitting Curves of USEPA Marginal Cost Data for CH ₄ Mitigation Technologies in the Energy Sector	130
Figure A-3: Methane removal technology model.	131
Figure A-4: Full Results of Sensitivity Analysis of the Year that CH ₄ Removal Starts to Important Parameters	132
Figure A-5: Estimated Average Cost for CH ₄ Control for Relevant Climate Goals in Different Scenarios	133

Chapter 1. Introduction

1.1. Background

As early as 1856, Eunice Foote suggested, based on her experiments, that a higher proportion of carbon dioxide (CO₂) in the atmosphere would increase the global temperature (Foote, 1856). However, the significance of this effect did not become prominent until approximately one hundred years later. Since 1970, the global average temperature has been increasing at a rate of 1.7°C per century, in contrast to the long-term decline of 0.01°C per century over the past 7,000 years (IPCC, 2022; Marcott et al., 2013; NOAA, 2016). Concurrently, there has been a surge in atmospheric concentrations of greenhouse gases (GHGs). As the two most potent GHGs, CO₂ reached a global mean concentration of 419 parts per million (ppm) in 2023 (Lan et al., 2024), and methane (CH₄) reached 1923 parts per billion (ppb) (Thoning et al., 2024), which are 147% and 240% of the values in 1850, respectively. These trends far exceed the historical natural changes and are caused by human activities (IPCC, 2023b).

The human-caused global warming triggers systematic climate change, which has far-reaching influences on the global environment, ecosystems, and human societies. One significant impact is the rise in sea levels, driven by the melting of polar ice caps and glaciers, which poses a threat to coastal communities and ecosystems (Cinner et al., 2012; Mousavi et al., 2011; K. Zhang et al., 2004). Another is the acidification of the surface

open ocean, a result of increased CO₂ absorption, adversely impacts marine biodiversity and fisheries (Doney et al., 2009, 2020; Wilson et al., 2020). Climate change also exacerbates weather and climate extremes, with increased frequency and intensity of heatwaves, heavy precipitation, droughts, and tropical cyclones observed in various regions across the globe (AghaKouchak et al., 2014, 2020; Easterling et al., 2000). These extreme weather events pose substantial threats to food security (Myers et al., 2017), water security (Eekhout et al., 2018), key infrastructure (Forzieri et al., 2018), and human physical and mental health (Cianconi et al., 2020; Ebi et al., 2021), causing wide economic and societal impacts in all regions (IPCC, 2023b).

As people become more aware of global warming and climate change, international efforts to address these issues have made important progress. The United Nations Framework Convention on Climate Change (UNFCCC), established in 1992, set the stage for international negotiation and cooperation to achieve “stabilization of greenhouse gas concentrations in the atmosphere at a level that would prevent dangerous anthropogenic interference with the climate system” (UNFCCC, 1992). This led to the Kyoto Protocol in 1997, the first legally binding treaty which requires developed countries to cut GHG emissions by around 5% below 1990 levels between 2008 and 2012 (UNFCCC, 1998). The Paris Agreement of 2015, building on the UNFCCC and lessons from the Kyoto Protocol, marked a major advance in global climate efforts. Unlike the Kyoto Protocol, the Paris Agreement requires all countries to submit nationally determined contributions (NDCs) to limit global temperature rise to well below 2°C,

aiming for 1.5°C (UNFCCC, 2015). These agreements have significantly shaped international climate policy, driving national and global efforts to address climate change. The implementation of the policy requires specific technical approaches as a foundation. The Institute of Environmental Management and Assessment (IEMA) suggests an IEMA GHG Management Hierarchy to systematically address GHG emissions, which consists of four key components: Eliminate, Reduce, Substitute, and Compensate (IEMA, 2020). First, the *Eliminate* component focuses on preventing GHG emissions at the source by influencing business decisions that impact the entire lifecycle of products and services. For instance, companies can create new business modes for a circular economy, which involves sharing, leasing, reusing, repairing, refurbishing and recycling materials and products as long as possible (Bocken et al., 2017; Velenturf & Purnell, 2021). Second, the *Reduce* component aims to reduce energy use which results in the reduction of GHG emissions. This can be accomplished through efficiency improvements, which are highly various across different sectors, such as those in agricultural (Engler & Krarti, 2021; Smith et al., 2015), industrial (Malinauskaite et al., 2020; Zuberi et al., 2020), and residential (De Boeck et al., 2015; Ramos et al., 2015) sectors. Third, the *Substitute* component involves replacing high-carbon energy sources with low-carbon or renewable alternatives. Examples include adopting on-site renewable energy generation (Al-Ghamdi & Bilec, 2016), switching to lower-carbon fuels (Van Dyk et al., 2022), purchasing green tariffs for electricity (MacDonald & Eyre, 2018), etc. Finally, the *Compensate* component addresses residual emissions that cannot be eliminated, reduced, or substituted. This involves investing in carbon offset projects, such as reforestation, carbon capture and

storage (CCS), and carbon mineralization (Minx et al., 2018). Compensation makes it possible to counterbalance unavoidable emissions, supporting broader climate goals.

In summary, to effectively control GHG emissions and address climate change, it is crucial to develop and optimize a portfolio of various technologies and policies based on current efforts.

1.2. Motivation

The renewable energy is a key factor to reduce GHG emissions through the *Substitute* component in the IEMA GHG Management Hierarchy. Renewable energy capacity has seen substantial growth over the past decade, with solar and wind energy leading the charge. According to the International Renewable Energy Agency (IRENA, 2018, 2024), global solar energy capacity reached approximately 1,419 GW in 2023, up from just 40 GW in 2010. Similarly, wind energy capacity expanded to about 1,017 GW in 2023, compared to 181 GW in 2010. The capacity growth is accompanied by significant cost reductions: from 2010 to 2022, the levelized cost of electricity (LCOE) for utility-scale solar photovoltaics (PV), concentrating solar power (CSP), onshore wind, and offshore wind decreased by 89%, 69%, 69%, and 59%, respectively (IRENA, 2023b).

In contrast to the rapid expansion of solar and wind, geothermal energy development has progressed at a slower pace. As of 2023, global geothermal power capacity was approximately 14.8 GW, a modest increase from 10.1 GW in 2010 (IRENA, 2018, 2024). Such a scale is disproportionate to the technical potential of geothermal resources, which is estimated at about 200 GW for electricity and more than 5000 GW for thermal use

(IRENA, 2023a). Indeed, geothermal energy has the potential to and should take on a larger role in renewable energy development.

First, geothermal energy has a unique role among renewable energy resources. Unlike other renewable sources, it offers the dual benefits of generating both electricity and heat, along with the added value of mineral extraction. Second, geothermal energy provides a continuous and reliable source of power, unlike wind and solar, which are intermittent. This makes geothermal energy more stable and capable of providing base-load power without the need for additional storage devices. Moreover, one of the most promising advancements in geothermal technology is the synergy with carbon capture and storage (CCS). The captured CO₂ can not only be injected into the geothermal reservoir for permanent storage, but also can be employed as the working fluid for the geothermal energy system. For example, CO₂ can be used in enhanced geothermal systems (EGSs), which are engineered reservoirs created to extract heat from low-permeability, hot rock formations by injecting fluid to enhance permeability and enable geothermal energy production (Pruess, 2006). In another type of geothermal system, the CO₂ plume geothermal (CPG) system, supercritical CO₂ is used as the primary working fluid circulated through naturally-permeable formations (Randolph & Saar, 2011). In summary, geothermal energy should be paid more attention to in research and practice. Just as geothermal energy needs more development in the renewable energy ecosystem, the importance of CH₄ has also been underestimated. People have been concentrating on CO₂, since it is widely recognized as the GHG driving climate change, contributing the most to the greenhouse effect due to its high atmospheric concentration and long lifetime.

In contrast, CH₄ has a much lower atmospheric concentration than CO₂, but its impact on climate change is disproportionately large. CH₄ is over 25 times more effective than CO₂ at trapping heat in the atmosphere over a 100-year period, making it a potent climate pollutant (IPCC, 2023b). This property potentially poses a greater threat to global warming, as the atmospheric concentration of CH₄ is increasing faster now than at any time since the 1980s. CH₄ also plays a role in the creation of ground-level ozone, which is responsible for around 500,000 premature deaths annually worldwide. Fortunately, CH₄ has a short atmospheric lifetime (~10 years), which indicates that immediate action on CH₄ control can swiftly lower its concentrations in the atmosphere, leading to rapid decreases in climate forcing and ozone pollution (UNEP & CCAC, 2021). In conclusion, we should address it specifically and focus more on controlling it to expand our opportunities to combat global warming.

As previously analyzed, geothermal energy and CH₄ control are crucial components in the effort to mitigate climate change. However, both are currently hindered by a lack of concentrated efforts and insufficient development. Therefore, this dissertation focuses on optimizing strategies for geothermal heat mining and CH₄ control, and aims to provide valuable insights that can enhance the future development of geothermal energy and methane control, ultimately contributing to the global effort to address climate change.

1.3. Dissertation Overview

This dissertation studies the problems of geothermal heat mining and CH₄ control through the lens of optimization. The geothermal heat mining problem is examined at the facility level, with the objective of determining the optimal strategy for dynamic heat mining to maximize profit (Chapter 2). This problem is formulated as an optimal control model, solved using a fully analytical algorithm, and further analyzed from an economic perspective. The CH₄ control problem is addressed at the system level from both a top-down (Chapter 3) and bottom-up (Chapter 4) perspective. Chapter 3 develops a comprehensive model called “Model for Optimization of Methane Emissions and removal with Negative Technologies Under climate Mitigation (MOMENTUM)”. This model provides the optimal pathways for CH₄ mitigation (control before emissions) and atmospheric removal (control after emissions) under various climate-technology scenarios. Chapter 4 establishes an agent-based model to simulate the interactions among the government, suppliers, and consumers following the introduction of a CH₄ emission market to initial commodity/service markets. The simulation offers insights into the optimal design of the CH₄ emission market.

Chapter 2. An Analytic Approach to Optimal Geothermal Heat Mining

2.1. Introduction

The surge of anthropogenic emissions of greenhouse gases (GHGs) is one of the main reasons of current concerning climate change. In order to mitigate GHG emissions, the energy production which is dominated by fossil fuels has been gradually converted to one accommodating more renewable energy sources (RESs), e.g., wind energy, solar radiation, hydropower, and geothermal energy.

From the perspective of “stock”, i.e., the energy stored in the initial form, geothermal energy is different from other RESs. Wind energy, solar radiation, and run-of-the-river hydropower do not have obvious stock attributes, which are not naturally stored and can only be instantly used, otherwise wasted. Reservoir-based hydropower has a clear stock attribute, as the water is stored in the reservoir, and the recharging speed of the stock is determined by inflows, which is not much related to the stock level. However, the recharging speed of geothermal energy stock, which is stored in underground reservoir, is largely determined by the temperature difference between interior of the reservoir and the surrounding media. Thus, from the perspective of stock recharging, geothermal energy is less uncertain than other RESs.

Moreover, geothermal energy is also different from some other natural resources like forests and fish. Without considering environmental limitation, the recharging rate of the

stock of forest or fish is positively correlated to the stock level, i.e., a larger forest or fish group increases faster. On the contrary, less geothermal stock level means lower temperature in the reservoir, which leads to faster recharging speed. Such an opposite recharging mode will lead to many differences in the exploitation of geothermal energy compared with forestry and fishery.

Given the special stock attribute of geothermal energy, its optimal exploitation strategy needs to be separately analyzed. Several studies were focused on this topic. As early in 1980s, Golabi et al. established optimization model with closed expressions to determine some important variables in geothermal extraction, such as optimal starting time and optimal extraction rate (Golabi et al., 1981; Golabi & Scherer, 1981). However, they didn't explicitly consider the recharging process in the model. Moreover, despite they gave some analytical analyses, the algorithm for obtaining final results was numerical, and the results were only for limited combinations of discount rate and real energy increasing rate. Sigurdardottir et al. applied the lumped parameter modelling with mixed integer linear programming and proposed a semi-analytical optimal model for geothermal utilization (Sigurdardottir et al., 2015). Yet the algorithm was also numerical with the help of a optimization solver, and only two scenarios were studied. Malafeh and Sharp discussed the influences from different royalties on the geothermal extraction, but the numerical results were limited within several situations of royalty choices (Malafeh & Sharp, 2015). Liang et al. drew detailed sensitivity analyses on technological parameters and natural conditions, yet relying on complex simulation software, TOUGH2 (Liang et al., 2018). Júlíusson et al. explored different types of geothermal stock models, which

were given in simple closed forms, and gave some representative analytical solutions of those models (Júlíusson & Axelsson, 2018). However, since the extraction rates were predefined as functions of geothermal stock, these solutions didn't involve optimality. Based on the above paper, Júlíusson et al. further developed a discrete optimization model for geothermal energy production, which was linked to different market price models for deeper analysis, but only one set of geothermal parameters was considered (Juliussen & Bjornsson, 2021). Spittler et al. utilized system dynamic approach to analyze the capacity expansion of a geothermal power plant, but the study depended on STELLA Architect software, resulting in representative but not transferable results (Spittler et al., 2020).

In conclusion, historical references have focused on the numerical analysis, which can simulate models with complex expression. However, compared with analytical methods, numerical methods are often computationally expensive, and thus hard to use for exploring large parameter space. More importantly, they cannot provide insight of solution structure for all possible parameters, which can be achieved through the analytical method.

To compensate for the disadvantages of numerical methods, a totally analytical method for the optimal geothermal heat mining (OGHM) problem is proposed in this paper. Specifically, this paper contributes in

- 1) Establishing an optimal control formulation of the OGHM problem. The formulation is simple enough for analytical algorithm, while not missing the most important details of geothermal power plants and reservoirs.

- 2) Proposing a totally analytical algorithm for solving the OGHM problem. The algorithm does not rely on any additional software, and can be realized by any programming languages. Four situations of optimal mass flow rates are given, which conclude the results under any possible combinations of input parameters.
- 3) Giving detailed economic interpretation for the results. By using the concept of “stationary rate of return on capital”, economic explanations are drawn for all possible combinations of input parameters under infinite horizon, which are further extended to finite horizons.

2.2. Methods

In this section, the OGHM problem is modelled as an optimal control problem, and an algorithm is proposed to solve it by utilizing the maximum principle (Weitzman, 2003).

2.2.1. Model

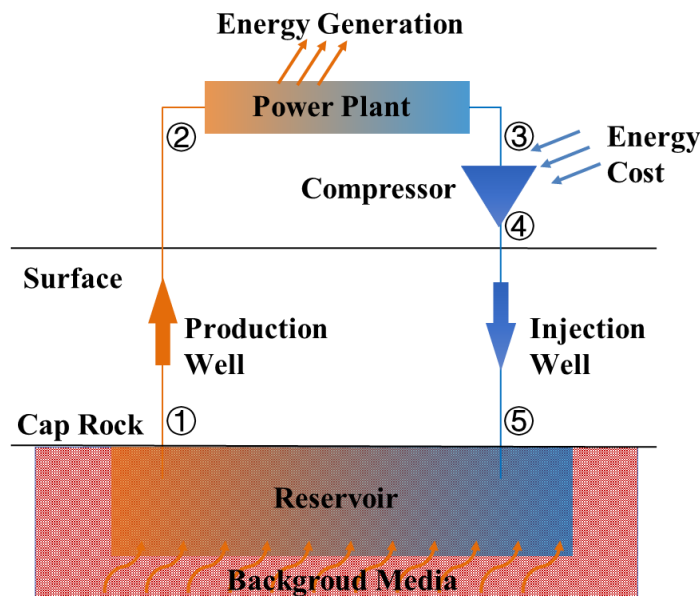


Figure 2-1. Geothermal Heat Mining and Energy Conversion

The objective is to maximize total profit, which is expressed as the present value of all net generated energy (W). At any point in time, the value of the objective function equals the useful produced energy less the energy needed to compress the fluid for injection. Let h be the specific enthalpy, and \dot{m} the mass flow rate. The useful energy is the difference in enthalpy flow between the inlet to the production well in the reservoir ($h_1\dot{m}$) and the injection wellhead ($h_3\dot{m}$) with an accommodation for an efficiency (η) penalty: $\eta(h_1 - h_3)\dot{m}$. This general framework allows for η to represent the efficiency in the production well and the use of the produced heat, regardless of the specific application (e.g., direct-use, electricity).

The energy for compression is estimated as the change in enthalpy flow of the fluid being injected by the compressor, i.e., $(h_4 - h_3)\dot{m}$. The objective function is the net present energy, which considers the discounts energy production over time back to the present. Moreover, it is assumed that the mass flow rate in the production well equals the mass flow rate in the injection well. As such, the objective function as

$$\max W = \int_{t=0}^{t=\tau} [\eta(h_1 - h_3)\dot{m}(t) - (h_4 - h_3)\dot{m}(t)]e^{-\delta t} dt \quad (2-1)$$

where t is the time index starting from 0 and ended at τ , e is the base of the natural logarithm function, and δ is the discount rate.

Since we only care about the change of reservoir stored heat, i.e., how much is extracted or recharged, we use “the change of reservoir stored heat (ΔQ_r)” throughout the model, which is defined as

$$\Delta Q_r(t) = Q_r(t) - Q_r(0) \quad (2-2)$$

where Q_r is the reservoir stored heat.

Before heat is extracted (i.e., $t = 0$), the reservoir temperature (T_r) is in equilibrium with the surrounding media temperature (T_e) in the aquifer, which we assume is constant over the relevant lifetime of geothermal heat extraction. We also assume that the contact conductance between the reservoir and surrounding media (H_{r-e}) is constant over time. When heat is extracted from the reservoir, T_r decreases below T_e . This difference in temperature results in heat flow from the surrounding media into the reservoir, which increases the reservoir temperature. As such, there are two competing factors (heat extraction rate, \dot{Q}_{extr} , and heat recharge rate, \dot{Q}_{rech}) that affect the reservoir temperature. These factors are modeled by the dynamic change in reservoir stored heat:

$$\frac{dQ_r(t)}{dt} = \frac{d\Delta Q_r(t)}{dt} = \dot{Q}_{rech}(t) - \dot{Q}_{extr}(t) \quad (2-3)$$

Through a simple representation of heat transfer due to conduction,

$$\dot{Q}_{rech} = [T_e - T_r(t)]H_{r-e} \quad (2-4)$$

The heat extraction rate \dot{Q}_{extr} is calculated by the difference in the enthalpy flow of heat extraction fluid between downhole of production well (h_1) and downhole of the injection well (h_5):

$$\dot{Q}_{extr}(t) = \dot{m}(t)(h_1 - h_5) \quad (2-5)$$

The reservoir temperature depends on the change of reservoir stored heat,

$$Q_r(t) = M_r c_{p,eff} [T_r(t) - T_e] \quad (2-6)$$

where M_r is the mass of reservoir, and $c_{p,eff}$ is the effective specific heat of reservoir (fluid/rock mixture).

The specific enthalpy of fluid downhole of production well, h_1 , depends on the change in T_r . Under isobaric conditions (constant pressure), the relationship between fluid enthalpy and temperature can be approximated as linear regarding the temperature.

$$h_1 = c_{p,1}T_r + h_{1,ic} \quad (2-7)$$

in which the slope is the specific heat of production fluid, $c_{p,1}$, and the intercept is $h_{1,ic}$.

The mass flow rate, \dot{m} , must be between 0 and a maximum value, \dot{m}_{max} ,

$$0 \leq \dot{m}(t) \leq \dot{m}_{max} \quad (2-8)$$

yet ΔQ_r does not need to be constrained: when $\Delta Q_r = 0$, the heat recharge rate (\dot{Q}_{rech}) is 0, which means the reservoir stored heat cannot increase anymore, i.e., the upper bound of ΔQ_r is naturally 0. As heat is extracted from the reservoir, T_r decreases, which reduces the heat extraction rate (\dot{Q}_{extr}) and increases the heat recharge rate (\dot{Q}_{rech}). At some point, the maximum extraction rate and recharge rate will be equal, i.e., \dot{Q}_{extr} with \dot{m}_{max} equals \dot{Q}_{rech} , and the reservoir heat cannot be reduced anymore. As a result, the lower bound of $\Delta Q_{r,t-0}$ is $\frac{\dot{m}_{max}(h_5 - h_{1,ic}) + H_{r-e}T_e}{\dot{m}_{max}c_{p,1} + H_{r-e}}$. These two natural bounds (i.e., not additionally constrained) of ΔQ_r avoid the situation where net negative heat is extracted from the reservoir (or net positive heat is injected into the reservoir).

Finally, the initial condition of the change of reservoir stored heat is

$$\Delta Q_r(0) = 0 \quad (2-9)$$

Equations (2-1), (2-3)-(2-9) can comprise the full model, which has two state variables (ΔQ_r and T_r) and two control variables (\dot{m} and q). Since one state variable or control variable can be determined by another, the current formulation is redundant. By substituting Equations (2-4)-(2-7) into (2-1) and (2-3), ΔQ_r is left as the only state variable, and $\dot{m}(t)$ is the only control variable. The final model is listed as follows:

$$\max W = \int_{t=0}^{t=\tau} \left\{ \underbrace{\eta \left[c_{p,1} \left(\frac{\Delta Q_r(t)}{M_r c_{p,eff}} + T_e \right) + h_{1,ic} - h_3 \right]}_{Revenue} - \underbrace{(h_4 - h_3)}_{Cost} \right\} \dot{m}(t) e^{-\delta t} dt \quad (2-10a)$$

subject to

$$\frac{d\Delta Q_r(t)}{dt} = -\frac{H_{r-e}}{M_r c_{p,eff}} \Delta Q_r(t) - \dot{m}(t) \left[c_{p,1} \left(\frac{\Delta Q_r(t)}{M_r c_{p,eff}} + T_e \right) + h_{1,ic} - h_5 \right] \quad (2-10b)$$

$$0 \leq \dot{m}(t) \leq \dot{m}_{max} \quad (2-10c)$$

$$\Delta Q_r(0) = 0 \quad (2-10d)$$

2.2.2. Algorithm

Model (2-10) is an optimal control problem, which can be solved by the maximum principle (Weitzman, 2003). The first step is to construct the current-value Hamiltonian (H_c), which is the profit at a single point in time plus the product of an additional costate variable and dynamic change function of the state variable (right-hand side of Equation (2-10b)):

$$\begin{aligned}
H_C &= \left\{ \eta \left[c_{p,1} \left(\frac{\Delta Q_r(t)}{M_r c_{p,eff}} + T_e \right) + h_{1,ic} - h_3 \right] - (h_4 - h_3) \right\} \dot{m}(t) + \\
&\quad \mu(t) \left\{ -\frac{H_{r-e}}{M_r c_{p,eff}} \Delta Q_r(t) - \dot{m}(t) \left[c_{p,1} \left(\frac{\Delta Q_r(t)}{M_r c_{p,eff}} + T_e \right) + h_{1,ic} - h_5 \right] \right\} \\
&= \left\{ \eta \cdot \left[c_{p,1} \left(\frac{\Delta Q_r(t)}{M_r c_{p,eff}} + T_e \right) + h_{1,ic} - h_3 \right] - (h_4 - h_3) - \mu(t) \left[c_{p,1} \left(\frac{\Delta Q_r(t)}{M_r c_{p,eff}} + \right. \right. \right. \\
&\quad \left. \left. \left. T_e \right) + h_{1,ic} - h_5 \right] \right\} \dot{m}(t) - \mu(t) \frac{H_{r-e}}{M_r c_{p,eff}} \Delta Q_r(t)
\end{aligned} \tag{2-11}$$

where μ is the costate variable for constraint (2-10b). H_C is a linear function regarding \dot{m} , and denote the coefficient of \dot{m} as

$$\begin{aligned}
\xi(t) &= \eta \cdot \left[c_{p,1} \left(\frac{\Delta Q_r(t)}{M_r c_{p,eff}} + T_e \right) + h_{1,ic} - h_3 \right] - (h_4 - h_3) - \mu(t) \left[c_{p,1} \left(\frac{\Delta Q_r(t)}{M_r c_{p,eff}} + \right. \right. \\
&\quad \left. \left. T_e \right) + h_{1,ic} - h_5 \right]
\end{aligned} \tag{2-12}$$

According to the maximum principle, the control variable \dot{m} must maximize the Hamiltonian at any time. Thus

$$\dot{m}(t) = \begin{cases} \dot{m}_{max}, & \text{if } \xi(t) > 0 \\ \text{arbitrary}, & \text{if } \xi(t) = 0 \\ 0, & \text{if } \xi(t) < 0 \end{cases} \tag{2-13}$$

Further the motion equation of the costate variable is

$$\frac{d\mu(t)}{dt} = \delta \mu(t) - \frac{\partial H_C}{\partial \Delta Q_r(t)} = \left(\frac{c_{p,1}}{M_r c_{p,eff}} \dot{m}(t) + \delta + \frac{H_{r-e}}{M_r c_{p,eff}} \right) \mu(t) - \frac{\eta c_{p,1}}{M_r c_{p,eff}} \dot{m}(t) \tag{2-14}$$

Finally the transversality condition is

$$\mu(\tau) = 0 \tag{2-15}$$

Equations (2-10b), (2-10d) and (2-12)-(2-15) are necessary and sufficient conditions to solve problem (2-10). Due to the ‘‘if’’ branches in Equation (2-13), it’s difficult to directly obtain the solution from these conditions. Thus alternatively, we construct solutions (of

the mass flow rate \dot{m}) that satisfy these conditions. A qualitative summary of all possible solutions is given in Figure 2-2, followed by the complete algorithm in Figure 2-3.

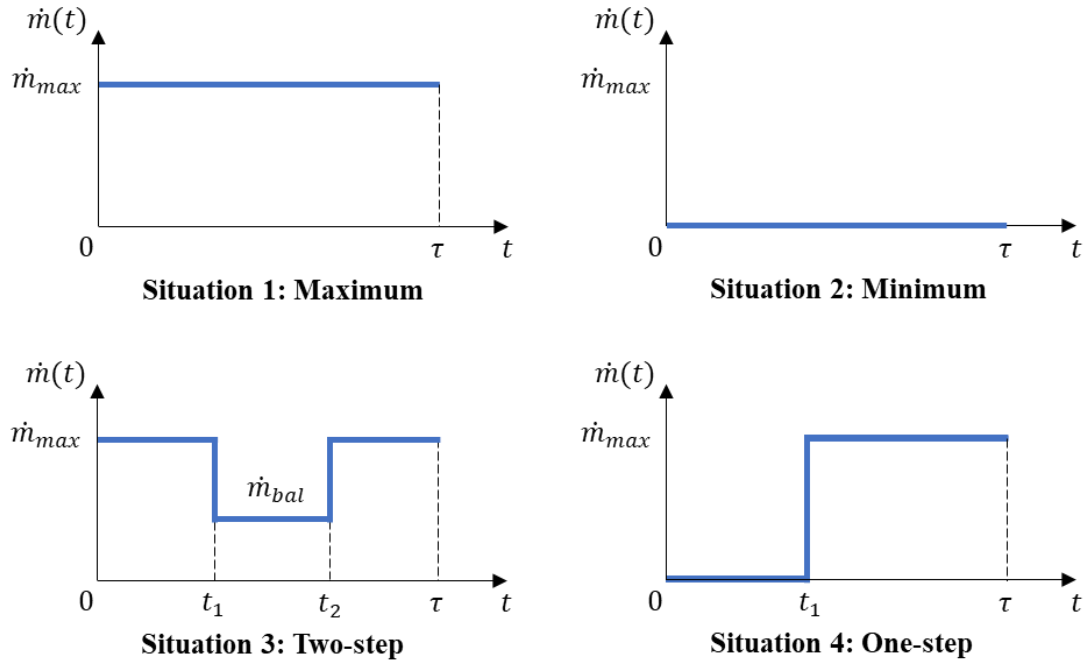


Figure 2-2. Situations of Mass Flow Rate Solutions for the OGHM Problem

All possible solutions can be categorized into four situations (Figure 2-2). In situation 1, the mass flow rate keeps the maximum through all the time, in contrast to, in situation 2, that the mass flow rate keeps as 0. In situation 3, the mass flow rate has three stages and two steps, distinguished by two time points, t_1 and t_2 . The mass flow rates of stages 1 and 3 are both the maximum, and of stage 2 is a balanced constant \dot{m}_{bal} that needs to be solved. In situation 4, the mass flow rate has two stages and one step, distinguished by time point t_1 . The mass flow rate starts as 0, and after some time changes to the maximum and keeps to the end.

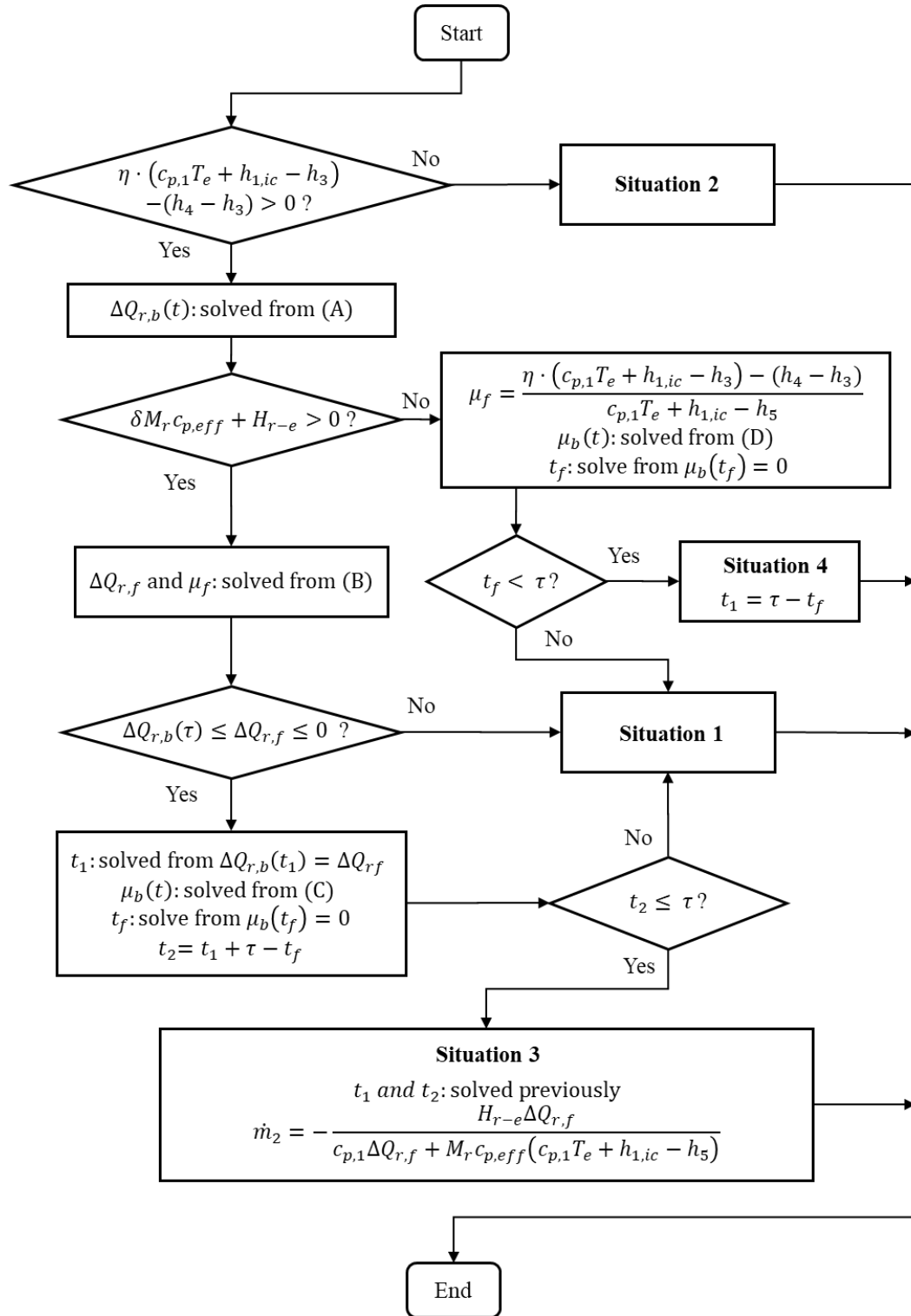


Figure 2-3. Flow Chart of Algorithm on Solving the Mass Flow Rate

Figure 2-3 shows the flow chart of the algorithm for solving the mass flow rate, in which formulas (A)-(E) are listed as follows. The subscript b means “base” functions obtained amid the algorithm, and f means “flag” values that are essential to determine the final solution.

$$\frac{d\Delta Q_{r,b}(t)}{dt} = -\frac{H_{r-e}}{M_r c_{p,eff}} \Delta Q_{r,b}(t) - \dot{m}_{max} \left[c_{p,1} \left(\frac{\Delta Q_{r,b}(t)}{M_r c_{p,eff}} + T_e \right) + h_{1,ic} - h_5 \right] \quad (A)$$

$$\Delta Q_{r,b}(0) = 0$$

$$\begin{aligned} \eta \cdot \left[c_{p,1} \left(\frac{\Delta Q_{r,f}}{M_r c_{p,eff}} + T_e \right) + h_{1,ic} - h_3 \right] - (h_4 - h_3) \\ - \mu_f \left[c_{p,1} \left(\frac{\Delta Q_{r,f}}{M_r c_{p,eff}} + T_e \right) + h_{1,ic} - h_5 \right] = 0 \end{aligned} \quad (B)$$

$$\frac{\delta}{M_r c_{p,eff}} \mu_f \Delta Q_{r,f} + \left(\delta + \frac{H_{r-e}}{M_r c_{p,eff}} \right) \left(T_e + \frac{h_{1,ic} - h_5}{c_{p,1}} \right) \mu_f + \frac{\eta H_{r-e}}{(M_r c_{p,eff})^2} \Delta Q_{r,f} = 0$$

$$\frac{d\mu_b(t)}{dt} = \left(\frac{c_{p,1}}{M_r c_{p,eff}} \dot{m}_{max} + \delta + \frac{H_{r-e}}{M_r c_{p,eff}} \right) \mu_b(t) - \frac{\eta c_{p,1}}{M_r c_{p,eff}} \dot{m}_{max} \quad (C)$$

$$\mu_b(t_1) = \mu_f$$

$$\frac{d\mu_b(t)}{dt} = \left(\frac{c_{p,1}}{M_r c_{p,eff}} \dot{m}_{max} + \delta + \frac{H_{r-e}}{M_r c_{p,eff}} \right) \mu_b(t) - \frac{\eta c_{p,1}}{M_r c_{p,eff}} \dot{m}_{max} \quad (D)$$

$$\mu_b(0) = \mu_f$$

where Formula (B) is made of two quadratic algebra equations and easy to solve. It is possible that Formula (B) has no real-number solutions. Formulas (A), (C) and (D) are all simple first-order linear differential equations, with the same mathematical form as

$$\frac{dy(t)}{dt} = \alpha y(t) + \beta \quad (2-16)$$

$$y(t_\gamma) = y_\gamma$$

where $y(t)$ is the variable dependent on t , α and β are constant coefficients of the differential equation, and t_γ and y_γ are constants in the initial condition. Equation (2-16) has a solution as follows, which can be used for solving Formulas (A), (C), and (D).

$$y(t) = \left(y_\gamma + \frac{\beta}{\alpha} \right) e^{\alpha(t-t_\gamma)} - \frac{\beta}{\alpha} \quad (2-17)$$

2.3. Economic Interpretation

The above algorithm and solutions are purely mathematical which cannot provide an intuitive understanding of the solution. To better interpret the solutions, some economic concepts and methods are utilized in this section to solve the OGHM problem with an infinite time horizon, which is further compared with the finite-time situations shown in Figure 2-2.

2.3.1. Stationary Rate of Return on Reservoir Stored Heat

The concept of “stational rate of return on capital” is essential for solving economic control problems (Weitzman, 2003). Here we employ this concept to analyze the OGHM problem, and since the “capital” in the problem is reservoir stored heat, it is renamed as “stationary rate of return on reservoir stored heat”.

Denote $G(\Delta Q_r(t), \dot{m}(t))$ as the current value of net generated energy at time t , which is extracted from Equation (2-10b):

$$G(\Delta Q_r(t), \dot{m}(t)) = \left\{ \eta \left[c_{p,1} \left(\frac{\Delta Q_r(t)}{M_r c_{p,eff}} + T_e \right) + h_{1,ic} - h_3 \right] - (h_4 - h_3) \right\} \dot{m}(t) \quad (2-18)$$

By substituting Equation (2-10b) into (2-18), convert G from a function of $\Delta Q_r(t)$ and

$\dot{m}(t)$ to a function of $\Delta Q_r(t)$ and $\frac{d\Delta Q_r(t)}{dt}$:

$$G\left(\Delta Q_r(t), \frac{d\Delta Q_r(t)}{dt}\right) = \left\{ \eta \left[C_{p,1} \left(\frac{\Delta Q_r(t)}{M_r C_{p,eff}} + T_e \right) + h_{1,ic} - h_3 \right] - (h_4 - h_3) \right\} \frac{-\frac{H_r - e}{M_r C_{p,eff}} \Delta Q_r(t) - \frac{d\Delta Q_r(t)}{dt}}{C_{p,1} \left(\frac{\Delta Q_r(t)}{M_r C_{p,eff}} + T_e \right) + h_{1,ic} - h_5} \quad (2-19)$$

where $\Delta Q_r(t)$ and $\frac{d\Delta Q_r(t)}{dt}$ are considered as mutually independent variables.

Consider a stationary state, where reservoir stored heat remains constant, i.e.,

$$G\left(\Delta Q_r(t), \frac{d\Delta Q_r(t)}{dt}\right) = G(\Delta Q_r, 0) = \text{constant} \quad (2-20)$$

Define partial derivatives as

$$G_1\left(\Delta Q_r(t), \frac{d\Delta Q_r(t)}{dt}\right) = \frac{\partial G\left(\Delta Q_r(t), \frac{d\Delta Q_r(t)}{dt}\right)}{\partial \Delta Q_r(t)} \quad (2-21)$$

$$G_2\left(\Delta Q_r(t), \frac{d\Delta Q_r(t)}{dt}\right) = \frac{\partial G\left(\Delta Q_r(t), \frac{d\Delta Q_r(t)}{dt}\right)}{\partial \frac{d\Delta Q_r(t)}{dt}}$$

If we transfer the stationary state from $(\Delta Q_r, 0)$ to $(\Delta Q_r + \epsilon, 0)$, the current value of net generated energy at time t will increase by $G_1(\Delta Q_r, 0)\epsilon$, and the total present-value of net

generated energy will increase by $\int_t^\infty G_1(\Delta Q_r, 0)\epsilon e^{-\delta t} dt = G_1(\Delta Q_r, 0)\epsilon \int_t^\infty e^{-\delta t} dt =$

$\frac{G_1(\Delta Q_r, 0)\epsilon e^{-\delta t}}{\delta}$. However, in order to have such a profit increase, we must temporarily put ϵ

of heat into the reservoir, which causes a temporary loss of profit at the point of time t as

$-G_2(\Delta Q_r, 0)\epsilon e^{-\delta t}$.

When the profit is more than the loss, the tiny increase of ΔQ_r is beneficial and we want to increase ΔQ_r until the profit equals the loss. In contrast, when the profit is less than the loss, the tiny increase of ΔQ_r is harmful and we want to decrease ΔQ_r until the profit equals the loss. If the profit equals the loss, we maintain the state.

Now introduce the concept of stationary rate of return on reservoir stored heat to describe the above relationships in another manner, which is defined as

$$R(\Delta Q_r) = \frac{G_1(\Delta Q_r, 0)}{-G_2(\Delta Q_r, 0)} \quad (2-22)$$

When $R > \delta$, we want to increase ΔQ_r until $R = \delta$; When $R < \delta$, we want to decrease ΔQ_r until $R = \delta$; When $R = \delta$, we maintain the state. Moreover, because the objective function is linear regarding $\frac{d\Delta Q_r(t)}{dt}$, the change towards $R = \delta$ should be the most rapid approach (MRA), i.e., in the optimal solution R should follow the trajectory with the fastest speed towards δ (Weitzman, 2003).

2.3.2. Solutions to Infinite-Time OGHM Problems

By using stationary rate of return on reservoir stored heat, the OGHM problem with an infinite time horizon is solved as follows.

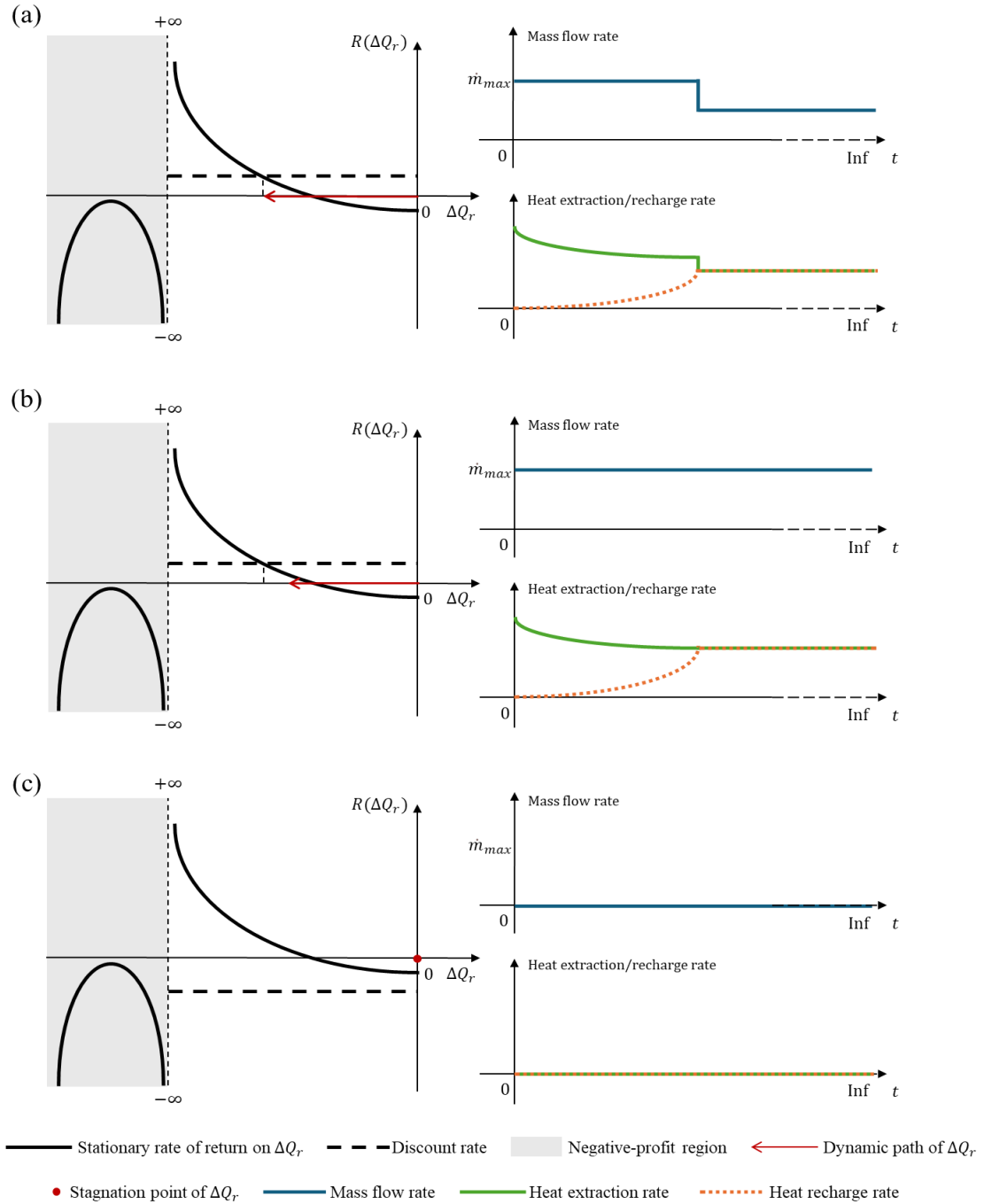


Figure 2-4. Solutions to Infinite OHM Problem Under Different Situations.

(a) $\eta[c_{p,1}T_e + h_{1,ic} - h_3] - (h_4 - h_3) > 0$ (can make positive profit), $\delta M_r c_{p,eff} + H_{r-e} > 0$ ($R(\Delta Q_r = 0) > \delta$), can reach where $R = \delta$.
 (b) $\eta[c_{p,1}T_e + h_{1,ic} - h_3] - (h_4 - h_3) > 0$ (can make positive profit), $\delta M_r c_{p,eff} + H_{r-e} > 0$ ($R(\Delta Q_r = 0) > \delta$), cannot reach where $R = \delta$.
 (c) $\eta[c_{p,1}T_e + h_{1,ic} - h_3] - (h_4 - h_3) > 0$ (can make positive profit), $\delta M_r c_{p,eff} + H_{r-e} \leq 0$ ($R(\Delta Q_r = 0) \leq \delta$)

As shown in Equation (2-18), if the coefficient $\eta \left[c_{p,1} \left(\frac{\Delta Q_r(t)}{M_r c_{p,eff}} + T_e \right) + h_{1,ic} - h_3 \right] - (h_4 - h_3)$ is non-positive, the best strategy is extracting no fluid to make a zero profit, otherwise the profit will be non-positive. Given that $\Delta Q_r \leq 0$ for all the time, the largest value of this coefficient is $\eta [c_{p,1} T_e + h_{1,ic} - h_3] - (h_4 - h_3)$, when $\Delta Q_r = 0$. If $\eta [c_{p,1} T_e + h_{1,ic} - h_3] - (h_4 - h_3) \leq 0$, the optimal strategy will be extracting no fluid through all the time. The situation where $\eta [c_{p,1} T_e + h_{1,ic} - h_3] - (h_4 - h_3) > 0$ is discussed in the following part.

The solid black curves in Figure 2-4 show the relationship between the stationary rate of return on reservoir stored heat (R) and reservoir stored heat (ΔQ_r). It can be proven that the initial value of R , i.e., $R(\Delta Q_r = 0)$, is always negative. As ΔQ_r decreases, R increases to positive infinity, then jumps down to negative infinity and stays negative.

For the left part of R (gray box), the aforementioned coefficient $\eta \left[c_{p,1} \left(\frac{\Delta Q_r(t)}{M_r c_{p,eff}} + T_e \right) + h_{1,ic} - h_3 \right] - (h_4 - h_3)$ is always negative, i.e., the profit is negative, so the left part of R will not be reached in the OGHM solutions.

When the initial value of R , $R(\Delta Q_r = 0)$, is lower than the discount rate δ [Figure 2-4(a) and (b)], according to the MRA (see at the end of Section 2.3.1), the mass flow rate should be the maximum so that ΔQ_r can decrease as fast as possible, i.e., R increase as fast as possible towards δ . As ΔQ_r decreases, the heat extraction rate decreases while the heat recharge rate increases. In Figure 2-4(a), the maximum heat extraction rate is always higher than the recharge rate before R reaches δ , so ΔQ_r keeps decreasing. Once reaching

δ , R should be unchanged to make the maximum profit, i.e., the heat extraction rate should immediately be adjusted to what equals the heat recharge rate and keep this balance forever. In contrast, as shown in Figure 2-4(b), it is also possible that the heat recharge process is so significant that the maximum heat extraction rate cannot keep higher than the recharge rate before R reaches δ . In this situation, at somewhere $R < \delta$, the maximum heat extraction rate equals the heat recharge rate, and ΔQ_r cannot decrease any more. Thus, the mass flow rate will be the maximum forever toward the unreachable point where $R = \delta$, and R will be stagnant at some value smaller than δ .

When the initial value of R is higher than the discount rate δ (Figure 2-4(c)), ΔQ_r should not decrease. Otherwise R will increase and have a large gap with δ , which violates the MRA. As a result, no heat will be extracted and ΔQ_r keeps zero forever. In other words, the discount rate is so negative that the optimal heat mining strategy is reserving the heat for the future forever.

2.3.3. Relationship Between Finite-Time and Infinite-Time OGHM problems

Figure 2-5 shows the solutions of the mass flow rate for OGMH problems, where the infinite-time problems are solved by using the stationary rate of return on reservoir stored heat (Section 2.3.2), and the finite-time problems are solved by the proposed mathematical algorithm (Section 2.2.2). In each sub-figure, there is one infinite-time case and four finite-time cases, of which all the input parameters are the same except for the time horizon (infinite time horizon vs. finite time horizons from τ_1 to τ_4).

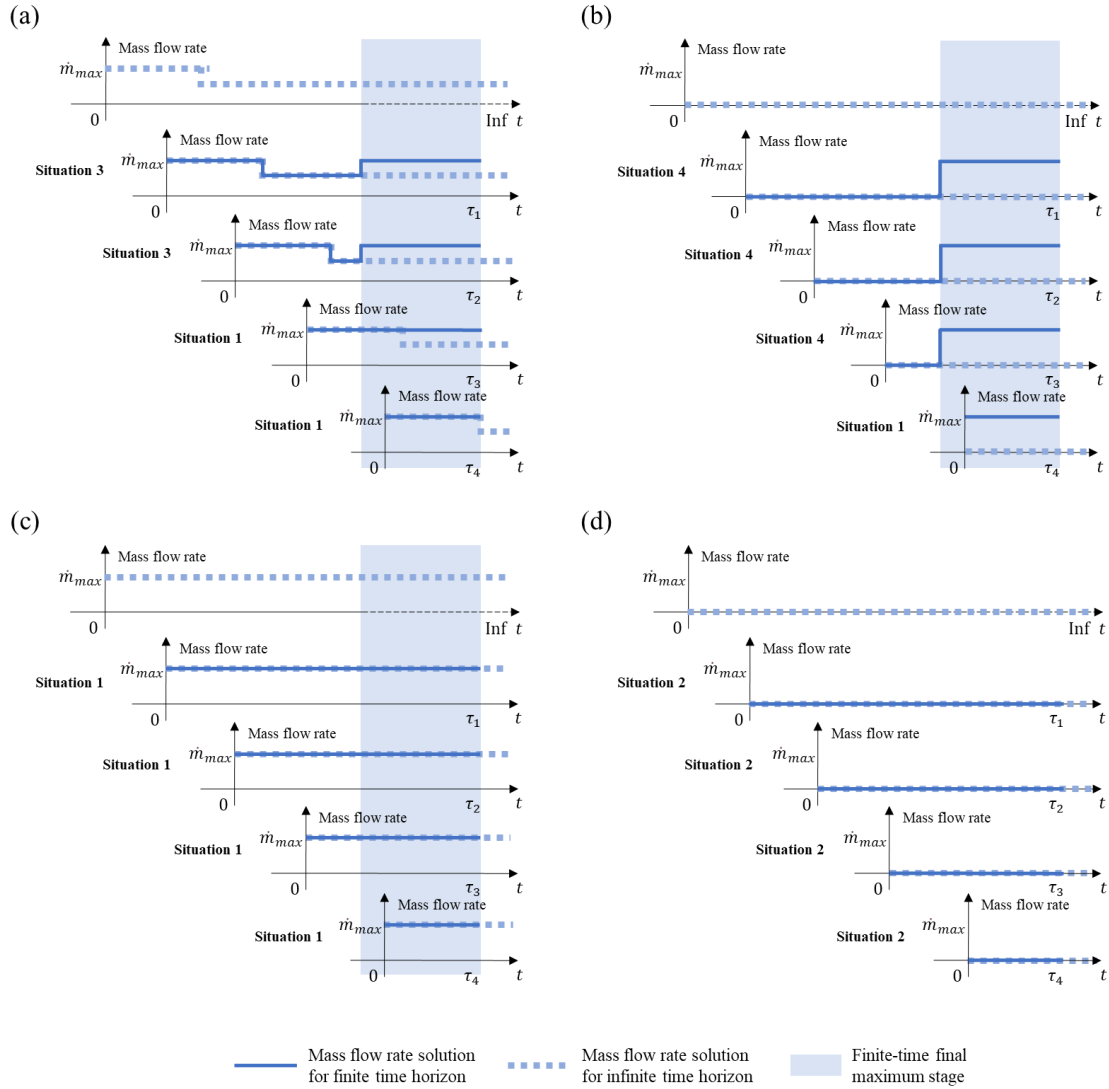


Figure 2-5. Relationship Between Finite-Time and Infinite-Time OGHM problems

In Figure 2-5(a), when the time horizon is infinite, the mass flow rate starts with the maximum value and keeps until reaching where $R = \delta$ [see Figure 2-4(a)]. Then the mass flow rate will forever keep the value which maintains $R = \delta$. However, for the finite-time cases, when close to the end, the mass flow rate goes back to the maximum and last to the end. This means that for finite-time cases, when there is not much time left, it is not

optimal to reserve any heat for the future, and the best strategy is extracting heat with the maximum mass flow rate until the end. Here we name this final stage where the mass flow rate goes back to the maximum, which is unique in finite-time OGHM problems, as the “*Finite-Time Final Maximum (FTFM) stage*”. Thus the mass flow rate solutions of finite-time OGHM problems can be considered as a combination of the solution of the infinite-time problem and one FTFM stage. Moreover, for finite-time OGHM problems with the same parameters except for the time horizon, the FTFM stage is the same, which is drawn as blue belts in Figure 2-5.

Such a combination varies with different finite-time horizons. In Figure 2-5(a), for the finite-time cases with time horizons as τ_1 and τ_2 , the FTFM stage is shorter than the stage where $R = \delta$ (i.e., the stage that keeps forever in the infinite-time case), and the combination of the infinite-time solution and the FTFM stage results in a “two-step” situation (situation 3 in Figure 2-2). However, when the time horizon decreases (τ_3 and τ_4), the FTFM stage becomes longer than and fully covers the stage where $R = \delta$. In other words, the mass flow rate starts as the maximum, and reaches the FTFM stage before reaching where $R = \delta$. As a result, the mass flow rate is always the maximum, and the two-step situation degrades to the maximum situation (situation 1 in Figure 2-2). In addition, if the FTFM stage is longer than the total time horizon (e.g., τ_4), all stages are covered by the FTFM stage, and the mass flow rate keeps maximum throughout the time horizon.

Similar to Figure 2-5(a), Figure 2-5(b) shows how the combination of the infinite-time solution and the FTFM stage leads to finite-time solutions. In Figure 2-5(b), the optimal

solution for the infinite-time OGHM problem is keeping zero mass flow rate, i.e., always reserving heat to the unreachable points where $R = \delta$ [see Figure 2-4(c)]. For the finite-time cases with time horizons as τ_1 , τ_2 , and τ_3 , the introduction of FTFM stage creates a “one-step” situation (situation 4 in Figure 2-2), where the mass flow rate starts as 0, changes to the maximum, and keeps the maximum to the end. In other words, it is optimal to reserve all heat for the future until reaching the FTFM stage, where the mass flow rate rises to the maximum. For finite-time horizon τ_4 , where the FTFM stage is longer than the total time horizon, the mass flow rate is always maximum, and the one-step situation is degraded to the maximum situation (situation 1 in Figure 2-2).

In Figure 2-5(c), for the infinite-time problem, the optimal solution always keeps the maximum mass flow rate [see Figure 2-4(b)]. In this case, the introduction of the FTFM stage makes no difference, since the mass flow rate is also the maximum in the FTFM stage. All finite-time cases in Figure 2-5(c) belong to the maximum situation (situation 1 in Figure 2-2).

Figure 2-5 (d) corresponds to the situation where extracting any amount of heat at any time cannot make positive profits, i.e., $\eta[c_{p,1}T_e + h_{1,ic} - h_3] - (h_4 - h_3) \leq 0$ (see Section 2.3.2). Thus, whether for the finite-time or the infinite-time problem, the optimal strategy is keeping the mass flow rate at zero, and there is no FTFM stage.

2.4. Results

Table 2-1: Baseline Parameters

Parameter	Value
Efficiency η	10%
Compression cost $h_4 - h_3$	12 J/g
h_3	262.93 J/g
h_5	287.93 J/g
$h_{1,ic}$	184.08 J/g
$c_{p,1}$	2.20 J/g-K
$c_{p,eff}$	0.92 J/g-K
H_{r-e}	2.5×10^5 W/K
M_r	1.5×10^{15} g
T_e	100 °C
T_3	22 °C
\dot{m}_{max}	100 kg/s
Discount rate δ	5%

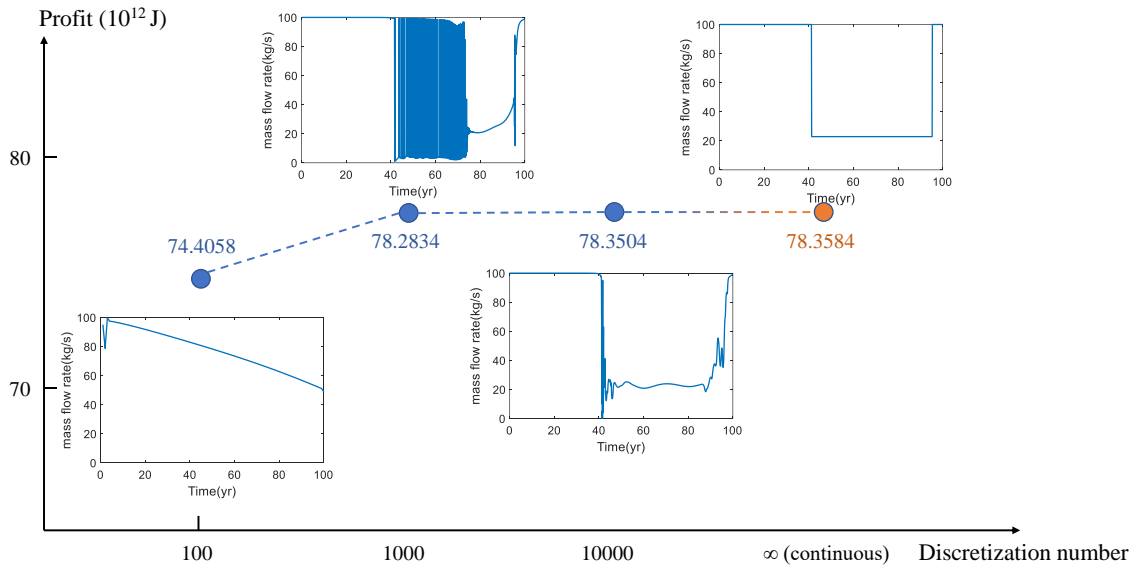


Figure 2-6: Numerical results from discretized models with different discretization numbers and analytical results from the continuous model.

To verify the analytical algorithm, the time-continuous optimal control problem (2-10) is discretized in time and solved numerically by using MATLAB 2021b with optimization toolbox YALMIP (Lofberg, 2004) and optimization solver IPOPT (Bertolazzi, 2022; Wächter & Biegler, 2006). By using the baseline parameters listed in Table 2-1, the numerical results are compared with the analytical result obtained by the algorithm proposed in this study (Section 2.2.2). As shown in Figure 2-6, the value of optimal profit shows good convergence as the discretization number increases, which gradually rises to the limit (infinite discretization number, i.e., continuous) as 78.3584×10^{12} J. Moreover, the shape of the optimal mass flow rate also “converges” as the discretization number increases, which becomes more similar to the two-step situation (situation 3 in Figure 2-2) that is solved by the analytical algorithm. In addition, the analytical algorithm does not rely on any other software and can be easily realized by any programming language, which makes the results more accurate and the computation speed faster. In conclusion, the comparison with numerical results verifies the correctness and shows the advantages of the analytical algorithm.

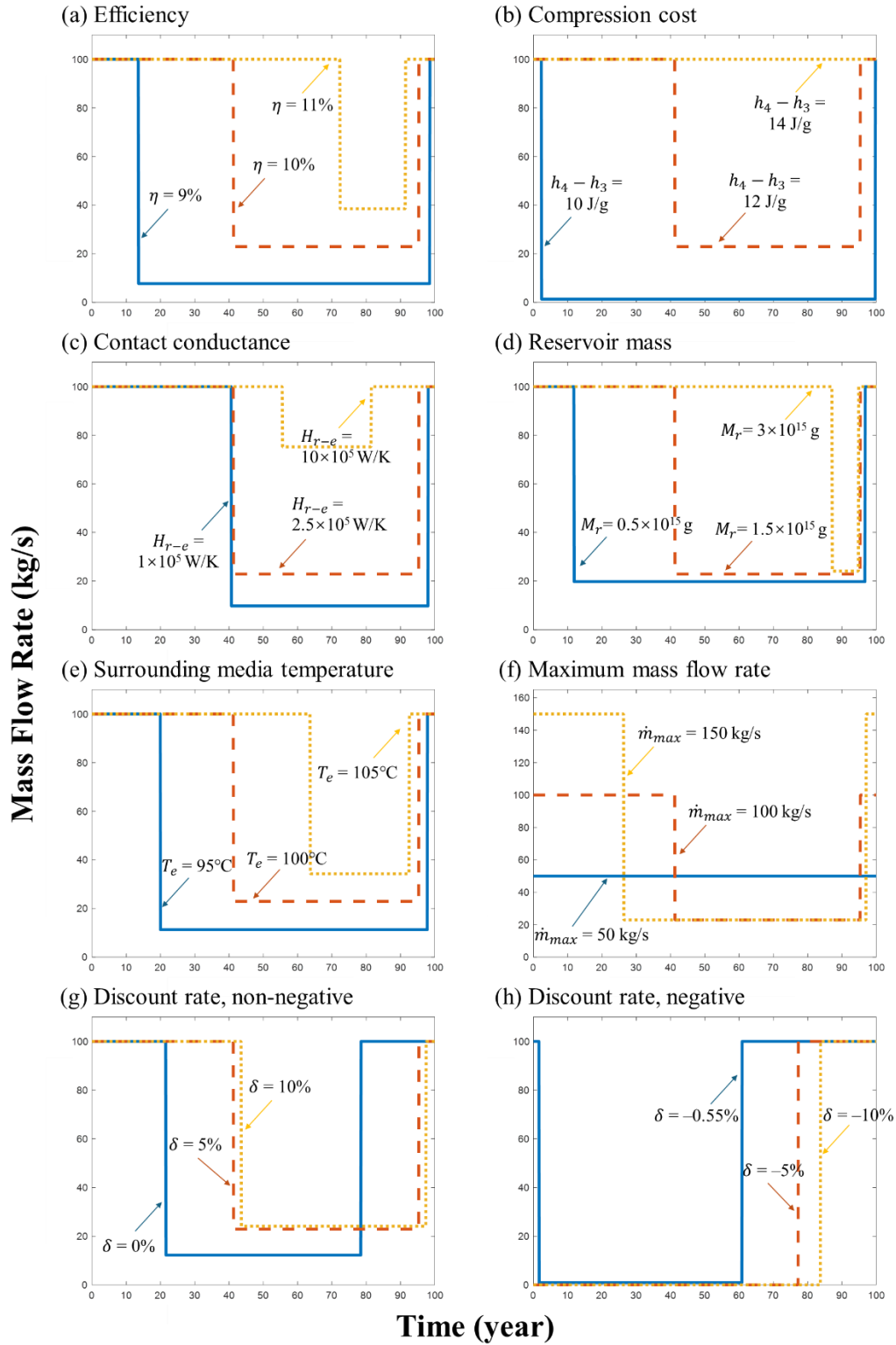


Figure 2-7: Sensitivity analysis of different techno-economic parameters on the optimal solution of mass flow rate

By using the parameter settings in Table 2-1 as the baseline case, different parameters are varied respectively to analyze the impact on the optimal solution of the mass flow rate. Only scenarios resulting in a positive profit are considered. In Figure 2-7(a)–(e), the change of the parameter (including efficiency, compression cost, contact conductance, reservoir mass, and surrounding media temperature) has similar influences [take Figure 2-7(a) as an example]. As the parameter value increases, 1) the time at which the mass flow rate decreases from the maximum to the value where $R = \delta$ occurs later (e.g., at ~year 12 when $\eta = 9\%$, and at ~year 41 when $\eta = 10\%$), 2) the time at which the mass flow rate recovered from the value where $R = \delta$ to the maximum occurs earlier (e.g., at ~year 98 when $\eta = 9\%$, and in ~year 95 when $\eta = 10\%$), and 3) the value of mass flow rate where $R = \delta$ becomes greater (e.g., ~8 kg/s when $\eta = 9\%$, and ~21 kg/s when $\eta = 10\%$). For convenience, name the time described in 1) as “*mass flow rate dropping time*”, the time in 2) as “*mass flow rate recovering time*”, and the value in 3) as “*mass flow rate balancing value*”. Specially, in Figure 2-7(b), when the compression cost is 14 J/g, the mass flow rate dropping time and recovering time overlap and the mass flow rate balancing value equals the maximum, leading to degradation from the two-step situation into the maximum situation (situation 3 and 1 in Figure 2-2). Additionally, changing the reservoir mass has little effect on the mass flow rate recovering time and balancing value, yet has a significant impact on the mass flow rate dropping time.

When the maximum mass flow rate decreases, as shown in Figure 2-7(f), the mass flow rate dropping time is delayed, the mass flow rate recovering time is advanced, but the mass flow rate balancing value remains unchanged. Specially, when the maximum mass

flow rate is 50 kg/s, it is so small that the heat extraction rate is not large enough to reach where $R = \delta$ before the FTFM stage. As a result, the mass flow rate keeps the maximum throughout the time horizon, and the two-step situation degrades into the maximum situation (situations 3 and 1 in Figure 2-2).

Figure 2-7(g) shows cases with varying discount rates that are non-negative. When the discount rate goes higher, the mass flow rate balancing value becomes greater, yet in contrast to the cases in Figure 2-7(a)-(f), the mass flow rate dropping time and recovering time are both postponed. Moreover, the lasting time of the mass flow rate balancing value remains almost the same (~55 years) regardless of the discount rate. In addition, when the discount rate is high enough (e.g., 5% and 10%), changing it will not have a significant influence on the mass flow rate solution.

Cases with different negative discount rates are tested as shown in Figure 2-7(h). when the discount rate is -0.55%, the mass flow rate solution shows a two-step situation (situation 3 in Figure 2-2). When the discount rate is reduced to -5% or -10%, the two-step situation changes to a one-step situation (situation 4 in Figure 2-2), where the mass flow rate starts with 0 and recovers to the maximum. The lower the discount rate, the later the mass flow rate jumps from 0 to the maximum. Further calculation shows that the threshold discount rate is about -0.5713%: if the discount rate is higher than the threshold, the solution is two-step; otherwise, the solution is one-step.

Using parameters in Table 2-1 as a benchmark, different parameters are varied from 90% to 110%, respectively, and their impacts on the optimal profit are shown in Figure 2-8.

The parameters are distinctly separated into two groups: the optimal profit is highly sensitive to three parameters, including surrounding media temperature, efficiency, and compression cost, whereas the other three, reservoir mass, maximum mass flow rate, and contact conductance, barely show influences on the optimal profit. Among all tested parameters, surrounding media temperature has the most significant influence on the optimal profit, and contact conductance has the least.

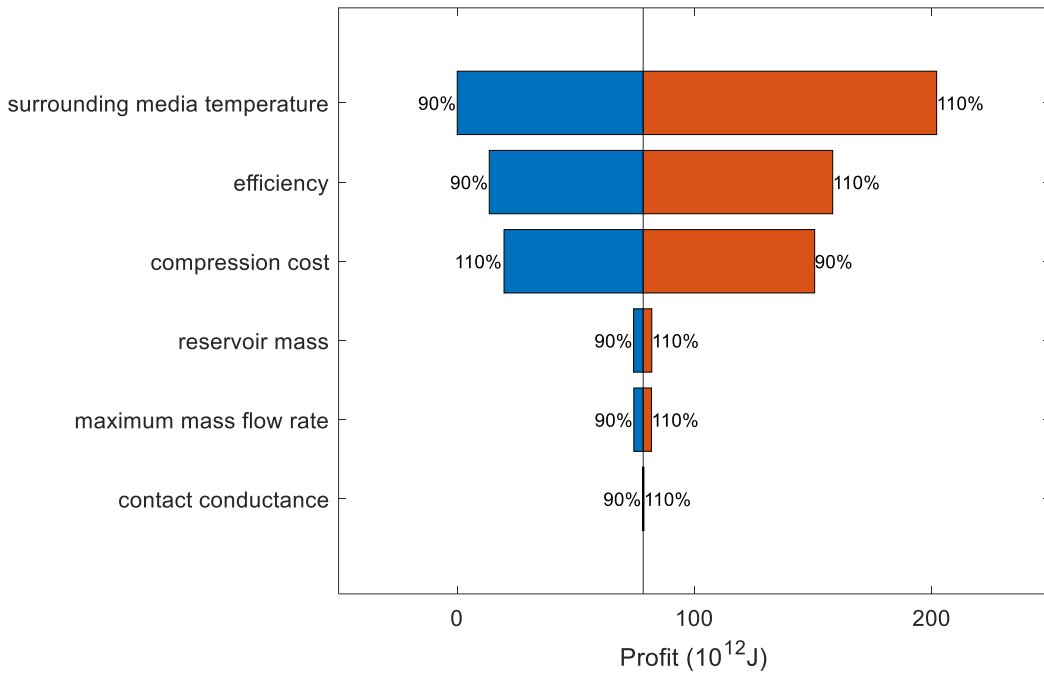


Figure 2-8: Sensitivity analysis of different techno-economic parameters on the optimal profit

Under a constant surface temperature, the surrounding media temperature is decided by the depth and the thermal gradient. The following case studies compare the optimal

profits of using CO₂ and water as the working fluid, under different depths and thermal gradients, with a surface temperature set as 15°C.

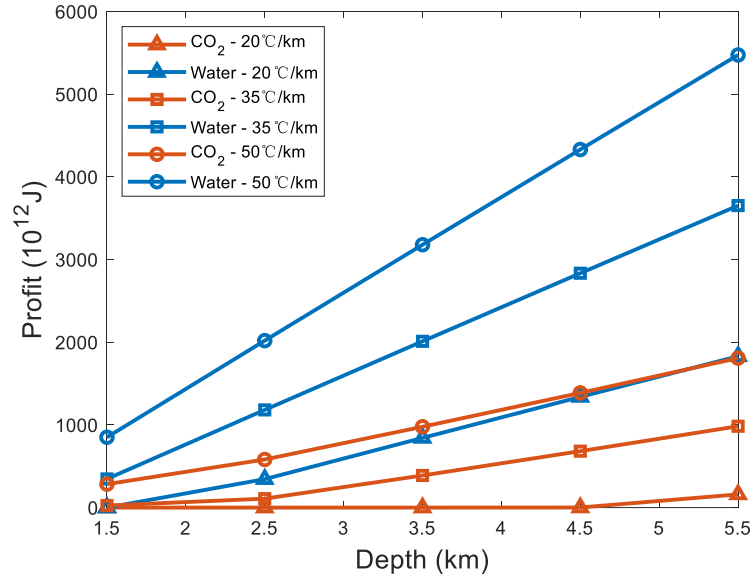


Figure 2-9: Profits of Using CO₂ and Water as the Working Fluid Under Different Depths and Thermal Gradients (Thermosiphon effect is not considered)

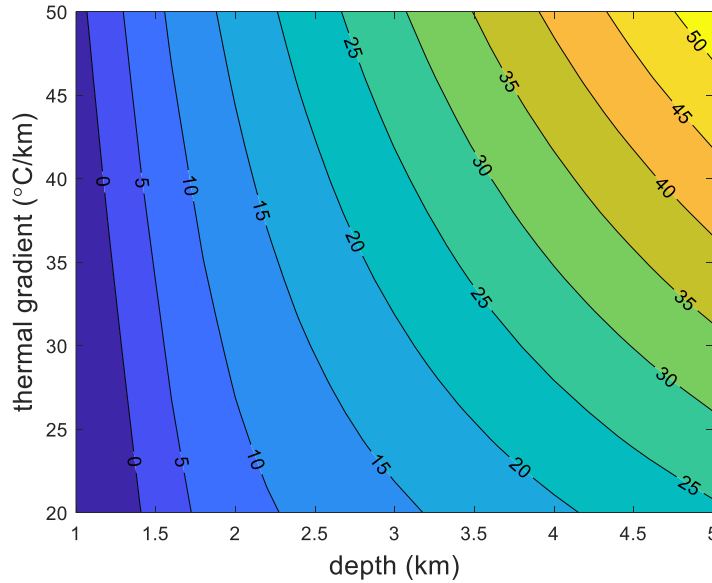


Figure 2-10: Minimum Required Thermosiphon Effect (J/g) for CO₂ to Be Same Profitable as Water.

The density of CO₂ is highly sensitive to temperature change, which results in a buoyancy-driven convection between the reservoir and wellheads, i.e., the thermosiphon effect. Such an effect can reduce or even eliminate the pumping energy needs. In contrast, since the density of water is almost constant with the fluid phase, its thermosiphon effect is negligible. In Figure 2-9, where the thermosiphon effect is not considered, using water as the working fluid can make more profits than using CO₂ under almost all situations of different combinations of depths and thermal gradients. However, the thermosiphon effect of CO₂ can possibly make CO₂ profit-competitive with water. Figure 2-10 shows the minimum thermosiphon effect required for CO₂ as the working fluid to make the same profit as water. When the depth is 5 km and the thermal gradient is 50 °C/km, the required thermosiphon effect is higher than 50 J/g. As the depth becomes shallower and the thermal gradient becomes smaller, CO₂ needs less thermosiphon energy to be the same profitable as water. In some cases where depth < 1.5km, even no thermosiphon energy is needed. In addition, the deeper the depth is, the more sensitive the required thermosiphon energy is to the thermal gradient. For example, when the depth is 2 km, the required thermosiphon energy ranges within 5-15 J/g for different thermal gradients, and that range is much larger (15-45 J/g) under a 4 km depth.

2.5. Conclusions

In this study, we formulated the optimal geothermal heat mining problem as an optimal control model, which is solved by a proposed analytical algorithm. Economic explanations are further developed to address the problem with infinite horizons and the

relationship with those under finite horizons. Cases with varying parameters are studied, and the main conclusions are listed as follows:

- 1) Solutions to the OGHM problem can be categorized into four situations. In situation 1, the mass flow rate keeps the maximum; In situation 2, the mass flow rate keeps as 0; In situation 3, the mass flow rate starts as the maximum, decreases to a constant value, and finally recovers to the maximum; In situation 4, the mass flow rate starts as 0, and changes to the maximum.
- 2) For the cases that have positive optimal profits, the solutions of finite-time OGHM problems can be considered as a combination of the solution of the infinite-time problem and one final stage with a maximum mass flow rate.
- 3) Surrounding media temperature, efficiency, and compression cost have significant influences on the optimal profit, and surrounding media temperature has the most.
- 4) Compared with water geothermal systems, CO₂ geothermal systems performs better for shallow, low-grade heat sources due to less requirement for the thermosiphon effect.

Chapter 3. Pathways of Methane Control to Address Climate Change

3.1. Introduction

Climate change is a result of human activities that emit carbon dioxide (CO₂), methane (CH₄), and other greenhouse gases (GHGs) to the atmosphere, where they accumulate and alter the energy balance of the earth by contributing to the radiative forcing that increases surface temperatures (IPCC, 2023b). Most efforts to date focus on slowing, stopping, and reversing CO₂ emissions by switching fuels, increasing renewable utilization, implementing CO₂ capture with geologic CO₂ storage (CCS), and deploying direct air CO₂ capture (DACC) and bioenergy with CCS (BECCS) (Boucher et al., 2014; Fawzy et al., 2020; Minx et al., 2018). The emphasis on CO₂ is understandable because it accounts for 64% (2.170 W/m²) of the total radiative forcing in the atmosphere (NOAA, 2023), and modern economies are organized around fuels and processes that produce CO₂ as a byproduct of using them. Yet while there is ~210x less CH₄ in the atmosphere than CO₂ (~1.8 ppm vs. ~420 ppm) (USEPA, 2021), addressing CH₄ should be a high priority as well: (a) since the beginning of the Industrial Revolution, the amount of CH₄ in the atmosphere has increased faster than the amount of CO₂ (~2.5x vs. ~1.5x) (USEPA, 2021); (b) CH₄ has radiative efficiency that is an order of magnitude greater than CO₂ (Myhre et al., 2013), (c) CH₄ presently contributes ~0.65 W/m² of radiative forcing (NOAA, 2023); (d) unlike with CO₂, there are worrisome temperature-driven positive

feedbacks that release CH₄ to the atmosphere (e.g., from permafrost, hydrates, clathrates) as temperatures increase (Cheng & Redfern, 2022; Dean et al., 2018; Matthews & Fung, 1987); and (e) the broad reliance on natural gas – the primary component of which is CH₄ – in energy and industrial systems is difficult to change (Ritchie et al., 2023b). While CH₄ control may not appear to be as important as addressing CO₂ because it has a shorter average lifetime in the atmosphere than CO₂ (~10 years vs. ~100 years), the concentration of CH₄ in the atmosphere is accelerating faster than that of CO₂ (UNEP & CCAC, 2021), and concern about CH₄ will likely increase as, (i) natural gas continues to displace coal in electricity generating systems (Ritchie et al., 2023a), and (ii) natural gas continues to be relied upon for heating (~40% of the primary energy for building heating) (IEA, 2023) with (iii) infrastructure that leaks fugitive CH₄ (Brandt et al., 2014; Weller et al., 2020); (iv) assets and geopolitical influences embedding natural gas (Osička & Černoch, 2022; Szabo, 2022); and (v) increasing meat production and associated CH₄ emissions from ruminants are contributing more CH₄ to the atmosphere (Ritchie et al., 2023c). Altogether, immediate near-term action to control the accumulation of CH₄ in the atmosphere could rapidly reduce the pace of global climate change.

A portfolio approach is urgently needed to slow, stop, and reverse the emissions of CH₄ to the atmosphere. While there are some early actions, such as the proposed CH₄ rules from the Biden Administration (The White House, 2021) followed by a \$350M grant (USEPA, 2023) and a Waste Emissions Charge (USEPA, 2024) for CH₄ emission reduction in oil and gas sector, there is relatively scant attention to addressing CH₄ emissions – especially with respect to the understanding that it will be essential to remove

GHGs from the atmosphere in order to have a chance at stabilizing climate change at levels that preserve the environmental envelope in which societies evolved and to which they are adapted (J. Forster et al., 2020; Waller et al., 2020). Some studies have focused on assessing the potentials and costs of CH₄ emissions abatement and begun to incorporate those assessments into integrated assessment models for scenario-based simulations (Harmsen et al., 2019; Höglund-Isaksson et al., 2020; Lucas et al., 2007; Staniaszek et al., 2022). But CH₄ removal, especially from the atmosphere, has hardly been considered in those scenario-based simulations. While there is debate on the viability of atmospheric CH₄ removal, the possibility is receiving attention as one of potential options for CH₄ control (Jackson et al., 2019, 2020; Lackner, 2020; Nisbet-Jones et al., 2022). Some potentially viable CH₄ removal technologies have been proposed (Abernethy et al., 2023; Jackson et al., 2021), including biological (Majdinasab & Yuan, 2017), heat-based (Brenneis et al., 2022), and light-based (Chen et al., 2016) approaches. Nevertheless, CH₄ removal approaches will be more difficult to realize than existing CO₂ abatement methods. Almost a generation elapsed between DAC being proposed and the first industrial-scale facility (IEA, 2020; Keith et al., 2006; Lackner et al., 1999; Sanz-Pérez et al., 2016), and the chemistry of removing CH₄ from dilute gasses is more complicated and less certain than for removing CO₂. As such, while there is some emerging research on specific approaches to separate CH₄ from dilute gas streams (Hu, May, et al., 2022; Hu, Zhao, et al., 2022), it will likely take longer to research, develop, and demonstrate CH₄ removal at the time where the effects of its increasing presence in the atmosphere are accelerating.

There are three main options to address the GHG pre-cursors to climate change: mitigation to avoid emissions, removal of what is in the atmosphere, and solar radiation management (SRM) to reduce the amount of energy from the sun that reaches the Earth's surface (Drake et al., 2021). Setting aside SRM because of its ethical conundrums (Preston, 2017; Svoboda & Irvine, 2014), this paper develops the *Model for Optimization of Methane Emissions and removal with Negative Technologies Under climate Mitigation (MOMENTUM)* to investigate pathways for CH₄ control. These pathways depend on the radiative forcing of all GHGs in the atmosphere, and thus the model incorporates trajectories for CO₂ and other emissions over several scenarios (Byers et al., 2022) in order to determine when society needs to mitigate or remove CH₄ emissions.

3.2. The *MOMENTUM* for Optimal CH₄ Control

The goal of the *MOMENTUM* is to provide insights for CH₄ control, particularly in the context of CH₄ atmospheric removal, through effective quantitative calculations. The *MOMENTUM* contains a climate model and a technology model (Figure 3-1) that are linked by two decision variables that determine the amount of CH₄ emissions to (1) mitigate or (2) remove each year. The objective function minimizes the total discounted cost each year, which is formulated from cost parameters in marginal cost curves for CH₄ mitigation and learning curves for CH₄ removal.

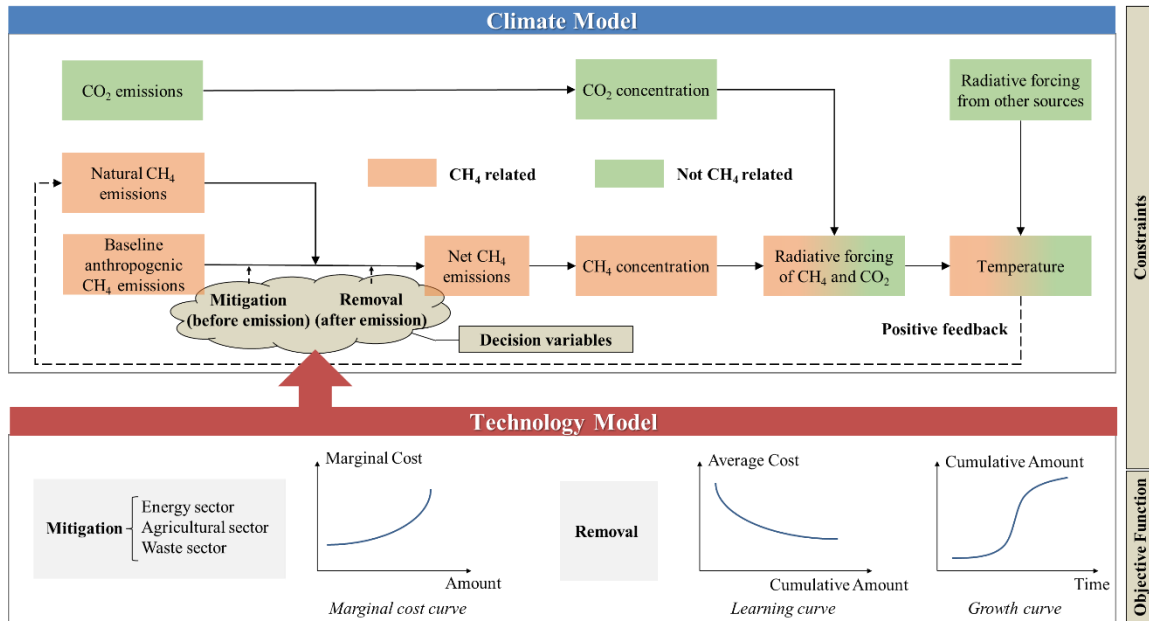


Figure 3-1: The Model for Optimization of Methane Emissions and removal with Negative Technologies Under Climate Mitigation (MOMENTUM) for Methane Pathways

3.2.1. *MOMENTUM*: The Global Climate Component

The global climate component of the *MOMENTUM* incorporates two ways in which CH₄ is treated differently than CO₂: 1) mitigation and removal technologies can be deployed to control net CH₄ emissions; and 2) there is positive feedback from CH₄ emissions that increase global mean surface temperatures that lead to more CH₄ emissions. In contrast to how CH₄ is incorporated, CO₂ emissions control is assumed to be implicitly included in input trajectories for CO₂ emissions and there are no temperature-related feedbacks.

1) Emissions and Concentrations

The global climate component of the *MOMENTUM* uses CO₂ emissions and CH₄ emissions as inputs to determine their accumulation and concentrations in the atmosphere

and their resulting contributions to total radiative forcing. Other GHGs and constituents in the atmosphere add a small amount to the total radiative forcing (<10%), and are directly used (i.e., are not estimated from emissions) with the radiative forcing from CO₂ and CH₄ to estimate the global mean surface temperature.

The net amount of CH₄ emitted to the atmosphere [Mt/yr] at a point in time ($\dot{E}_{CH_4}(t)$) equals the sum of (a) the CH₄ emissions from anthropogenic sources without any control ($\dot{E}_{CH_4,a}(t)$) and (b) the CH₄ emissions from natural sources ($\dot{E}_{CH_4,n}(t)$), less (c) the CH₄ emissions that would be emitted but are instead mitigated ($\dot{E}_M(t)$) and (d) removal of accumulated emissions from the atmosphere ($\dot{E}_R(t)$):

$$\dot{E}_{CH_4}(t) = \dot{E}_{CH_4,a}(t) + \dot{E}_{CH_4,n}(t) - \dot{E}_M(t) - \dot{E}_R(t) \quad (3-1)$$

Natural CH₄ emissions are assumed to be determined by the global mean surface temperature. For example, rising temperatures enhance archaeal CH₄ production in wetlands, which is one of the major sources of $\dot{E}_{CH_4,n}(t)$ (Dean et al., 2018). The relationship between $\dot{E}_{CH_4,n}(t)$ and global mean surface temperature [°C, relative to the mean between 1850 and 1900] is formulated as a Q_{10} relationship, which describes the exponential temperature sensitivity of CH₄-related chemical and biological processes (Delwiche et al., 2021; Mundim et al., 2020),

$$\dot{E}_{CH_4,n}(t) = \dot{E}_{CH_4,n,0} \times Q_{10}^{\frac{T(t)-T_{CH_4,n,0}}{10}} \quad (3-2)$$

where Q_{10} is 2.57 (Delwiche et al., 2021), $\dot{E}_{CH_4,n,0}$ is 215 Mt/yr (Saunois et al., 2020), $T_{CH_4,n,0}$ is 0.841 °C (Fyfe et al., 2021). These values for $\dot{E}_{CH_4,n,0}$ and $T_{CH_4,n,0}$ are the

averages between 2000 and 2009. The concentration of CH₄ in the atmosphere (Boucher et al., 2009) is

$$C_{CH_4}(t) = C_{CH_4}(t_0) + \frac{1}{2.85} \int_{t_0}^t \dot{E}_{CH_4}(\tau) \cdot IRF_{CH_4}(t - \tau) d\tau \quad (3-3)$$

where IRF_{CH_4} is the impulse response function of CH₄, which characterizes how an impulse of CH₄ emitted to the atmosphere decays over time, beginning at time t_0 . The integral in Equation (3-3) gives the increase of the mass of CH₄ in the atmosphere [Mt], which is converted to the increase in atmospheric concentration [ppb] by dividing by 2.85, which is the product of mass of the atmosphere (5.1480×10^{18} kg), and the molecular weight of CH₄ (16.04 g/mol) divided by the molecular weight of air (28.96 g/mol). With the average lifetime of CH₄ in the atmosphere as L_{CH_4} ,

$$IRF_{CH_4}(t) = e^{-\frac{t}{L_{CH_4}}} \quad (3-4)$$

Similarly, the concentration of CO₂ in the atmosphere (Joos et al., 2013) is,

$$C_{CO_2}(t) = C_{CO_2}(t_0) + \frac{1}{7.82} \int_{t_0}^t \dot{E}_{CO_2}(\tau) \cdot IRF_{CO_2}(t - \tau) d\tau \quad (3-5)$$

where

$$IRF_{CO_2}(t) = 0.2173 + 0.2240 \cdot e^{-\frac{t}{394.4}} + 0.2824 \cdot e^{-\frac{t}{36.54}} + 0.2763 \cdot e^{-\frac{t}{4.304}} \quad (3-6)$$

2) Radiative Forcing

The radiative forcing [W/m²] for CH₄ ($F_{CH_4}(t)$) is a subduplicate function of its concentration in the atmosphere, C_{CH_4} [ppb],

$$F_{CH_4}(t) = F_{CH_4}(t_0) + a_{CH_4}(\sqrt{C_{CH_4}(t)} - \sqrt{C_{CH_4}(t_0)}) \quad (3-7)$$

and the radiative forcing for CO₂ is a logarithmic function of its concentration,

$$F_{CO_2}(t) = F_{CO_2}(t_0) + a_{CO_2} \ln\left(\frac{C_{CO_2}(t)}{C_{CO_2}(t_0)}\right) \quad (3-8)$$

where a_{CH_4} is 0.038 W/m² and a_{CO_2} is 5.36 W/m² (Etminan et al., 2016). The total radiative forcing is the sum of $F_{CH_4}(t)$, $F_{CO_2}(t)$, and the radiative forcing of other constituents in the atmosphere ($F_{other}(t)$),

$$F(t) = F_{CH_4}(t) + F_{CO_2}(t) + F_{other}(t) \quad (3-9)$$

3) Temperature

Using a deep-layer energy balance model, the global mean surface temperature, $T(t)$, results from $F(t)$ (Drake et al., 2021; Geoffroy et al., 2013; Held et al., 2010), according to

$$T(t) = \frac{F(t)}{\beta + \gamma} + \frac{\gamma}{\beta} \int_{t_0}^t \frac{e^{-\frac{\tau-t}{\delta}}}{\delta} \frac{F(\tau)}{\beta + \gamma} d\tau \quad (3-10)$$

where $\beta = 1.13$ W/(m²K) is the climate feedback parameter, $\gamma = 0.73$ W/(m²K) is the ocean heat uptake rate, and $\delta = 240$ yr is a slow deep ocean timescale. Note that historical CH₄ emissions and total radiative forcing (i.e., before t_0) are considered in the calibration of the model. (See the details in Appendix A.1)

3.2.2. Technology Model

1) Methane Mitigation Technology Model

Marginal cost curves for CH₄ emissions mitigation in different sectors (e.g., energy, agriculture, waste) are based on data from the U.S. Environmental Protection Agency

(USEPA, 2019). These USEPA data embed considerations of technological change and provide comprehensive forecasts of CH₄ mitigation potentials and corresponding costs for each mitigation method and each country at five-year increments from 2015 to 2050. Directly using the cost-quantity pairs by countries and by technologies would require many discrete, step-like curves which cannot be simply expressed with a mathematical function. Accommodating these data directly would substantially increase the complexity of the Methane Mitigation Technology model. In keeping with the goal of an accurate yet parsimonious model, these forecasts are simplified to establish explicit and continuous marginal cost functions. To do so, the timescale, resolution, and baseline scenario are aligned to the IPCC AR6 data (Byers et al., 2022). We use data for approaches with marginal costs between $-\$500/\text{tCO}_2\text{e}$ and $\$500/\text{tCO}_2$ and, for consistency with the rest of the model, the years 2020 – 2050. These data account for 90% of the total data from the EPA dataset. Technological changes in cost reductions and efficiency improvements are embedded in the USEPA data (Figure 2a). Those discretized data are fitted with least-squares regression into two-term exponential functions for each sector, such that

$$c_M(\dot{E}_{M_{sect}}, t) = m_1(t)e^{n_1(t)\dot{E}_{M_{sect}}(t)} + m_2(t)e^{n_2(t)\dot{E}_{M_{sect}}(t)} \quad (3-11)$$

where c_M is the marginal cost of CH₄ mitigation, $\dot{E}_{M_{sect}}$ is the mitigation capacity for a sector, and m_1 , m_2 , n_1 , and n_2 are coefficients that are estimated by the regression. To incorporate the structural characteristics of the marginal costs for each sector without influence from the maximum capacities that are outliers, the marginal cost curves for each sector are normalized by changing the absolute mitigation capacity into percentages of the maximum potentials. To do so, we implement compression transformations so that

the maximum capacity is normalized to 100%. These transformations reveal other minor but important structural impact factors beyond cost reduction and efficiency improvement that affect the cost curves. To align the timescale and resolution with our model, the marginal cost curves are then linearly interpolated and extrapolated along the temporal dimension. Figure 3-2 provides an example of this process for the energy sector.

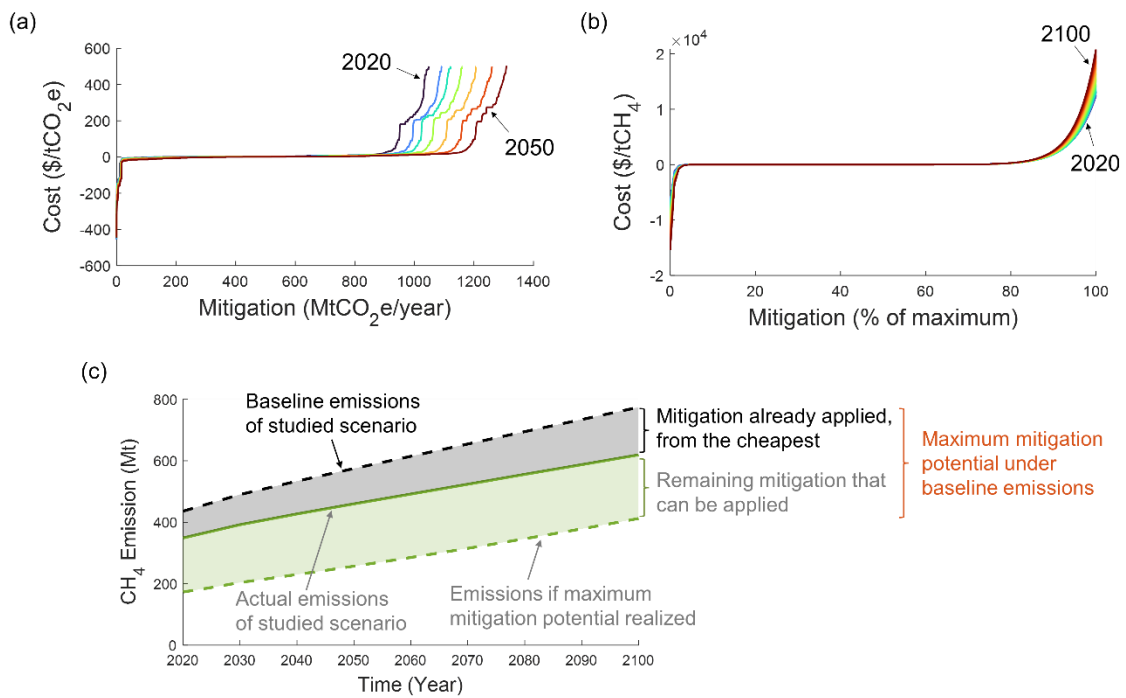


Figure 3-2: Example Alignment from the Energy Sector. (a) Marginal Cost Curves for CH₄ Mitigation Technologies, every five years from year 2020 to year 2050 (USEPA, 2019). (b) Alignment of the Marginal Cost Curves in (a) after harmonizing them. (c) Alignment of Maximum Mitigation Potentials for Non-Baseline Emissions.

The maximum mitigation potentials, as percentages of baseline CH₄ emissions in the USEPA data, are also linearly interpolated or extrapolated along the temporal dimension. The baseline here refers to the Business-As-Usual (BAU) conditions, where scenarios with emission rates are consistent with historical levels and do not include policy changes. For baseline emissions of other scenarios from the AR6 data for the SSPs, the percentage-based maximum mitigation potentials for each sector are assumed to be the same as those in the USEPA data. For non-baseline emissions (Figure 3-2c), we consider the differences from baseline emissions to be mitigation efforts that have already been applied. The assumption is that the cheapest approaches are implemented until their individual capacity is exhausted before more expensive approaches are implemented. The mitigation potential that has not been used is incorporated into decision variables in the model.

2) Methane Removal Technology Model

Given the nascent development of CH₄ removal approaches, a logarithmic learning curve, or experience curve, and sigmoid growth curve are employed to describe future development of CH₄ removal technologies. These mathematical representations are typically applied to projections of learning and diffusion for emerging technologies (Lackner & Azarabadi, 2021; Rogers, 2003; van der Kam et al., 2018; van der Zwaan & Rabl, 2003). The cost of CH₄ removal technologies is

$$c_R = c_{R_0} \left[\frac{\dot{E}_R}{\dot{E}_{R,0}} \right]^{\log_2(1-l_R)} \quad (3-12)$$

where c_R [\$/tCH₄] is the average cost of CH₄ removal at removal ability R , $\dot{E}_{R,0}$ [Mt/yr] is the initial CH₄ removal ability at $t = 0$, and l_R [%] is the learning rate of the CH₄ removal technology. The growth of the deployment of CH₄ removal technology is

$$\dot{E}_R(t) = \frac{\dot{E}_{R,max}}{1 + e^{-g_{\dot{E}_R,max}(t-t_{mid})}} \quad (3-13)$$

where $\dot{E}_{R,max}$ [Mt/yr] is the maximum removal potential, $g_{\dot{E}_R,max}$ [%] is the maximum relative growth rate, and t_{mid} [yr] is the time when the removal ability reaches half of the maximum of the removal potential. The growth rate [%/yr] of the removal, $g_{\dot{E}_R}(t)$, is

$$g_{\dot{E}_R}(t) = \frac{d\dot{E}_R(t)}{dt} \frac{1}{\dot{E}_R(t)} = \frac{g_{\dot{E}_R,max}}{1 + e^{g_{\dot{E}_R,max}(t-t_{mid})}} \quad (3-14)$$

It can be deduced that $\dot{E}_R(t)$ and $g_{\dot{E}_R}(t)$ are linearly correlated by

$$g_{\dot{E}_R}(t) = -\frac{g_{\dot{E}_R,max}}{\dot{E}_{R,max}} \dot{E}_R(t) + g_{\dot{E}_R,max} \quad (3-15)$$

As the initial expression of the sigmoid growth rate, Equation (3-13) is non-convex and is thus more likely to result in a locally optimal solution. As a result, the *MOMENTUM* uses Equation (3-15), which is a linear equivalent of Equation (3-13). Moreover, considering that the growth curve is likely to not strictly follow the sigmoid pattern, the relative growth rate defined by (3-15) is set as the maximum relative growth rate and (3-15) is relaxed into

$$0 \leq g_{\dot{E}_R}(t) \leq -\frac{g_{\dot{E}_R,max}}{\dot{E}_{R,max}} \dot{E}_R(t) + g_{\dot{E}_R,max} \quad (3-16)$$

3.2.3. Optimization Model

The objective function is minimizing the total discounted cost of CH₄ mitigation and removal,

$$\min Cost = \sum_t \left[\sum_{sect} c_M(\dot{E}_{M_{sect}}(t), t) + c_R(\dot{E}_R(t)) \right] (1 + \rho)^{-t} \quad (3-17)$$

The constraints are defined by other relationships in the climate model and the technology model, with an additional climate goal given as

$$T(t_{end}) \leq T_{goal} \quad (3-18)$$

The optimization model is implemented in MATLAB 2021b using the optimization toolbox YALMIP (Lofberg, 2004) and optimization solver IPOPT (Bertolazzi, 2022; Wächter & Biegler, 2006).

3.2.4. Scenarios

Five representative shared socioeconomic pathways (SSPs) are used with the *MOMENTUM* to study optimal pathways for CH₄ control: SSP1-1.9, SSP1-2.6, SSP2-4.5, SSP3-7.0, and SSP5-8.5. The SSPs are global scenarios that have become a standard for integrated assessment modeling to determine pathways for mitigating global climate change (O'Neill et al., 2020). The SSPs are based on alternative future worlds with different narratives (e.g., SSP1) describing alternative socio-economic developments, followed by a value of nameplate radiative forcing (e.g., 1.9 W/m²) that is possible to reach by 2100 under the narrative (Riahi et al., 2017). Since SSP1-1.9, SSP1-2.6, and SSP2-4.5 are not baseline scenarios, the baseline scenarios (which describe future developments in the absence of new climate policies) of SSP1 and SSP2 are also

considered. Data for the climate model are from IPCC AR6 dataset (Byers et al., 2022), and data for CH₄ mitigation technology model are based on USEPA data (as described in Section 3.2.2). Baseline parameters for CH₄ removal technology model are shown in Table 3-1.

Table 3-1: Baseline Parameters for CH₄ Removal Approaches

Initial CH ₄ Removal Ability	Maximum CH ₄ Removal Potential	Maximum CH ₄ Removal Growth Rate	Initial CH ₄ Removal Cost	CH ₄ Removal Learning Rate
0.01Mt/yr	200Mt/yr	30%	\$30k/t	20%

Table 3-2: Summary of Shared Socioeconomic Pathway (SSP) Scenarios Used in This Study

	Challenges for Mitigation / Adaptation (O’Neill et al., 2017)	Radiative Forcing in 2100 (W/m ²)	Temperature in 2100 above Pre-Industrial in 2100(°C) [range], climate goal
SSP1	Low/Low	1.9	[1.03, 1.34], 1.2
		2.6	[1.42, 1.71], 1.5
SSP2	Intermediate/Intermediate	4.5	[2.38, 2.63], 2.5
SSP3	High/High	7.0	[3.76, 4.07], 3.9
SSP5	High/Low	8.5	[4.52, 4.84], 4.7

For each SSP scenario, a specific climate goal is input into the *MOMENTUM* to determine the optimal CH₄ mitigation and CH₄ removal pathways. These climate goals are more stringent, in terms of lower global mean surface temperatures, than the

representative SSP scenarios and are based on a range of possible temperatures in 2100 – from no CH₄ control to full CH₄ control.

Table 3-2 summarizes the SSP scenarios used in this study, where the possible ranges of temperature above the pre-industrial in 2100 are simulated under baseline parameters of CH₄ mitigation and removal.

3.3. Results

3.3.1. Optimal CH₄ Control Costs and Pathways for Several Shared Socioeconomic Pathways

Figure 3-3 contains the results for CH₄ emissions mitigation and CH₄ emissions removal for specific climate goals in each SSP scenario.

For SSP1-1.9 and SSP1-2.6, where the climate goals are respectively 1.2°C and 1.5°C above pre-industrial temperatures, the optimal CH₄ control strategies are similar. The results in Figure 3-3(a - d) show a small amount of CH₄ emissions mitigation occurs early in the timeframe (2020-2030). A small amount of CH₄ removal begins around the middle of the century and increases substantially around 2075. Of the total amount of CH₄ control, less than 20% relies on CH₄ emissions mitigation, whereas the rest (>80%) relies on CH₄ emissions removal. Further, the cost of CH₄ emissions mitigation in each sector are negative and small (~-0.1T\$), whereas the total cost of CH₄ removal is enormous (~\$3T/~\$5T).

There is more CH₄ mitigation potential in SSP2-4.5 than in SSP1-1.9 and SSP1-2.6 because it has more allowable emissions which leads to a higher temperature. The results in Figure 3-3(e-f) show that CH₄ emissions mitigation accounts for ~30% of the total CH₄ control. The CH₄ mitigation costs in the agricultural and waste sectors are negative, but

the CH₄ mitigation costs in the energy sector are positive and total CH₄ mitigation cost is much smaller than that of CH₄ removal (<\$0.1T vs. ~\$3.3T). In addition to CH₄ mitigation beginning early (2020-2030), some CH₄ mitigation is also deployed along with CH₄ removal in the later years (around 2085).

The SSP3-7.0 scenario is the baseline scenario for SSP3, with the climate goal set to 3.9°C above pre-industrial temperatures. As the baseline SSP3 scenario with a high climate goal, a discontinuity in total CH₄ mitigation cost becomes apparent around the year 2030 because the marginal abatement cost curves of the agriculture sector in the U.S. EPA dataset have a distinct difference before and after 2030. Figure 3-3(g-h) show that the large amount of CH₄ mitigation potential keeps total costs negative until around 2085 – which suggests that it is economically beneficial to mitigate CH₄ emissions under the baseline conditions for SSP3 – until a few years after CH₄ removal substantially accelerates, which occurs around 2080. In Figure 3-3(i-j) for the least stringent climate goal (4.7°C) we investigate (SSP5-8.5), mitigation is the primary means for CH₄ control, although CH₄ removal begins to accelerate around the year 2080. Initial CH₄ emissions stabilize during 2050-2070 and start to decrease after 2070, mainly due to a peak and subsequent reduction in population and demand for food (Kriegler et al., 2017; Riahi et al., 2017).

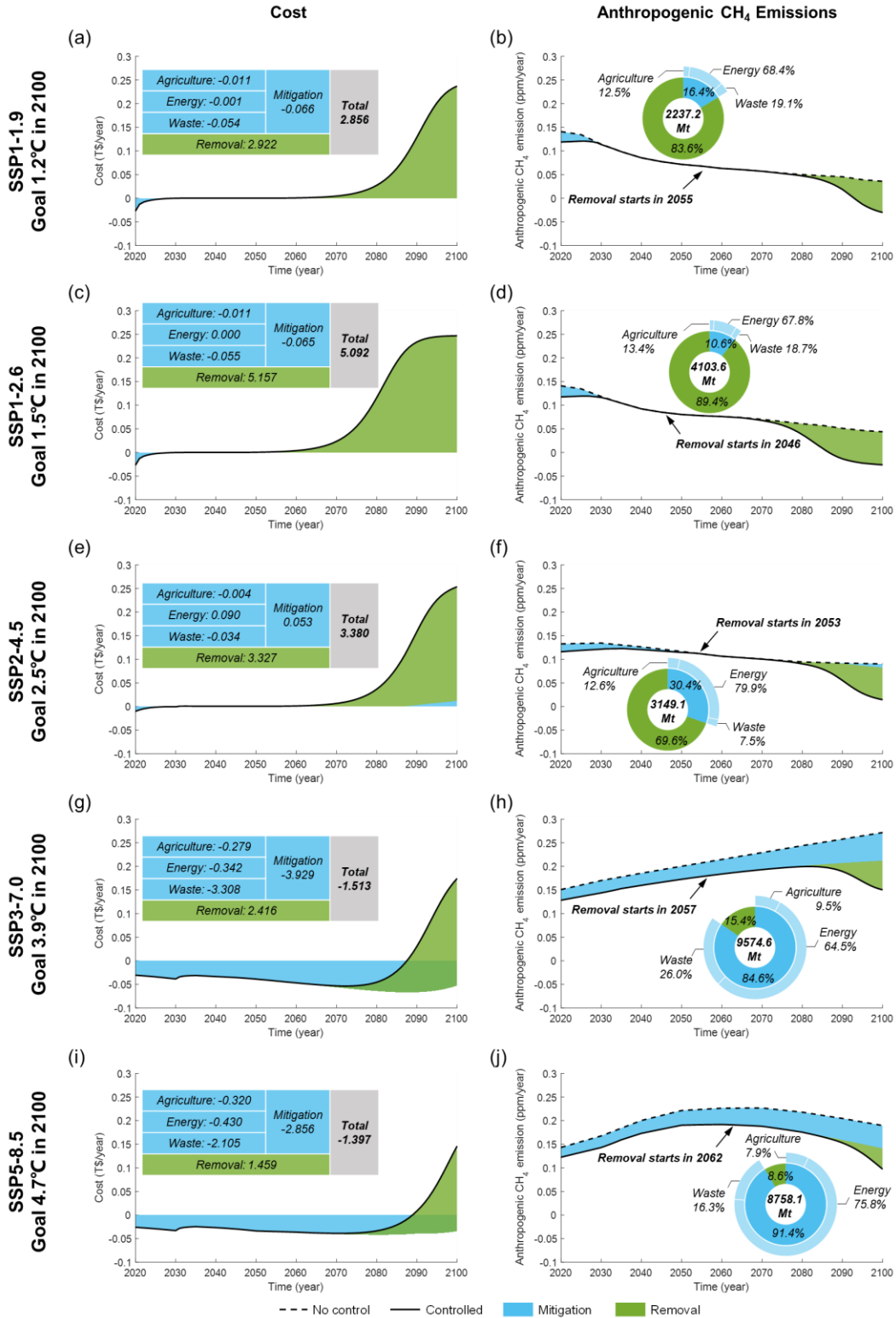


Figure 3-3: Optimal CH₄ Control Costs and Pathways for Several Shared Socioeconomic Pathways (SSPs) and Global Mean Surface Temperature Goals in 2100.

There are some notable trends across the five SSPs and their climate goals. Methane removal begins at small levels around the middle of the century, yet in the SSPs that have more mitigation potential, CH₄ mitigation accounts for more of the total CH₄ control (e.g., 16.4% in SSP1-1.9 vs. 91.4% in SSP5-8.5) and CH₄ removal is less relied upon and tends to start later in time (e.g., 2055 in SSP1-1.9 vs. 2062 in SSP5-8.5). While the results from SSP1-1.9 and SSP1-2.6 do not strictly follow this trend (e.g., SSP1-2.6 has more CH₄ mitigation potential but less CH₄ mitigation), the 1.5°C climate goal for SSP1-2.6, which was chosen to be consistent with the 2016 Paris Agreement (UNFCCC, 2015), is more demanding than the 1.2°C goal for SSP1-1.9. That is, the difference in radiative forcing for the same SSP makes it more difficult to achieve a 1.5°C goal with radiative forcing consistent with RCP 2.6 than a 1.2°C climate goal consistent with RCP 1.9. Finally, for all SSPs, the energy sector consistently has the most CH₄ mitigation while the waste sector consistently has the cheapest CH₄ mitigation. These results suggest that, from a societal standpoint, the energy sector must be prioritized for CH₄ emission reductions and the waste sector can offset total costs.

3.3.2. Sensitivity of Climate Goals in 2100 by Shared Socioeconomic Pathway

The results in Figure 3-3 are for the subsets of the climate goals that are achievable for each SSP. Figure 3-4 provides an overview of the results of five representative SSPs under the full range of achievable climate goals in 2100. Within these ranges for each SSP, the maximum is the “business as usual” pathway and is the same as the initial SSP with no additional CH₄ control. The minimum represents the case where all the

mitigation and removal potential are applied and any climate goal under this value is unrealizable.

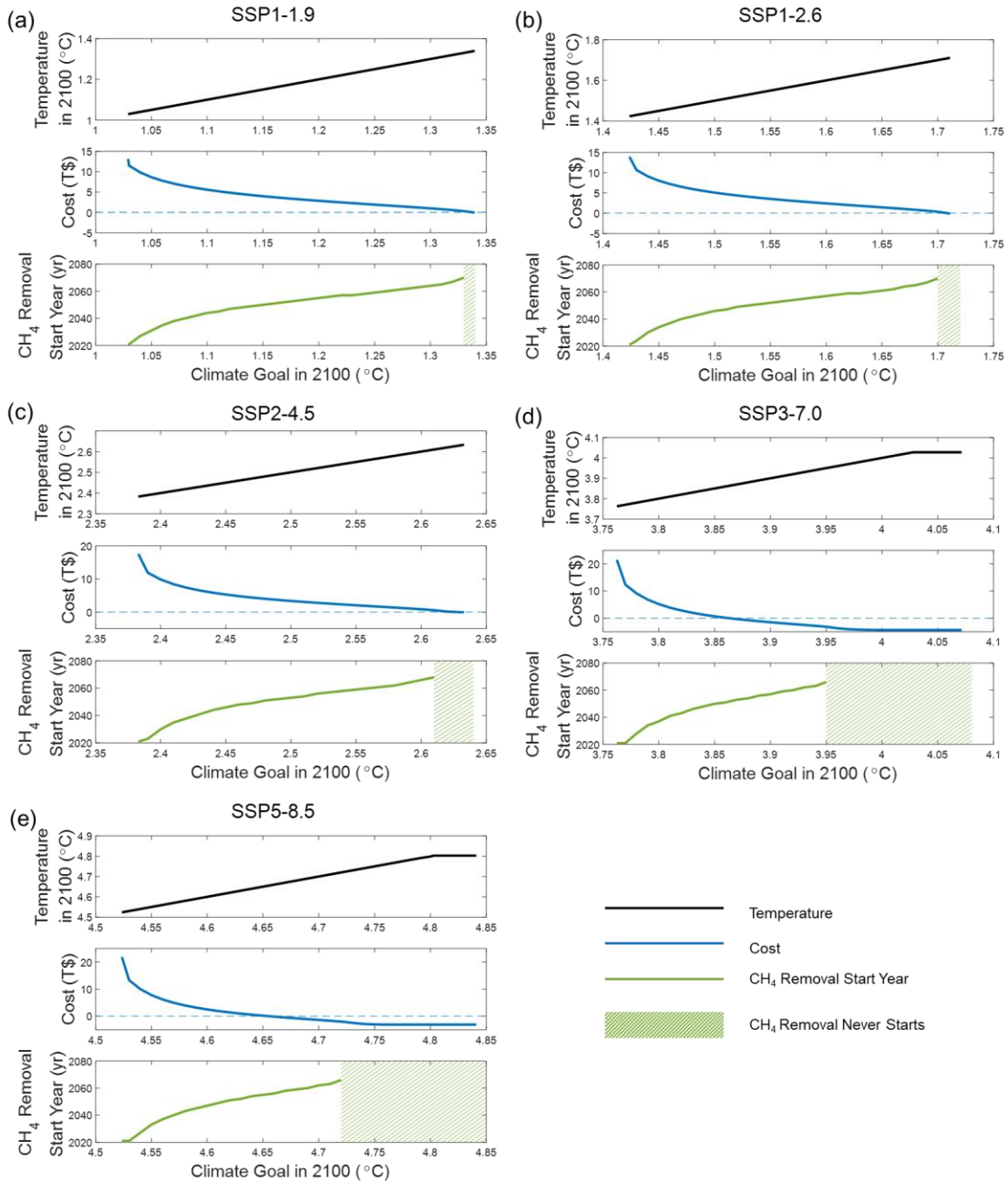


Figure 3-4: Sensitivity Analysis of Climate Goals in 2100 for Five Representative SSPs

As shown in the top subplots for each panel (black curves) for each SSP, the temperature in 2100 after the optimal CH₄ control is not necessarily same as the climate goal. This difference is clear for SSP3-7.0 and SSP5-8.5. As the climate goal increases, the temperature in 2100 initially equals the climate goal until at some point that the temperature plateaus. This result occurs because the mitigation approaches with negative costs are economically beneficial and will be applied, and the temperature in 2100 with all the negative-cost mitigation approaches may thus be lower than the climate goal. For instance, the plateau for SSP3-7.0 occurs around a climate goal of 4.03°C, where all the negative-cost mitigation approaches are the only mitigation approaches that are applied. If the temperature in 2100 is forced to be higher than 4.03°C, less mitigation approaches with negative costs will be applied and the overall cost will be higher. As a result, climate goals higher than 4.03°C in SSP3-7.0 will not have a real influence on the results. This phenomenon is not apparent for the SSP1 and SSP2 scenarios due to the limited mitigation potentials that are available. The middle subplots (blue curves) show the total cost for each SSP as a function of the climate goal in 2100. Across the SSPs, the slope of the curve is higher with more stringent climate goals (i.e., lower temperatures in 2100) it is more and more costly to achieve per unit of climate goal. For the SSP1 and SSP2 scenarios, the costs under almost all the achievable climate goals are positive, whereas for SSP3-7.0 and SSP5-8.5 a range of climate goals are achievable with negative costs because of the larger availability of mitigation potential. The bottom subplots (green curves) for each SSP show when CH₄ removal should start. When CH₄ removal begins earlier, there is more total CH₄ removal and a lower climate goal can be achieved. For all

SSPs, to reach the most ambitious climate goal, the removal must start immediately at the beginning of the simulation period (i.e., year 2020). The CH₄ removal begins later as the climate goal increases, but never after the year 2070. In these situations, for high climate goals, the ability to remove CH₄ stays consistent at the initial baseline amount of 0.01 MtCH₄/yr. CH₄ removal never begins to exceed the baseline level after 2080 because it is too late to develop CH₄ removal technology; there is insufficient time before 2100 to scale CH₄ removal to the point where the high average CH₄ removal cost decreases enough for it to be cost-effective to rely on CH₄ removal. Additionally, the range of climate goals in which CH₄ removal never occurs widens from SSP1-1.9 to SSP5-8.5, because almost all the CH₄ control is realized by mitigation and latter SSPs (e.g., SSP5-8.5) have more mitigation potential (especially those with negative costs).

3.3.3. Dependence of Total Cost of CH₄ Control on Several Key Parameters

Figure 3-5 shows the results of sensitivity analyses of the total cost of CH₄ control on six important parameters for CH₄ removal: (1) *initial CH₄ removal cost* vs. (2) *maximum CH₄ removal potential*; (3) *CH₄ removal learning rate* vs. (4) *maximum CH₄ removal growth rate*; and (5) *CH₄ mitigation cost* vs. (6) *maximum CH₄ mitigation potential*. For each of these six parameters, five values are used in the sensitivity analysis. The values for each parameter are indicated on the axes of each panel in Figure 3-5 (e.g., Figure 3-5a(i) shows the values considered for *initial CH₄ removal cost* are \$3k, \$10k, \$30k, \$100k, and \$300k/tCH₄ and the values considered for *maximum CH₄ removal potential* are 50, 100, 200, 300, and 400 MtCH₄), and the middle value is the baseline that is presented in Section 3.2.2 (for CH₄ mitigation) or Table 3-1 (for CH₄ removal).

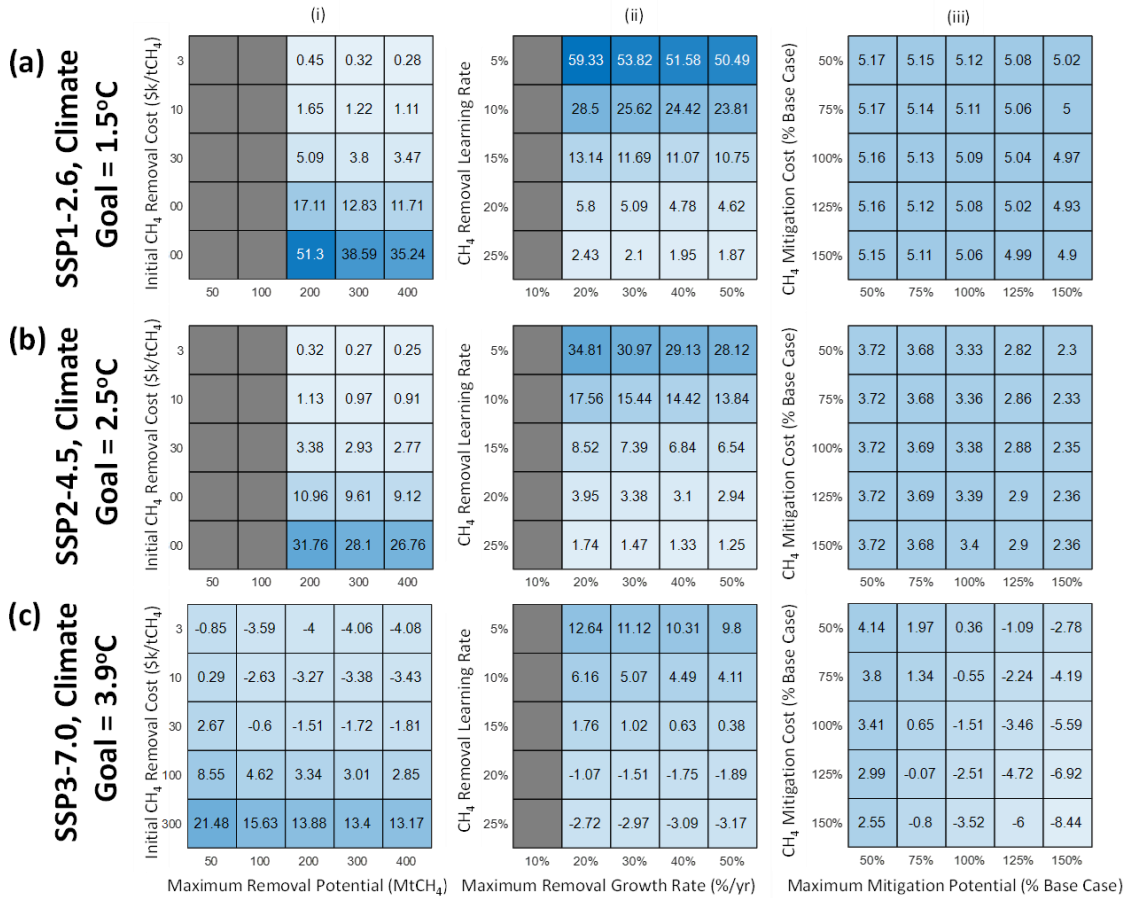


Figure 3-5: Sensitivity of Total Cost of CH₄ Control to Important Parameters. (i) Initial CH₄ Removal Rate vs. Maximum CH₄ Removal Potential; (ii) CH₄ Removal Learning Rate vs. Maximum CH₄ Removal Growth Rate; (iii) CH₄ Mitigation Cost vs. Maximum CH₄ Mitigation Potential. Dark grey = no feasible solution.

In column (i) of Figure 3-5, the initial CH₄ removal cost influences the total cost of CH₄ control more than the maximum CH₄ removal potential. While the total cost of CH₄ control decreases with increases in maximum CH₄ removal potential, those differences are less than the increases in the total cost of CH₄ control with increases in the initial CH₄ removal cost. Throughout the results presented in column (i) of Figure 3-5, the total cost of CH₄ control approximately triples with an approximate tripling of the initial CH₄

removal cost, holding *maximum CH₄ removal potential* fixed. That is, the relationship between total cost is roughly linear. In contrast, when *maximum CH₄ removal potential* is halved, the total cost of CH₄ control increases between 5% and 46%, holding *initial CH₄ removal cost* constant. For the range of values for *maximum CH₄ removal potential* we consider in this sensitivity analysis, the total cost of CH₄ control tends to increase proportionally less than the decrease in *maximum CH₄ removal potential*. In addition, when the *maximum CH₄ removal potential* is low ($\leq 100\text{Mt/yr}$), or the *maximum CH₄ removal growth rate* is low ($\leq 10\%$), the results here suggest that the climate goal cannot be attained.

As with column (i), the results in column (ii) of Figure 3-5 show that *CH₄ removal learning rate* has more effect on the total cost of CH₄ control than the *maximum CH₄ removal growth rate*. In each panel corresponding to different SSP-RCP combinations and associated climate goals, the proportional changes in the total cost of CH₄ removal with differences in the *CH₄ removal learning rate* (the rows) are greater than with differences in *maximum CH₄ removal growth rate*.

Finally, while the cost and potential of CH₄ mitigation (respectively the y and x axes of the panels in column (iii) of Figure 3-5) both influence the total cost of CH₄ control, the variations of each key variable we investigate result in less total costs than the variations in the other key variables in columns (i) and (ii). The total cost of CH₄ control is more sensitive to the variations in *maximum CH₄ mitigation potential* we investigated than the variations in *CH₄ mitigation cost* we investigated, but these key variables exert less

overall influence on the total cost of CH₄ control than the other key parameters in columns (i) and (ii) of Figure 3-5.

3.3.4. Dependence of the Year CH₄ Removal Begins on Key Parameters

Table 3-3 provides a summary of the results of the sensitivity analyses for the year that CH₄ removal starts. The parameters and their values are the same as in Section 3.3.3.

(The full results are provided in Figure A-4.) For example, for SSP1-2.6 with a climate goal of 1.5°C, CH₄ removal starts in the year 2046 when (a) the *maximum CH₄ removal potential* is 200 MtCH₄/yr, regardless of the *initial cost of CH₄ removal* we investigate; (b) the *maximum CH₄ removal growth rate* is 30%/yr, regardless of the *CH₄ removal learning rate* we investigate; and (c) when the *maximum CH₄ mitigation potential* is 50 – 150% of the baseline value. In contrast, CH₄ removal starts later and with increasing variability as the climate goals are less stringent. For example, when the *maximum CH₄ removal potential* is 200 MtCH₄/yr, CH₄ removal starts between 2052 and 2054 in SSP2-4.5 with a climate goal of 2.5°C and between 2053 and 2063 in SSP3-7.0 with a climate goal of 3.9°C. Within each cell of the table when there is a range in the year in which CH₄ removal begins, this removal begins later when the *initial cost of CH₄ removal* is costlier, the *CH₄ removal learning rate* is higher, and the *CH₄ mitigation cost* is costlier. In general, the columns in Table 3-3 show that CH₄ removal begins later with increases in the *maximum CH₄ removal potential*, the *maximum CH₄ removal growth rate*, and the *maximum CH₄ mitigation potential*. Aside from the case with the lowest *maximum CH₄ removal potential* in the SSP with the highest amount of radiative forcing and temperature increase (SSP3-7.0, 3.9°C, shown in Figure A-4), the results in Table 3-3

indicate that the year in which CH₄ removal starts is generally insensitive to the variations in, respectively, *initial CH₄ removal cost*, *CH₄ removal learning rate*, and *CH₄ mitigation cost*. That is, in each cell of Table 3-3 there is a narrow range of years in which CH₄ removal starts.

Table 3-3: Summary of Results for Start Year for CH₄ Removal Depending on Several Key Parameters.

In each cell, the results are for variations in another parameter: for *Maximum CH₄ Removal Potential* the *Initial CH₄ Removal Price* is varied from \$3k/tCH₄ to \$300k/tCH₄; for *Maximum CH₄ Removal Growth Rate* the *CH₄ Removal Learning Rate* is varied between 5% and 25%; for *Maximum CH₄ Mitigation Potential* the *CH₄ Mitigation Cost* is varied between 50% and 150% of the base case. Full results are provided in Figure A-4 in the Supplemental Information.

	Maximum CH ₄ Removal Potential (MtCH ₄ /yr) ^a			Maximum CH ₄ Removal Growth Rate Per Year ^b				Maximum CH ₄ Mitigation Potential (% of Baseline) ^c				
	200	300	400	20%	30%	40%	50%	50%	75%	100%	125%	150%
SSP1-2.6 Climate Goal = 1.5°C	2046	2053	2055	2028	2046	2055	2060	2046	2046	2046	2046	2046
SSP2-4.5 Climate Goal = 2.5°C	2052-2054	2056-2057	2057-2058	2035-2037	2053-2054	2062-2063	2067-2068	2052	2052	2053-2054	2055-2056	2057-2058
SSP3-7.0 Climate Goal = 3.9°C	2053-2062	2056-2062	2057-2063	2038-2047	2055-2062	2064-2070	2069-2075	2045-2048	2052-2054	2056-2059	2060-2064	2066-2069

^a When the Maximum CH₄ Removal Potential is 50 and 100MtCH₄/yr, there is no feasible solution for Initial CH₄ Removal Costs between \$3k/tCH₄ and \$300k/tCH₄.

^b When the Maximum CH₄ Removal Growth Rate is 10%, there is no feasible solution for CH₄ Removal Learning Rates of 5%, 10%, 15%, 20%, and 25%.

^c When Maximum CH₄ Mitigation Potential is 150% of the base case, CH₄ removal never occurs cost of 50%, 75%, and 100% of the base case.

3.4. Discussion and Conclusions

Among the substantial efforts that address the need to evolve energy systems and deploy approaches that slow, stop, and reverse the flow of greenhouse gases to the atmosphere, we are not aware of prior work that investigates the deployment CH₄ removal approaches at scale and how those approaches can work in tandem with CO₂ mitigation, CO₂ removal, and CH₄ mitigation approaches to achieve climate goals. The present work addresses this gap by developing and implementing the *MOMENTUM* with scenarios about the possible socioeconomic evolutions that are pertinent to addressing climate change. This work addresses questions around when CH₄ removal will be needed to be deployed at scale in order to minimize climate change. While this analysis is relatively agnostic to the technical approach for removing CH₄ from free air – the nature of which is challenging (Jackson et al., 2021) – the need to understand the necessary timing of the availability of these approaches is the point of departure for this investigation. The results show that developing and deploying these CH₄ removal technologies is essential, and we can provide several generalizable conclusions.

- 1) Negative-cost CH₄ mitigation options should be implemented, and the barriers to their implementation should be addressed. From a purely economic perspective, negative cost options such as adding propionate precursors to animal feed to reduce enteric CH₄ emissions, should be pursued for their ability to account for more than half of the negative-cost CH₄ mitigation potential in 2030 (USEPA, 2019). Yet absent local incentives to do so, it is unlikely that these strategies will be implemented. For example, livestock farmers would incur the added expense for a more global solution.

- As such support by policy to implement and share these techniques and other CH₄ mitigation techniques is essential.
- 2) Relying solely on mitigating CH₄ emissions is not feasible to meet climate goals; it is imperative that CH₄ removal technologies are developed and deployed at a substantial scale, and policy to stimulate these developments through the energy technology innovation spectrum (Gallagher et al., 2012) are needed. While CH₄ removal appears to be expensive, it is an important and substantial component of the cost-effective portfolios of options to achieve climate goals. Further, while it is common to consider costly interventions such as CH₄ removal to be “backstop technologies” to be employed late in time when other approaches have not yielded the scale of intervention that is needed, waiting increases costs and puts the ability to preserve the present environmental envelope at risk.
 - 3) The emergence of options for CH₄ removal will likely be similar to the emergence of other energy technologies, where approaches are identified and developed over time. Each option may have its own characteristics (NREL, 2024), such as efficiency and learning rate. In our results, *Initial CH₄ Removal Cost* and *CH₄ Removal Learning Rate* have more impact on the total cost of CH₄ control than the *Maximum CH₄ Removal Potential* or the *Maximum CH₄ Removal Growth Rate*. As a result, emphasis on research and development activities early in the energy technology innovation spectrum is important for their influences on the initial costs and learning rates of the approaches, yet these emphases should not come at the expense of demonstration and deployment efforts. These efforts later in the energy technology

- innovation spectrum affect the pace and scale of implementation and the degree to which CH₄ removal diffuses and costs decrease by technological learning.
- 4) If there is a desire to achieve ambitious climate goals with least cost, concerted efforts to develop CH₄ removal approaches need to be initiated decades in advance of the year 2075 so that they can be deployed and diffuse at industrial scale by the year 2075. Across the range of stringency of climate action as manifest in the combinations of Shared Socioeconomic Pathways, Representative Concentration Pathways, climate goals, and sensitivity analyses of key parameters we investigate, in our results CH₄ removal always begins by the year 2075. If CH₄ removal were deployed after 2075, total costs would be higher or the climate goal would need to be less stringent (i.e., higher temperature).
 - 5) The year when CH₄ removal needs to begin is influenced by scale-related parameters (e.g., *maximum CH₄ removal potential*, *maximum CH₄ removal growth rate*) much more than by cost-related parameters (e.g., *initial CH₄ removal cost*, *CH₄ mitigation cost*). As such, roadmaps for the development of CH₄ removal can be established with less focus on present and future costs and more focus on timelines for initiating research, development, and demonstration of the CH₄ removal approaches so that they can scale in time to contribute to the portfolio of efforts to minimize global climate change.
 - 6) Society has a vested interest in controlling CH₄ emissions. Across all the scenarios we investigate with the relevant climate goals, the average cost of CH₄ control we find is always below \$4,300/tCH₄ (See details in Figure A-5), which is the minimum

estimate of the social cost of CH₄ emissions (UNEP & CCAC, 2021). This indicates that, if we take the avoided social cost into consideration, all CH₄ control can be implemented with net benefits.

Chapter 4. Agent-Based Analysis for Methane Emission Control

4.1. Introduction

How to combat climate change has become one of the most essential and compelling topics globally, especially as we are unfortunately moving away from the 1.5°C climate goal appealed in the Paris Agreement (P. M. Forster et al., 2020; UNFCCC, 2015). Most approaches to studying climate change related issues can be categorized into two groups: system-based modeling (SBM) and agent-based modeling (ABM). SBM, as a top-down method, aggregates and abstracts the components in the system into representative parameters and variables, and uses equations to analyze the system as a whole. ABM, as a bottom-up method, involves individual agents, each with their own rules and behaviors, interacting within the environment, which can be used to explain and predict macro patterns of the system (Castro et al., 2020). Compared to SBM, ABM is more effective in capturing the heterogeneity of individual behaviors and local interactions, potentially revealing emergent phenomena that are difficult to realize from a system-level perspective (Crooks & Heppenstall, 2012; Van Dyke Parunak et al., 1998). Therefore, for climate-change topics involving policy and market dynamics, which involves individual decision-making and interactions, ABM holds a distinct advantage and has been widely applied in studies, such as emission reduction (Tang et al., 2015; Zhu et al., 2018),

technology diffusion (Al Irsyad et al., 2019; Kangur et al., 2017), and energy conservation (Moglia et al., 2018; Niamir et al., 2018).

One of the most famous market-based emission control approaches is the Emission Trading Scheme (ETS), also known as the cap-and-trade system. In the ETS, the participants are limited by an emission cap and are issued equivalent amount of emission allowances that can be traded. They cannot emit more than the emission allowances they hold, otherwise they will receive a penalty. Many studies have employed ABM to analyze the behaviors of participants in the ETS (Dong & Fan, 2023; Richstein et al., 2014; Tang et al., 2015, 2017; Wei et al., 2023; H. Zhang et al., 2017; Zhu et al., 2018). However, these studies often have at least one of the following limitations. The first one is only considering a single sector in the ETS system, such as the electricity sector. Since the ETS system involves participants from various sectors, focusing on one sector does not comprehensively reflect the ETS system. Secondly, only considering the dynamics in the ETS system, while barely considering those in the commodity/service markets related to the ETS system. However, participation in the ETS will change the income and expenses of the participants and potentially influence their decision-making in the commodity/service market.

The third limitation is that current ETSs primarily consider carbon dioxide (CO₂) emissions, which is understandable since CO₂ is the most important GHG. Nevertheless, methane (CH₄) emissions are also significant and should be controlled in a separate ETS. One of the main reasons is that CH₄ has a short atmospheric lifetime of approximately 10 years. This suggests that immediate action on CH₄ control could lead to a rapid decrease

in its concentration and an effective slowdown in global warming. Also, as a more powerful GHG than CO₂ (which is indicated by its CO_{2e}, 25), CH₄ is increasing faster than CO₂, and faster now than at any time since the 1980s. In addition, CH₄ plays a crucial role in the formation of ground-level ozone, which is detrimental to human health (UNEP & CCAC, 2021). As a conclusion, handling CH₄ separately in an ETS system could be more beneficial for better tackling climate change.

To address the aforementioned limitations, this study proposes an ABM-based model on CH₄ emission control, with considerations of both the emission market and commodity/service markets. The model includes agriculture, energy, and waste sectors, which account for ~90% of CH₄ emissions in the US (USEPA, 2022a). The government, suppliers and consumers constitute the three types of agents, and the latter two are modeled with heterogeneity, local interactions, and adaptations. Finally, case studies are conducted based on 2030 projected data in Ohio, US.

4.2. Methods

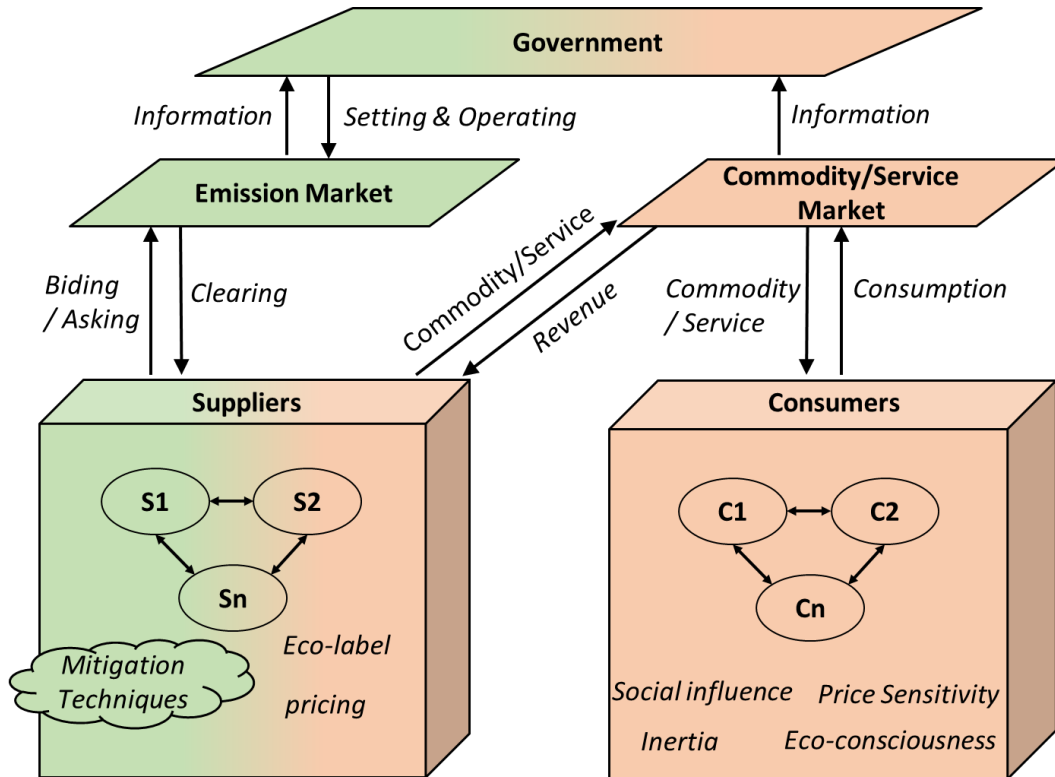


Figure 4-1. A Schematic Diagram of the Agent-Based Model for Methane Emission Control

The agent-based model for CH₄ emission control includes three types of agents (government, suppliers, and consumers) and two types of markets (emission market and commodity/service market) (see Figure 4.1). Each year, the government sets an emission cap and allocates CH₄ emission allowances to suppliers. At the end of the year, suppliers are required to surrender emission allowances equal to their current-year emissions to the government. To meet the emission cap, suppliers can apply mitigation techniques to reduce emissions or trade emission allowances in the emission market, which is established and regulated by the government. In the commodity/service market, suppliers

offer commodities/services with varying attributes, and consumers select products based on their preferences. Suppliers and consumers are heterogeneous and interact locally within their respective groups. Finally, the government collects data from both markets to evaluate the effectiveness of the emission regulations.

The following sections provide a detailed explanation of the model.

4.2.1. System Boundary and Settings

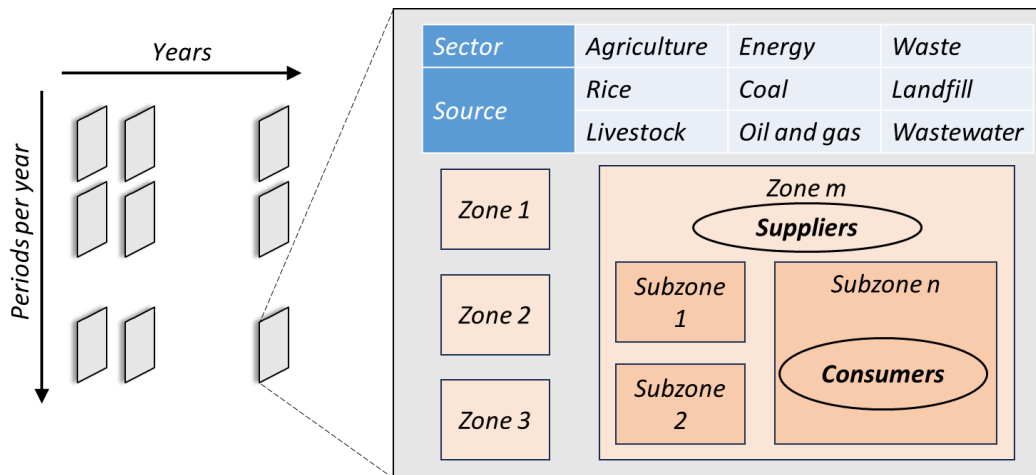


Figure 4-2. System Boundary and Settings of the Agent-Based Model for Methane Emission Control

The system boundary and settings are determined through three dimensions: time, space, and sector (Figure 4-2).

- 1) Time: The number of years (e.g., 10 years) limits the time boundary, and the number of periods per year (e.g., 12 periods per year) determines the time step. During each period, each agent only takes action (or a set of actions) once, i.e., the same type of action will not be repeated during the same period.

- 2) Space: The system is limited within a given space, e.g., a country or a state. The space is divided into zones, and the suppliers vary among different zones. Each zone is further divided into subzones, and the consumers can only mutually interact in the same subzone, i.e., one consumer cannot influence another consumer in a different subzone.
- 3) Sector: The CH₄ control is limited within three sectors which account for most of the CH₄ emissions: agriculture, energy, and waste. Each sector is subdivided into two sources, including (following the order of sectors) rice and livestock, coal and oil & gas, and landfill and wastewater. Any other sectors or sources are not considered.

4.2.2. Government

The primary goal of the government is to control CH₄ emissions to help address climate change. To achieve this, the government sets CH₄ emission reduction targets for major CH₄ emitters (i.e., suppliers in this study), which are specified by an annually decreasing CH₄ emission cap. This cap should be clear and fixed; for example, the maximum CH₄ emission is reduced by 2% of the benchmark per year. The benchmark CH₄ emission is calculated based on the historical CH₄ emissions of each supplier. To motivate suppliers to reduce CH₄ emissions, the government establishes a CH₄ emission market system, including CH₄ emission allowance allocation, trade, and surrender.

Each year, the government allocates free CH₄ allowances to each supplier, matching the emission cap for that year. This allocation gives suppliers permission to emit CH₄ within the specified cap. At the end of the year, suppliers must surrender CH₄ emission allowances equivalent to their actual emissions to the government. If a supplier exceeds

the available emission allowances, they will be fined heavily for the excess CH₄ emissions. If suppliers satisfy the emission cap, they will be allowed to mark this achievement on their products/services with an “ecolabel”.

The difficulty of mitigating CH₄ emissions varies among sectors and sources: some suppliers can mitigate CH₄ emissions cheaply, whereas others face high mitigation costs. As a result, for the whole system, CH₄ emissions are not reduced in the most cost-effective manner. To address this, the government allows suppliers to trade CH₄ emission allowances in the emission market. Suppliers with inexpensive CH₄ mitigation options are encouraged to mitigate more and sell their surplus allowances to the market for profit. Those facing higher mitigation costs can buy allowances from the market to offset their allowance deficits. Consequently, CH₄ emission mitigation is achieved with less total cost. Additionally, the government sets a reference price for emission allowance trading when the emission market is first established. More details of the CH₄ emission allowance trading scheme are put in section 4.2.3.

Finally, the government collects information from the emission market and the commodity/service market to evaluate the influence of the emission regulations and provide suggestions for future CH₄ control.

4.2.3. Emission market: Trading Scheme

In the emission market, CH₄ emission allowances are traded following the “double auction” rule. The suppliers can choose to be buyers, who submit CH₄ emission allowance bid price and quantity, or sellers, who submit CH₄ emission allowance ask price and quantity. The emission market institution will choose a price that clears the

market: 1) all the sellers who ask equal to or less than the clearing price sell, and all the buyers who bid equal to or more than the clearing price buy, both at the clearing price; 2) the selling quantity and buying quantity are exactly equal, i.e., the emission market itself would not gain any emission allowance or create any additional emission allowance.

Note that the successful seller who asks the highest price may not be able to sell all the ask quantity, and the successful buyer who bids the lowest price may not be able to buy all the bid quantity. In particular, the emission market institution determines the clearing price by the following steps.

- 1) Order the participants. Order the buyers in descending order of their bid prices, and order the sellers in ascending order of their ask prices.
- 2) Match a buyer and a seller. If the bid price of the first buyer (i.e., the one with the highest bid price) is more than or equal to the ask price of the first seller (i.e., the one with the lower ask price), match the buyer and the seller, and the trading quantity is the smaller of the bid quantity and the ask quantity. Remove the trading quantity from the buyer and seller, and remove the one who has zero bid/ask quantity from the order.
- 3) Repeat Step 2) until no pair of buyer and seller meets the matching criteria, or no buyer/seller is left in the order. The total trading quantity is the sum of all trading quantities realized in Step 2).
- 4) Determine the clearing price. Following initial orders given in Step 1), Denote the bid price of the last successful buyer b_1 , the ask price of last successful seller s_1 , the bid price of the first unsuccessful buyer b_2 , and the ask price of the first unsuccessful

seller s_2 . Note that by the matching criteria in Step 2, $b_1 \geq s_1$, and $b_2 < s_2$. The clearing price is determined as shown in Table 4.1.

Under several special situations, the total trading quantity can be zero: 1) the highest bid price is lower than the lowest ask price, where the clearing price is the average of the two prices; 2) no buyer, where the clearing price is the lowest ask price; 3) no seller, where the clearing price is the highest bid price; and 4) no buyer nor seller, where no clearing price is determined.

Table 4-1. Algorithm for Determining Clearing Price in the Emission Market

Conditions	$s_2 > b_1$	$s_2 \leq b_1$
$s_1 > b_2$	$(s_1 + b_1)/2$	$(s_1 + s_2)/2$
$s_1 < b_2$	$(b_1 + b_2)/2$	$(s_2 + b_2)/2$

Each period, the clearing results including the total clearing quantity and the clearing price are announced publicly, but the details of the successful buyers and sellers are not.

4.2.4. Suppliers

The decision rule for suppliers is maximizing the profit (i.e., revenue minus cost) considering both the emission market and the commodity/service market. Particularly, suppliers will decide (i) whether and which CH₄ emission mitigation technique to apply, (ii) the price change of the commodity/service, and (iii) the price and quantity of emission allowances to bid (to buy) or ask (to sell) in the emission market.

(i) Decision on CH₄ emission mitigation techniques

Each supplier has its own set of available CH₄ emission mitigation techniques with specific costs and CH₄ emission intensity reduction. Some techniques are competing, i.e.,

one supplier cannot have more than one technique among those that are competing. At the start of each period, at most one mitigation technique can be applied, and any mitigation technique will take the whole period to be fully implemented and thus will be effective starting from the next period. Once the mitigation technique is applied, it will be kept for all following periods. For each period, the decision on CH₄ emission mitigation techniques follows the steps below.

- 1) Check available mitigation techniques. If all available mitigation techniques have been applied, do nothing; otherwise, go to Step 2).
- 2) Find the mitigation technique with the lowest cost among those that have not been applied. If the cost is non-negative, apply the technique; otherwise, go to Step 3).
- 3) Estimate total CH₄ emissions in the current year, which is calculated by summing up
 - a) the CH₄ emissions that already occurred during past periods in the current year and
 - b) the CH₄ emissions that will occur in the current and following periods assuming the production amount and CH₄ intensity remain the same as the previous period. If the estimated annual CH₄ emissions are higher than the emission cap (i.e., allocated emission allowances), go to Step 4); otherwise, do nothing.
- 4) Predict the clearing price in the emission market in the current period. The clearing price is predicted based on the previous one, varying through random sampling to reflect the heterogeneity of suppliers. If the lowest mitigation technique cost is equal to or lower than the predicted clearing price, apply the technique; otherwise, do nothing.

(ii) Decision on commodity/service prices

Before the establishment of the emission market, it is assumed that the commodity/service market is under a Nash equilibrium where no supplier can make more profit by changing its own price, and thus all prices remain unchanged (See Section 4.2.6 for more details). The introduction of the emission market changes the costs of commodities/services, which breaks the initial Nash equilibrium and suppliers will accordingly adjust prices to make maximum profits. The steps are:

- 1) Estimate the additional cost per unit commodity/service. The additional unit cost is comprised of a) the cost of applied mitigation techniques per unit commodity/service and b) the cost from trading emission allowances per unit commodity/service. To obtain part b), estimate the total cost of trading emission allowances in the current and following periods (which is the product of the estimated emission allowance deficit and the predicted clearing price) and the total production amount in the current and following periods (by assuming that the production amount remains the same as the previous period), and divide the former by the latter.
- 2) Determine the price. Transfer some percentage of the additional unit cost to the initial price. This cost transfer percentage is obtained through random sampling for different suppliers, and it is fixed for all periods in the same year.

One supplier will learn from other suppliers' annual financial reports released at the end of each year, which contain information about the cost transfer percentage. In the following year, the supplier will adjust its cost transfer percentage to align more closely

with that of the supplier whose profit increased the most in the current year. The level of the alignment is also obtained through random sampling.

(iii) Decision on trading emission allowances

- 1) Estimate total CH₄ emissions in the current year, which is calculated by summing up
 - a) the CH₄ emissions that already occurred during past and current periods and b) the CH₄ emissions that will occur in the following periods assuming the production amount and CH₄ intensity remain the same as the current period.
- 2) Determine bid/ask price. If the estimated annual CH₄ emissions are higher than the emission cap, buy emission allowances with a bid price set at 50% to 100% of the cost of the cheapest unapplied mitigation technique. Conversely, if the emissions are below the cap, sell emission allowances with an ask price set at 100% to 200% of the cost of the most expensive applied mitigation technique. The above percentages are obtained through random sampling.
- 3) Determine bid/ask quantity. The maximum available bid/ask quantity is the difference between the estimated annual CH₄ emissions and the emission cap. Bid/ask a quantity of 0% to 100% (obtained through random sampling) of the maximum. If it is the final period of the year, bid/ask the maximum quantity.

4.2.5. Consumers

The decision rule for consumers is modeled based on random utility theory: within the available alternatives, the consumer will select the commodity/service that maximizes the utility. The interactions between commodity/service markets in different sectors and sources are not considered in this study, and consumers will make decisions in each

commodity/service market respectively. The following theory is applicable to each commodity/service market.

The set of available alternatives are called “choice set”. For consumers in a subzone, their choice set is made up of all commodities/services provided by suppliers in the zone that the subzone belongs to.

The utility is modeled as a random variable (U), which consists of a deterministic part (V) and a stochastic part (ε). For consumer i , the utility of commodity/service j at period t is

$$U_{ijt} = V_{ijt} + \varepsilon_{ijt} \quad (4-1)$$

We use the logit discrete choice model to model the utility further. Under this model, the stochastic part ε is assumed to be independent and identically Gumbel distributed, and the density function is

$$f(\varepsilon) = e^{-\varepsilon} e^{-e^{-\varepsilon}} \quad (4-2)$$

where e is the base of the natural logarithm function.

It can be further proven that the probability that consumer i selects commodity/service j at period t is

$$P_{ijt} = \frac{e^{V_{ijt}}}{\sum_j e^{V_{ijt}}} \quad (4-3)$$

The deterministic part V is modeled by a linear function

$$V_{ijt} = (\mathbf{a}_i)^T \mathbf{x}_{ijt} + C_{ij} \quad (4-4)$$

where \mathbf{a}_i is a vector reflecting the individual-specific taste of consumer i for attributes of choices in the choice set, \mathbf{x}_{ijt} is a vector reflecting the attributes of choice j for consumer i at period t , C_{ij} is the utility of all other attributes of choice j for consumer i not

modeled by \mathbf{a}_i and \mathbf{x}_{ijt} , and superscript T is the transpose symbol. Note the C_{ij} is assumed to be a constant through all periods.

Specifically, the components of \mathbf{a}_i and \mathbf{x}_{ijt} are

- 1) Price. Since consumers tend to select choices with lower prices given that other attributes are same, a^{price} is negative.
- 2) Inertia. It is assumed that consumers have some extent of inertia, i.e., they tend to stick with the previous choice regardless of changes, and $a^{inertia}$ is non-negative. If choice j was chosen by consumer i at period $t - 1$, $x_{ijt}^{inertia} = 1$; otherwise, $x_{ijt}^{inertia} = 0$.
- 3) Social influence. It is assumed that one consumer is to some extent influenced by the choices of neighboring consumers, i.e., they tend to select the commodity/service selected by others, and a^{social} is non-negative. As mentioned in Section 4.2.1, one consumer can only be influenced by other consumers in the same subzone. Denote the market share of choice j in consumer i 's subzone s at period t as M_{sjt} ($i \in s$), and the consumption percentage (i.e., weight) of consumer i in subzone s as w_{si} . x_{ijt}^{social} equals the market share of choice j among consumers other than consumer i at period $t - 1$. If choice j was chosen by consumer i at period $t - 1$, $x_{ijt}^{social} = \frac{M_{sj(t-1)} - w_{si}}{1 - w_{si}}$ ($i \in s$); otherwise, $x_{ijt}^{social} = \frac{M_{sj(t-1)}}{1 - w_{si}}$ ($i \in s$).
- 4) Eco-consciousness. It is assumed that consumers, to some extent, tend to select choices that are more eco-friendly, i.e., choices with an ecolabel (See Section 4.2.2),

and a^{eco} is non-negative. If choice j has an ecolabel at period t , $x_{jt}^{eco} = 1$; otherwise, $x_{jt}^{eco} = 0$.

Equation (4.4) can be rewritten in a decomposed form

$$V_{ijt} = a_i^{price} x_{jt}^{price} + a_i^{inertia} x_{ijt}^{inertia} + a_i^{social} x_{ijt}^{social} + a_i^{eco} x_{jt}^{eco} + C_{ij} \quad (4-5)$$

In the logit discrete choice model, the consumption amount of each consumer is fixed, i.e., only which commodity/service the consumer selects is determined. However, the amount of consumption also needs to be considered. To address this, we allow the consumer to select none of the choices in the choice set. In this case, one consumer agent does not directly represent one consumer in reality, but represents the aggregation of a number of real consumers with same/similar tastes. For example, if the price of a commodity increases, the probability of it being selected by a consumer agent decreases, while the probability of the consumer agent selecting other commodities or none increases. This is equivalent to, for the real consumers that the consumer agent represents, that some consumers turn to select other commodities, while others keep selecting the commodity but consume less.

Denote selecting none as choice “0”, and the only two attributes are inertia and social influence, i.e., $x_{0t}^{price} = x_{0t}^{eco} = C_{i0} = 0$. Thus, the deterministic part V for consumer i at time t is

$$V_{i0t} = a_i^{inertia} x_{i0t}^{inertia} + a_i^{social} x_{i0t}^{social} \quad (4-6)$$

4.2.6. Commodity/service market

In the commodity/service market, consumers accept the market price, while suppliers adjust their production amounts based on market demand. In this study, it is simplified

that in each period the production amount of each supplier is exactly equal to the demand, i.e., there is no situation where consumers cannot purchase according to their preferences due to a shortage of commodities/services, nor is there a situation where suppliers have to store or dispose of excess commodities/services due to a surplus.

The commodity/service market is influenced by the introduction of the emission market.

In the emission market, the suppliers are encouraged to apply mitigation techniques and trade emission allowances, resulting in receiving a penalty or an ecolabel, which will change the attributes (price and ecolabel) of the commodity/service. To easily analyze the influence of the emission market on the commodity/service market, it is assumed that before the introduction of the emission market, 1) the commodity/service market is in a stable state where the market share of each supplier is fixed, and 2) this stable state is a Nash equilibrium regarding the pricing strategy where no supplier can make more profit by changing the price of its own commodity/service. Details are as follows.

If consumer i selects choice j_1 at period $t - 1$, the deterministic utility of choice j_1 for consumer i at period t is

$$V_{ij_1t} = a_i^{price} x_{jt}^{price} + a_i^{inertia} + a_i^{social} \frac{M_{sj(t-1)} - w_{si}}{1 - w_{si}} + a_i^{eco} x_{j_1t}^{eco} + C_{ij_1} \quad (4-7)$$

$i \in \text{subzone } s$

For choices other than j_1 ,

$$V_{ij_2t} = a_i^{price} x_{j_2t}^{price} + a_i^{social} \frac{M_{sj(t-1)}}{1 - w_{si}} + a_i^{eco} x_{j_2t}^{eco} + C_{ij_2} \quad (4-8)$$

$i \in \text{subzone } s, j_1 \neq j_2$

Based on Equation (4-3), for consumer i , the transition probability of from selecting choice j_1 at period $t - 1$ to selecting choice j_1 at period t is

$$X_{i(j_1 \rightarrow j_1)(t-1 \rightarrow t)} = \frac{e^{a_i^{price} x_{jt}^{price} + a_i^{inertia} + a_i^{social} \frac{M_{sj(t-1)}^{-w_{si}}}{1-w_{si}} + a_i^{eco} x_{j_1 t}^{eco} + C_{ij_1}}}{e^{a_i^{price} x_{jt}^{price} + a_i^{inertia} + a_i^{social} \frac{M_{sj(t-1)}^{-w_{si}}}{1-w_{si}} + a_i^{eco} x_{j_1 t}^{eco} + C_{ij_1}} + \sum_{j_1 \neq j_2} e^{a_i^{price} x_{j_2 t}^{price} + a_i^{social} \frac{M_{sj(t-1)}}{1-w_{si}} + a_i^{eco} x_{j_2 t}^{eco} + C_{ij_2}}}, \quad (4-9)$$

$i \in \text{subzone } s$

The transition probability of from selecting choice j_1 at period $t - 1$ to selecting choice j_2 at period t is

$$X_{i(j_1 \rightarrow j_2)(t-1 \rightarrow t)} = \frac{e^{a_i^{price} x_{j_2 t}^{price} + a_i^{social} \frac{M_{sj(t-1)}}{1-w_{si}} + a_i^{eco} x_{j_2 t}^{eco} + C_{ij_2}}}{e^{a_i^{price} x_{jt}^{price} + a_i^{inertia} + a_i^{social} \frac{M_{sj(t-1)}^{-w_{si}}}{1-w_{si}} + a_i^{eco} x_{j_1 t}^{eco} + C_{ij_1}} + \sum_{j_1 \neq j_2} e^{a_i^{price} x_{j_2 t}^{price} + a_i^{social} \frac{M_{sj(t-1)}}{1-w_{si}} + a_i^{eco} x_{j_2 t}^{eco} + C_{ij_2}}}, \quad (4-10)$$

$i \in \text{subzone } s$

Equations (4-9) and (4-10) give the expression of elements in the transition probability matrix. Denote $\mathbb{X}_{i(t-1 \rightarrow t)}$ as consumer i 's transition probability matrix of choice transition from period $t - 1$ to period t , and \mathbf{P}_{it} as consumer i ' choice probability vector which contains the probabilities of selecting each choice at period t . The transition function for consumer i is

$$\mathbf{P}_{it} = \mathbb{X}_{i(t-1 \rightarrow t)} \mathbf{P}_{i(t-1)} \quad (4-11)$$

Sum up the choice probability vectors of all consumers by their weight and denote \mathbf{M}_{st} as subzone s ' market share vector which contains the market shares of each choice (containing selecting none) at period t , and we have

$$\mathbf{M}_{st} = \sum_{i \in S} \mathbf{P}_{it} w_i = \sum_{i \in S} \mathbb{X}_{i(t-1 \rightarrow t)} \mathbf{P}_{i(t-1)} w_i = \sum_{i \in S} \mathbb{X}_{i(t-1 \rightarrow t)} \mathbf{M}_{s(t-1)} \quad (4-12)$$

In a market under a stable state, the attributes of commodities/services and consumers' choice probabilities both remain unchanged, so transition probability matrices and market shares will both be unchanged for any period. In this case, the time subscripts can be removed from Equation (4-12), and we have

$$\mathbf{M}_s^{stable} = \sum_{i \in S} \mathbb{X}_i^{stable} \mathbf{M}_s^{stable} \quad (4-13)$$

where the superscript *stable* represents the stable state. Note that \mathbb{X}_i^{stable} ($i \in S$) is a function of \mathbf{M}_s^{stable} .

The stable market shares in subzone s can be obtained by solving \mathbf{M}_s^{stable} from Equation (4-13). Since direct solving is highly complex, it is realized by numerical iterations (See Appendix B.1 for details).

For supplier j in zone z , the total market share under a stable state considering all subzones that belong to zone z is

$$M_{zj}^{stable} = \sum_{s \in Z} \left(M_{sj}^{stable} \sum_{i \in S} w_{zi} \right) \quad (4-14)$$

where w_{zi} represents the consumption percentage (i.e., weight) of consumer i in zone z .

Further the profit under the stable state is

$$F_j^{stable} = M_{zj}^{stable} (x_j^{price,stable} - c_j) \quad (4-15)$$

where $x_j^{price,stable}$ is the price of commodity/service j under the stable state, c_j is the cost of commodity/service j which is a constant.

Under a Nash equilibrium, all suppliers have adjusted the price of its own commodity/service to make the maximum profit and the price is fixed. Thus, for any suppliers in zone z , we have

$$x_j^{price,nash} = \operatorname{argmax}_{x_j^{price,stable}} F_j^{stable} = \operatorname{argmax}_{x_j^{price,stable}} [M_{zj}^{stable}(x_j^{price,stable} - c_j)], \quad (4-16)$$

$$\forall j \in zone z$$

where $x_j^{price,nash}$ is the price of commodity/service j under the Nash equilibrium. Note that M_{zj}^{stable} is a function of $x_j^{price,stable}$. Similar to Equation (4-13), Equation (4-16) is also solved by numerical iterations (See Appendix B.2 for details).

4.2.7. Simulation process

The whole simulation process is summarized as shown in Figure 4-3. After initialization, the government sets up the emission market system, including regulations of CH₄ emission allowance allocation, trade, and surrender. At the start of each year, the government allocates emission allowances to suppliers, and at the end of the year suppliers surrender emission allowances back to the government and receive penalties or ecolabels depending on whether satisfying the emission cap. During each period within the year, suppliers first make decisions on emission mitigation techniques, and change commodity/service prices based on this decision and other estimations. Consumers make their choices on commodities/services (choosing one or nothing) according to their preferences, which determines the current-period market shares of suppliers. At the end of each period, suppliers decide on whether and how to bid/ask in the emission market, and the governmental institution clears the emission market by a uniform price.

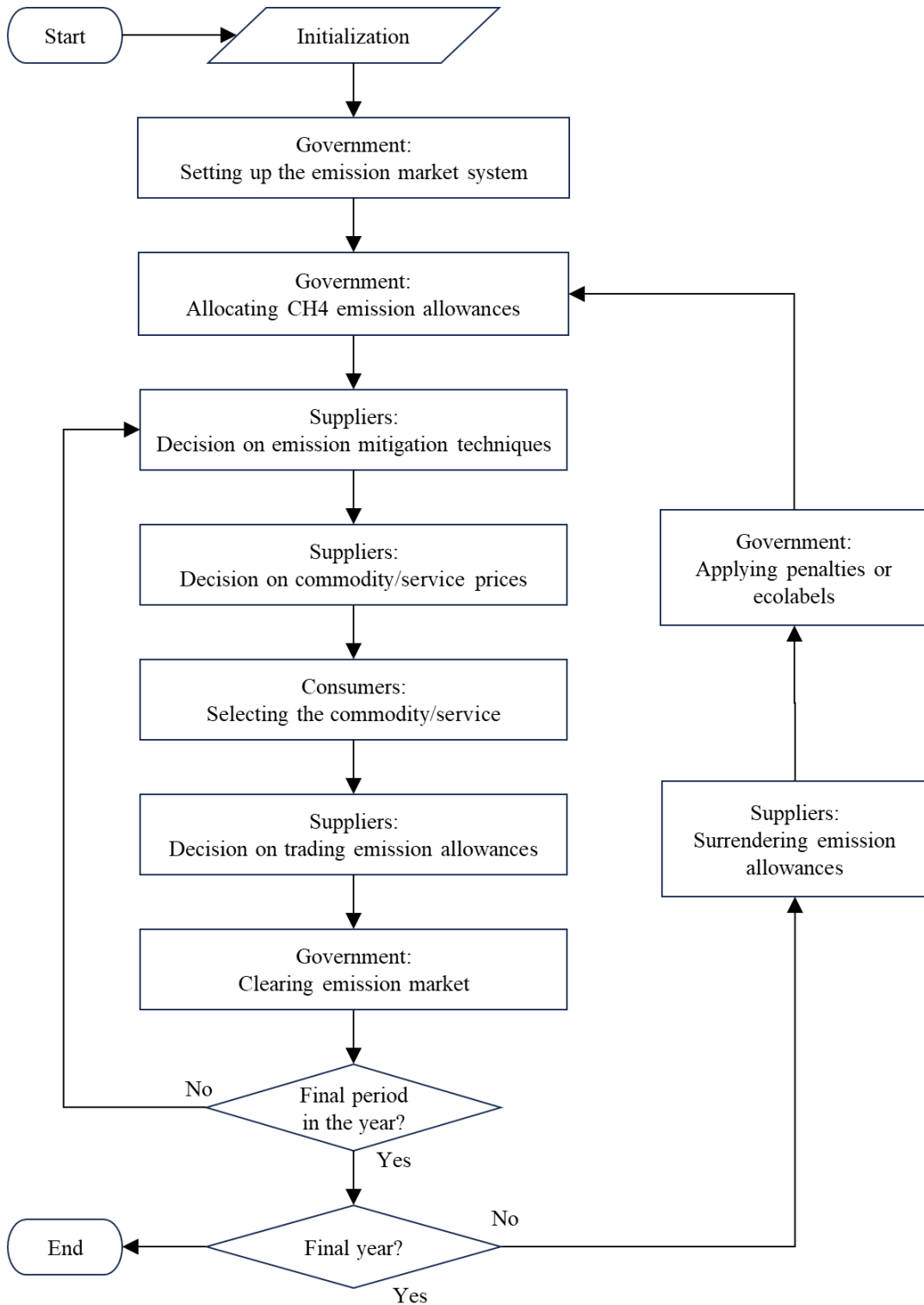


Figure 4-3: Simulation Process of the Agent-Based Model for Methane Emission Control

4.2.8. Scenarios

In this study, we constructed scenarios of CH₄ emission and control based on 2030 projected data in Ohio, US. The time is bounded within 10 years, and the time step is one month. Five sources are included: Livestock, coal, oil and gas, landfill, and wastewater. The rice source is not considered since Ohio barely produces rice. The suppliers in the waste sector (landfill and wastewater) are simplified as monopolies within their own zones, since consumers have very limited alternatives and usually they are not the direct decision-makers. The whole state is divided into 27 zones, each having 10 subzones. Each zone has a unique combination of consumer parameters, including inertia, social influence, and eco-consciousness. Data for CH₄ emissions and mitigation techniques are from USEPA (USEPA, 2022b). Five random seeds (same for all cases) are used for the simulation. Other details of the base-case parameters are listed in Table 4-2.

Table 4-2. Base-case Parameters for CH₄ Emission Control Agent-Based Model

Government					
<i>Emission cap reduction rate</i>	3%/year				
<i>Emission market penalty price</i>	\$2500/tCH ₄				
<i>Emission market reference price</i>	\$500/tCH ₄				
Suppliers					
<i>Source</i>	Livestock	Coal	Oil and Gas	Landfill	Wastewater
<i>Initial Emissions</i>	1.7×10 ⁵ tCH ₄	2.3×10 ⁴ tCH ₄	3×10 ⁵ tCH ₄	2.4×10 ⁵ tCH ₄	1.9×10 ⁴ tCH ₄
<i>Scale per year</i>	\$7×10 ⁹	\$1.25×10 ⁸	\$3.75×10 ¹⁰	2×10 ⁷ t	4.9×10 ⁶ households
<i>Ave. No. per zone</i>	20	5	5	1	1
<i>Ave. own price elasticity of demand</i>	-0.31	-0.18	-0.6	---	---
<i>Ave. profit rate</i>	10%	10%	10%	---	---
<i>Heterogeneity Percent</i>	30%				
Consumers					
<i>No. total</i>	10000				
<i>Parameters set (inertia, social influence, eco-consciousness)</i>	(0, 0.5, 1)				
<i>Heterogeneity Percentage</i>	70%				

4.3. Results

Figure 4-4 shows the emission trajectories under different emission cap reduction rates set by the government. In the base case [Figure 4-4(b)], where the emission cap is reduced by 3% per year and to 70% at the end, the agriculture and energy sectors meet the emission cap throughout the time horizon. However, the waste sector fails to do so starting from year 2, and its emissions remain at approximately 95% of the initial level from year 6 until the end. As a result, total emissions exceed the emission cap starting from year 5, ultimately only reduced to around 80%. When the emission cap is relaxed to a 1% reduction per year, resulting in a final cap of 90% of the initial emissions, the agriculture and energy sectors successfully reduce their emissions to below 90% (~88% and ~80%, respectively) by the second year and maintain these levels thereafter.

However, the waste sector still cannot meet the emission cap and only minimally reduces its emissions. Despite this, total emissions remain below the cap throughout the time horizon. If the emission cap reduction rate is increased to 5% per year, the agriculture and energy sectors can satisfy the emission cap until year 7, when their emissions are reduced to about 68% of the initial level yet stop decreasing in the following years, and the waste sector only reduces its emissions to a minimum of ~93% of initial level. Starting from year 4, total emissions become higher than the emission cap, and decrease to about 75% of the initial emission between year 8 and year 10. In general, a higher emission cap reduction rate will lead emissions across all sectors to decrease more significantly, but will also result in more sectors violating the emission cap earlier.

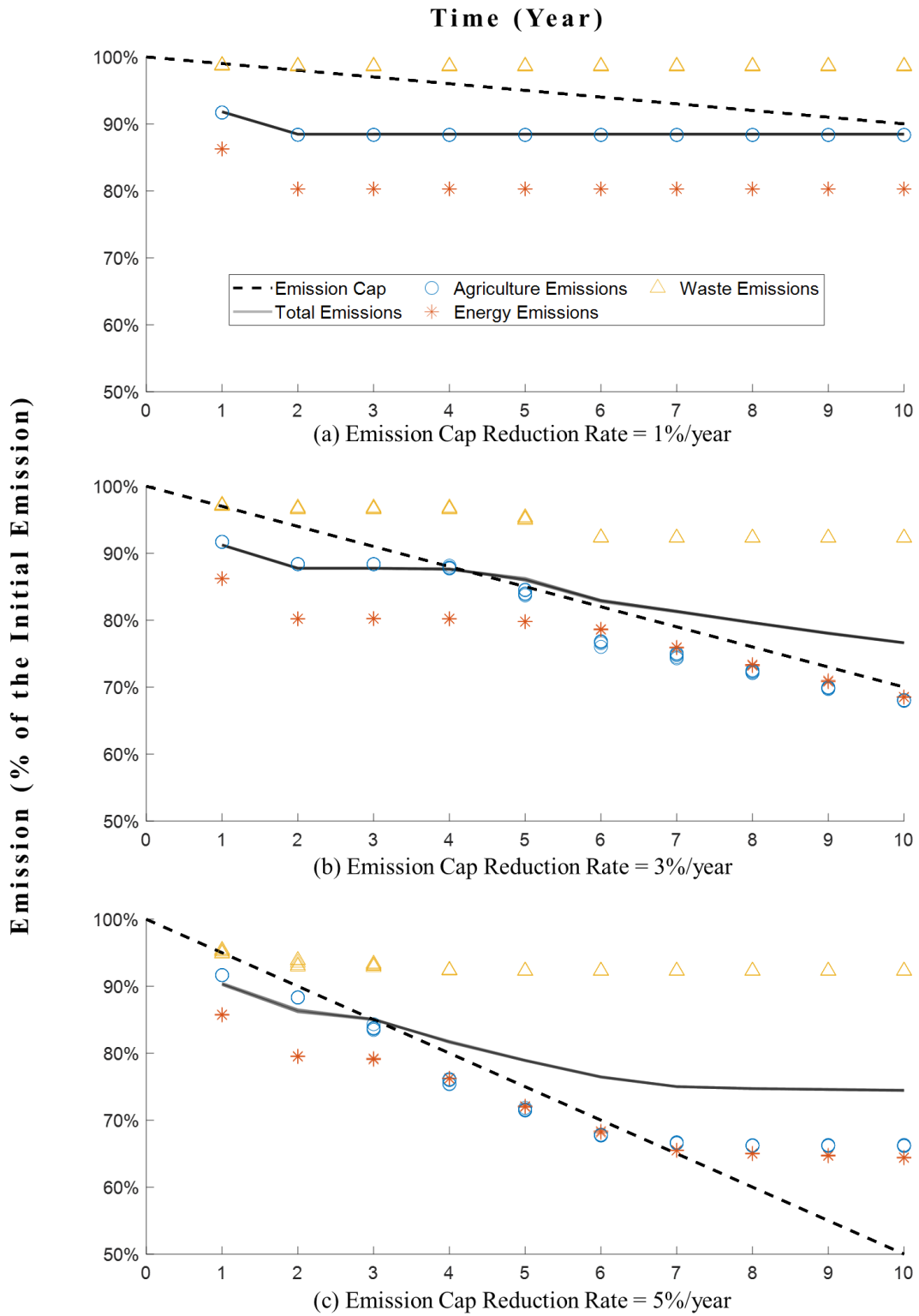


Figure 4-4. Dynamics of Emissions Under Different Emission Cap Reduction Rates. Allowance trading is not taken into account.

Intuitively, to encourage emissions reduction and decrease instances of exceeding emission caps (e.g., those shown in Figure 4-4), the government can set up a higher penalty price in the emission market. However, as shown in Table 4-3, under the same emission cap reduction rate, the change of penalty price (\$1250-3750/tCH₄) has almost no influence on the final total emissions (<1% for all cases). Since the suppliers would ultimately apply mitigation techniques that cost less than the penalty price, this indicates that mitigation techniques with costs ranging from \$1250/tCH₄ to \$3750/tCH₄ are extremely limited. Under such a situation, increasing the penalty price will not be helpful in satisfying a demanding emission cap.

Table 4-3. Final Total Emissions as Percentages of the Initial Emission (Average of All Simulation Seeds)

<i>Emission Cap Reduction Rate</i>	1%/year	3%/year	5%/year
<i>Emission Market Penalty Price</i>			
\$1250/tCH ₄	88.46%	76.88%	75.00%
\$2500/tCH ₄	88.46%	76.62%	74.45%
\$3750/tCH ₄	88.46%	76.62%	74.43%

Figure 4-5 presents the influence of government-set parameters on the trajectory of the clearing price in the emission market. When one parameter varies, all other parameters use base-case values. As shown in Figure 4-5(a), when the emission cap reduction rate is set as 1% per year, the emission market clearing price remains nearly zero throughout all years. Under a higher reduction rate as 3% per year, the clearing price starts at around \$700/tCH₄, and quickly decreases to nearly zero within the first year. This price is maintained until the start of year 5, when the clearing price begins to surge, reaching

\$2500/tCH₄ (the penalty price) within a year, and remains at that value until the end. If the reduction rate rises to 5% per year, the clearing price begins at \$2500/tCH₄ and drops rapidly to nearly zero during the first year. From the start of year 3, the clearing price rises and reaches \$2500/tCH₄ during year 4, staying at that value until the end.

The emission market penalty price [Figure 4-5(b)] does not have an obvious influence on the clearing price during the first five years, when all clearing prices are relatively low (< \$1000/tCH₄). Instead, it determines the highest clearing price that maintains during the latter five years. In other words, the penalty price performs as a “ceiling” preventing the clearing price from increasing to higher than that value. This is because no buyer in the emission market would bid a price higher than the penalty price, otherwise the cost of buying emission allowance would be higher than receiving the penalty.

In contrast to the penalty price, the emission market reference price only impacts the clearing price at the starting stage [Figure 4-5(c)]. When the reference price is \$250/tCH₄, the initial clearing price is ~\$300-400/tCH₄, which rises to ~\$600-800/tCH₄ with a reference price of \$500/tCH₄, and ~\$800-1200/tCH₄ with a reference price of \$750/tCH₄. This indicates that the initial clearing price is likely to be higher than the reference price. Within the first year, clearing price trajectories with different reference prices quickly converge to one bunch with tiny differences, which means that the reference price has no obvious influence on the emission market throughout the time horizon.

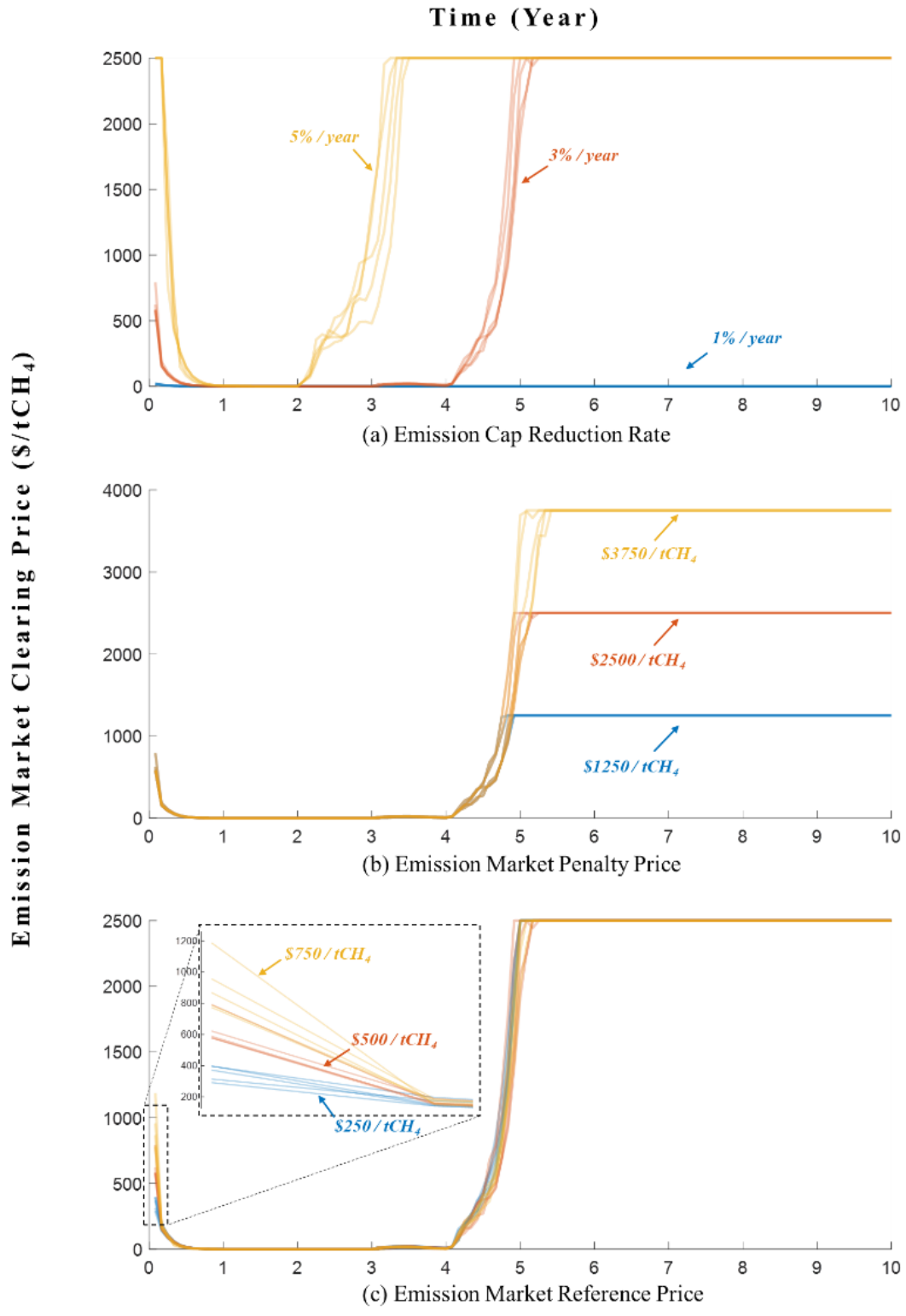


Figure 4-5. Dynamics of Emission Market Clearing Price Under Different Emission Market Settings.

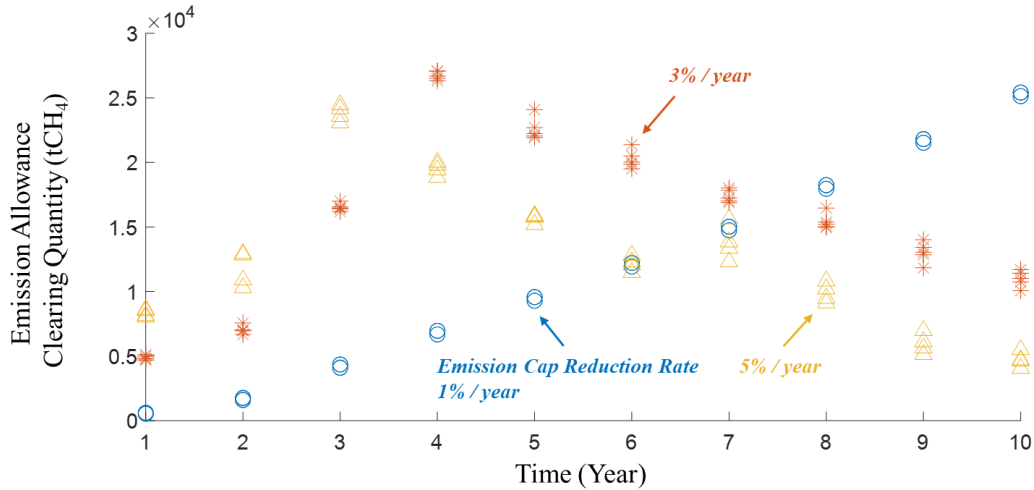


Figure 4-6. Dynamics of Emission Allowance Clearing Quantity Under Different Emission Cap Reduction Rates.

Figure 4-6 shows the influence of the emission cap reduction rate on the trajectory of the allowance clearing quantity in the emission market. Under an emission cap reduction rate of 1% per year, the clearing quantity starts from nearly zero in the first year, and steadily increases over time, reaching ~26 ktCH₄ by the end. This is mainly due to the requirement of emission allowances from the waste sector, which increases as the emission cap reduces. This also explains the reason why in year 1 the clearing quantity becomes higher (~5 ktCH₄) when the emission cap is reduced by 3% per year. However, unlike the case with a 1% reduction cap, the clearing quantity peaks in year 4 (~27 ktCH₄) and subsequently continues to decline, finally reaching ~1.2 ktCH₄. The main reason is that starting from year 5, more suppliers are faced with difficulty in complying with the emission cap, and those who used to sell emission allowances turned to buying. When the quantity of bids to buy exceeds the quantity of bids to sell, the clearing quantity will primarily depend on the quantity of sell bids, which is reduced over time. A similar

pattern can be observed when the emission cap reduction rate goes to 5% per year. In this case, the initial clearing quantity (~0.8 ktCH₄) is higher than that in the other two cases, the peak occurs in year 3, and the final clearing quantity (~0.5 ktCH₄) is less than that in the other two cases. In summary, a higher emission cap reduction rate will result in a higher clearing quantity in the early stage and a lower one in the later stage. A low emission cap reduction rate leads to a constant increase in the clearing quantity, while a high enough one will create a peak (an increase followed by a decrease) in the trajectory of the clearing quantity.

Table 4-4. All-Time Costs and Percents of Penalty Receivers (Average of All Simulation Seeds)

<i>Emission Cap Reduction Rate</i>		1%/year	3%/year	5%/year
<i>All-Time Costs of Technique Application (10⁶ \$)</i>	Agriculture	-368.4	-307.4	-250.1
	Energy	-209.7	-176.0	-72.2
	Waste	-74.8	-40.1	-24.0
	All Sectors	-653.0	-523.5	-346.3
<i>All-Time Costs of Emission Allowance Trade (10⁶ \$)</i>	Agriculture	0.004	-83.7	-34.1
	Energy	-0.007	-111.6	-126.5
	Waste	0.003	195.3	160.6
	All Sectors	0	0	0
<i>All-Time Total Costs (10⁶ \$)</i>	Agriculture	-368.4	-391.1	-284.2
	Energy	-209.7	-287.6	-198.7
	Waste	-74.8	155.2	136.6
	All Sectors	-653.0	-523.5	-346.3
<i>All-Time Percent of Penalty Receivers</i>	Agriculture	0%	1.43%	39.55%
	Energy	0%	1.80%	19.63%
	Waste	0%	56.48%	73.75%
	All Sectors	0%	5.17%	35.37%

Table 4-4 lists the costs of applying mitigation techniques and trading emission allowances for all sectors under different emission cap reduction rates. As the emission

cap reduction rates increase, the cost of technique application also increases for all sectors, resulting from applying more expensive techniques to meet a stricter emission cap. All costs of mitigation technique application are negative, even under the highest emission cap reduction rate, which indicates that all sectors have a net benefit from applying mitigation techniques. Even if some techniques have positive costs, they cannot fully offset the benefit from negative-cost techniques. One of the main reasons is that positive-cost techniques are applied later and the cost is accumulated over a shorter time than negative-cost techniques.

When the emission cap reduction rate is 1%/year, the costs from trading emission allowances are all nearly zero for all sectors, since the clearing price keeps extremely low [Figure 4-5(a)]. With an emission cap reduction rate as 3%/year, the agriculture and energy sectors receive \$83.7M and \$111.6M, respectively, from selling emission allowances, which are paid by the waste sector. When the emission cap reduction rate is 5%/year, the agriculture sector benefits less from the emission market, while the energy sector benefits more. Their total benefit becomes less, leading to less expenditure of the waste sector to the emission market.

By considering both types of costs, all the sectors can gain benefits except for the waste sector under an emission cap reduction rate of 3%/year or 5% per year. As the emission cap reduction rate rises, the total cost of all sectors increases but remains below zero, and the entire state can benefit by at least 0.35 billion dollars from controlling CH₄ emissions. In addition, under a 1%/year emission cap reduction rate, no supplier in any sector is punished by the government. Although the waste sector actually emits more than the

emission cap [Figure 4-4(a)], it offsets the emission allowance deficit through trading in the emission market. With a 3%/year emission cap reduction rate, some suppliers in agriculture and energy sectors receive penalties in some years, yet the percentages are very low (1%-2%). In contrast, the penalty receivers in the waste sector surge to more than 50%. The percentages of penalty receivers increase across all sectors under a higher emission cap reduction rate (5%/year), with the energy sector the lowest (~20%) and waste sector the highest (~74%). In general, the waste sector is faced with the highest risk of receiving a penalty, while the energy sector has the lowest.

Finally, Figure 4-7 depicts the change in prices for the waste sector under different emission cap reduction rates. It is important to note that the price changes of other sectors (agriculture and energy) are minimal (<1%) in all cases throughout the entire time, so these results are not shown in Figure 4-7. The prices in the landfill and wastewater sources change with similar patterns. When the emission cap is low (reduced by 1%/year), the prices hardly change. With a base-case emission cap (reduced by 3%/year), the prices rise obviously from year 6, ultimately reaching ~\$6/t and ~\$3/household-year higher than initial prices for landfill and wastewater sources, respectively. A 5%/year emission cap reduction rate leads to higher prices, which by the end reach ~\$12/t and ~\$4.5/household-year higher than initial prices for landfill and wastewater sources, respectively. Compared with the rate in Franklin County Sanitary Landfill, Ohio at \$39.75/t (SWACO, 2024) and the average annual household sewer rate in Ohio at \$489.95 (Gingerich et al., 2023), the landfill price can rise up to 30% while the wastewater price only rises less than 1%.

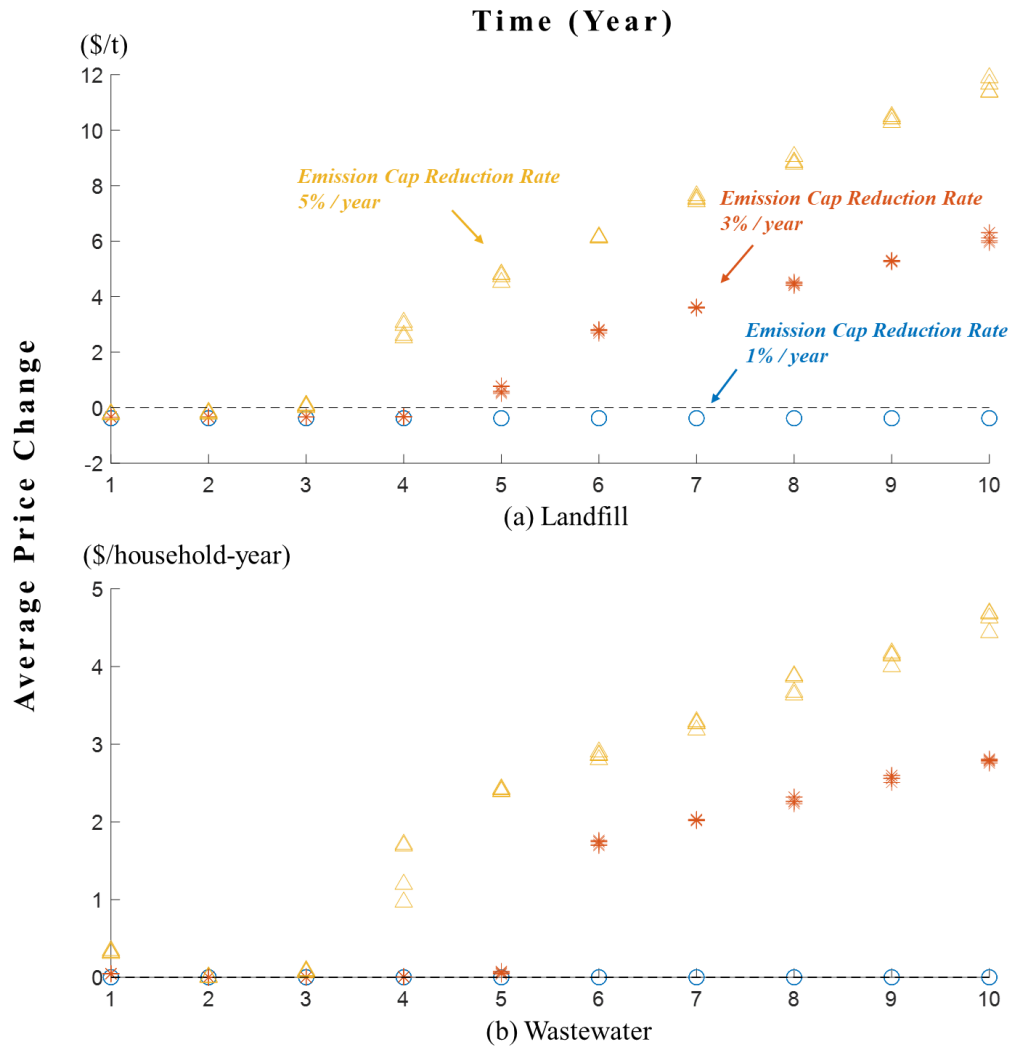


Figure 4-7. Dynamics of Price Change (Average of All Simulation Seeds) Under Different Emission Cap Reduction Rates. Only the results of waste sector are shown. *The price changes of other sectors (agriculture and energy) are all <1%.*

4.4. Discussion and Conclusions

This study establishes a comprehensive model for CH₄ emission control analysis with the agent-based method. The model consists of three types of agents, including the government, suppliers, and consumers. The suppliers and consumers are modeled with

heterogeneity, local interactions, and adaptations. Both the emission market and commodity/service markets are considered, covering agriculture, energy, and waste sectors. Case studies on Ohio, US that are based on projected data in 2030 indicate primary conclusions as follows:

- 1) The emission cap, which is determined by the emission cap reduction rate, is the main factor that influences CH₄ control, while the emission market penalty price has a tiny effect. If total emissions fail to satisfy the emission cap, it is ineffective to encourage more CH₄ mitigation by increasing the penalty (within the range of \$1250-3750/tCH₄).
- 2) The emission cap should be set carefully in the most cost-effective way for the whole system. A tighter emission cap will result in less CH₄ emissions and higher mitigation costs, but that relationship is not linear. As shown in this study, total CH₄ emissions can be reduced to ~88% with a 1%/year emission cap reduction rate. If the rate is 3%/year, total CH₄ emissions can decrease by an additional 11.84% with an extra cost of \$129.5M. However, under a rate of 5%/year, the additional emission reduction is 14.01% yet leading to a \$306.7M extra cost, which indicates that it is not cost-effective to set an excessively tight emission cap.
- 3) In all cases studied, the CH₄ control exhibits a negative total cost, i.e., a net total benefit. One of the main reasons is that suppliers always apply negative-cost techniques first, of which the negative costs accumulate over a longer period than positive-cost techniques. Those techniques with negative costs should have been applied before the introduction of the emission market, which would have led to more

cumulative benefits from CH₄ control. However, in reality a fair amount of negative-cost techniques still remain unapplied due to various barriers. Thus, the government should implement more incentives to encourage earlier deployments of negative-cost CH₄ mitigation techniques.

- 4) The waste sector faces the most difficulties in mitigating CH₄ emissions. In all cases studied, compared with the agriculture and energy sectors, the waste sector realizes the least CH₄ emission reduction with the highest cost, and the suppliers are penalized the most frequently. This leads to considerable price increases in the landfill source, up to 30% of the initial price. Therefore, the government should pay more attention to and provide greater support for the waste sector, especially the landfill source, in an effort to control CH₄ emissions.

Chapter 5. Conclusions

The Paris Agreement proposed the 1.5°C and 2°C pathways, but we are diverging from these targets. According to UNEP predictions, even with the full implementation of conditional Nationally Determined Contributions (NDCs), the temperature increase will still be limited to only 2.5°C above pre-industrial levels. To bridge the emission cap and address climate change, a portfolio of emission control approaches must be implemented in a more comprehensive and more optimized way.

This dissertation focuses on two components that can play a role in combating climate change yet are currently insufficiently developed: geothermal utilization and CH₄ control. Specifically, the dissertation explores optimizing strategies for their most effective implementations under different scenarios. Main conclusions are discussed as follows.

5.1. Geothermal Heat Mining

1) The optimal way to mine geothermal heat has four situations. In situation 1, the mass flow rate keeps the maximum; In situation 2, the mass flow rate keeps as 0; In situation 3, the mass flow rate starts as the maximum, decreases to a constant value, and finally recovers to the maximum; In situation 4, the mass flow rate starts as 0, and changes to the maximum. Setting aside situation 2 (where mining heat cannot make any profit) and situation 4 (where the discount rate is negative), the other two situations both contain a stable state where the extracted heat remains constant. This

- is perfectly consistent with the common practice of utilizing geothermal energy as base loads. Note that such a consistency is under the assumption that the energy price is constant. With a fluctuating energy price, the facility-level optimal strategy will not necessarily have such a stable state. This suggests that it could be better to set the geothermal energy price as a constant (e.g., the average of energy prices in a year) for a stable and profit-maximized use of geothermal heat.
- 2) The optimal geothermal heat mining profit is highly sensitive to surrounding media temperature, efficiency, and compression cost, yet barely influenced by reservoir mass, maximum mass flow rate, and contact conductance. This indicates that, to make the best profit, we should locate the geothermal plant at a site with high underground temperature, but not necessarily with a large reservoir or good thermal conductivity. Moreover, we should not focus on the scale of the plant (which is reflected by the maximum mass flow rate) but more on the energy-saving techniques (which is reflected by the efficiency and compression cost).
 - 3) Compared with water geothermal systems, CO₂ geothermal systems perform better for shallow, low-grade heat sources due to less requirement for the thermosiphon effect. Thus, when deciding the type of working fluid for geothermal heat mining, we should consider the depth and thermal gradient of the underground reservoir. To achieve better synergy between geothermal energy and carbon storage while maintaining cost-effectiveness, we should prioritize the utilization of shallow, low-grade heat sources.

5.2. Methane Control

- 1) Negative-cost CH₄ mitigation strategies should be put into action, and obstacles to their use should be overcome. Economically, these strategies are beneficial, but without local incentives, they are unlikely to be used. Therefore, policy support to promote and share CH₄ mitigation techniques is crucial, especially for those with negative costs. An earlier deployment of more cost-effective CH₄ mitigation strategies would accumulate more benefits for potential CH₄ mitigation efforts with positive costs in the future.
- 2) Relying only on mitigating CH₄ emissions is not enough to meet climate goals. We must develop and use CH₄ removal technologies on a large scale, and policies are needed to encourage these developments. Although CH₄ removal may seem expensive, it is a crucial and significant part of cost-effective strategies to reach climate targets. If we aim to achieve ambitious climate goals at the lowest cost, we need to start developing CH₄ removal methods decades before 2075, so they can be implemented on an industrial scale by then. The timing of when to start CH₄ removal depends more on scale-related parameters (e.g., *maximum CH₄ removal potential*, *maximum CH₄ removal growth rate*), rather than on cost-related parameters (e.g., *initial CH₄ removal cost*, *CH₄ mitigation cost*). Therefore, plans for developing CH₄ removal should focus less on current and future costs and more on timelines for starting research, development, and testing of these approaches.
- 3) The emission market is an effective tool to encourage CH₄ emission reduction, where participants can benefit from trading emission allowances. The government should

carefully set the emission cap: a cap that is too high is not sufficient to meet the climate goal, while if it is too low, the whole system will control CH₄ emissions in a cost-ineffective way. Additionally, the government should focus less on setting penalty prices for the emissions market. If total emissions exceed the cap, increasing the penalty is ineffective in encouraging further CH₄ mitigation.

- 4) In the effort to control CH₄ emissions, the government should pay more attention to and provide greater support for the waste sector, especially landfill sources. Case studies in Ohio, US indicate that the waste sector faces the most significant challenges in mitigating CH₄ emissions. Compared to the agriculture and energy sectors, the waste sector achieves the least CH₄ emission reduction at the highest cost, leading to substantial price increases in landfill sources, up to 30% of the initial price. The government can offer more incentives or subsidies to the waste sector or establish an emission cap reduction goal at a slower pace for it.

Bibliography

- Abernethy, S., Kessler, M. I., & Jackson, R. B. (2023). Assessing the potential benefits of methane oxidation technologies using a concentration-based framework. *Environmental Research Letters*, *18*(9), 094064. <https://doi.org/10.1088/1748-9326/acf603>
- AghaKouchak, A., Cheng, L., Mazdidasni, O., & Farahmand, A. (2014). Global warming and changes in risk of concurrent climate extremes: Insights from the 2014 California drought. *Geophysical Research Letters*, *41*(24), 8847–8852. <https://doi.org/10.1002/2014GL062308>
- AghaKouchak, A., Chiang, F., Huning, L. S., Love, C. A., Mallakpour, I., Mazdidasni, O., Moftakhari, H., Papalexioiu, S. M., Ragno, E., & Sadegh, M. (2020). Climate Extremes and Compound Hazards in a Warming World. *Annual Review of Earth and Planetary Sciences*, *48*(Volume 48, 2020), 519–548. <https://doi.org/10.1146/annurev-earth-071719-055228>
- Al Irsyad, M. I., Halog, A., & Nepal, R. (2019). Estimating the impacts of financing support policies towards photovoltaic market in Indonesia: A social-energy-economy-environment model simulation. *Journal of Environmental Management*, *230*(September 2018), 464–473. <https://doi.org/10.1016/j.jenvman.2018.09.069>
- Al-Ghamdi, S. G., & Bilec, M. M. (2016). On-Site Renewable Energy and Green Buildings: A System-Level Analysis. *Environmental Science & Technology*, *50*(9), 4606–4614. <https://doi.org/10.1021/acs.est.5b05382>
- Bertolazzi, E. (2022). *mexIPOPT*. <https://github.com/ebertolazzi/mexIPOPT>

- Bocken, N. M. P., Olivetti, E. A., Cullen, J. M., Potting, J., & Lifset, R. (2017). Taking the Circularity to the Next Level: A Special Issue on the Circular Economy. *Journal of Industrial Ecology*, 21(3), 476–482. <https://doi.org/10.1111/jiec.12606>
- Boucher, O., Forster, P. M., Gruber, N., Ha-Duong, M., Lawrence, M. G., Lenton, T. M., Maas, A., & Vaughan, N. E. (2014). Rethinking climate engineering categorization in the context of climate change mitigation and adaptation. *Wiley Interdisciplinary Reviews: Climate Change*, 5(1), 23–35. <https://doi.org/10.1002/wcc.261>
- Boucher, O., Friedlingstein, P., Collins, B., & Shine, K. P. (2009). The indirect global warming potential and global temperature change potential due to methane oxidation. *Environmental Research Letters*, 4(4), 044007. <https://doi.org/10.1088/1748-9326/4/4/044007>
- Brandt, A. R., Heath, G. A., Kort, E. A., O’Sullivan, F., Pétron, G., Jordaan, S. M., Tans, P., Wilcox, J., Gopstein, A. M., Arent, D., Wofsy, S., Brown, N. J., Bradley, R., Stucky, G. D., Eardley, D., & Harriss, R. (2014). Methane Leaks from North American Natural Gas Systems. *Science*, 343(6172), 733–735. <https://doi.org/10.1126/science.1247045>
- Brenneis, R. J., Johnson, E. P., Shi, W., & Plata, D. L. (2022). Atmospheric- and Low-Level Methane Abatement via an Earth-Abundant Catalyst. *ACS Environmental Au*, 2(3), 223–231. <https://doi.org/10.1021/acsenvironau.1c00034>
- Byers, E., Krey, V., Kriegler, E., Riahi, K., Schaeffer, R., Kikstra, J., Lamboll, R., Nicholls, Z., Sandstad, M., Smith, C., van der Wijst, K., Al -Khourdajie, A.,

- Lecocq, F., Portugal-Pereira, J., Saheb, Y., Stromman, A., Winkler, H., Auer, C., Brutschin, E., ... van Vuuren, D. (2022). *AR6 Scenarios Database* (1.1) [dataset]. Zenodo. <https://doi.org/10.5281/ZENODO.5886911>
- Castro, J., Drews, S., Exadaktylos, F., Foramitti, J., Klein, F., Konc, T., Savin, I., & van den Bergh, J. (2020). A review of agent-based modeling of climate-energy policy. *WIREs Climate Change*, *11*(4), e647. <https://doi.org/10.1002/wcc.647>
- Chen, X., Li, Y., Pan, X., Cortie, D., Huang, X., & Yi, Z. (2016). Photocatalytic oxidation of methane over silver decorated zinc oxide nanocatalysts. *Nature Communications*, *7*(1), Article 1. <https://doi.org/10.1038/ncomms12273>
- Cheng, C.-H., & Redfern, S. A. T. (2022). Impact of interannual and multidecadal trends on methane-climate feedbacks and sensitivity. *Nature Communications*, *13*(1), 3592. <https://doi.org/10.1038/s41467-022-31345-w>
- Cianconi, P., Betrò, S., & Janiri, L. (2020). The Impact of Climate Change on Mental Health: A Systematic Descriptive Review. *Frontiers in Psychiatry*, *11*. <https://doi.org/10.3389/fpsy.2020.00074>
- Cinner, J. E., McClanahan, T. R., Graham, N. A. J., Daw, T. M., Maina, J., Stead, S. M., Wamukota, A., Brown, K., & Bodin, Ö. (2012). Vulnerability of coastal communities to key impacts of climate change on coral reef fisheries. *Global Environmental Change*, *22*(1), 12–20. <https://doi.org/10.1016/j.gloenvcha.2011.09.018>
- Crippa, M., Guizzardi, D., Pagani, F., Banja, M., Muntean, M., Schaaf, E., Becker, W. E., Monforti-Ferrario, F., Brandao De Melo, J., Grassi, G., Vignati, E., SAN-

- MIGUEL-AYANZ, J., JACOME FELIX OOM, D., Rossi, S., & BRANCO, A. (2023). *EDGAR v8.0 Greenhouse Gas Emissions* [dataset]. European Commission, Joint Research Centre (JRC). <https://doi.org/10.2905/B54D8149-2864-4FB9-96B9-5FD3A020C224>
- Crooks, A. T., & Heppenstall, A. J. (2012). Introduction to Agent-Based Modelling. In A. J. Heppenstall, A. T. Crooks, L. M. See, & M. Batty (Eds.), *Agent-Based Models of Geographical Systems* (pp. 85–105). Springer Netherlands. https://doi.org/10.1007/978-90-481-8927-4_5
- De Boeck, L., Verbeke, S., Audenaert, A., & De Mesmaeker, L. (2015). Improving the energy performance of residential buildings: A literature review. *Renewable and Sustainable Energy Reviews*, 52, 960–975. <https://doi.org/10.1016/j.rser.2015.07.037>
- Dean, J. F., Middelburg, J. J., Röckmann, T., Aerts, R., Blauw, L. G., Egger, M., Jetten, M. S. M., de Jong, A. E. E., Meisel, O. H., Rasigraf, O., Slomp, C. P., in't Zandt, M. H., & Dolman, A. J. (2018). Methane Feedbacks to the Global Climate System in a Warmer World. *Reviews of Geophysics*, 56(1), 207–250. <https://doi.org/10.1002/2017RG000559>
- Delwiche, K. B., Knox, S. H., Malhotra, A., Fluet-Chouinard, E., McNicol, G., Feron, S., Ouyang, Z., Papale, D., Trotta, C., Canfora, E., Cheah, Y.-W., Christianson, D., Alberto, Ma. C. R., Alekseychik, P., Aurela, M., Baldocchi, D., Bansal, S., Billesbach, D. P., Bohrer, G., ... Jackson, R. B. (2021). FLUXNET-CH4: A global, multi-ecosystem dataset and analysis of methane seasonality from

freshwater wetlands. *Earth System Science Data*, 13(7), 3607–3689.

<https://doi.org/10.5194/essd-13-3607-2021>

Doney, S. C., Busch, D. S., Cooley, S. R., & Kroeker, K. J. (2020). The Impacts of Ocean Acidification on Marine Ecosystems and Reliant Human Communities. *Annual Review of Environment and Resources*, 45(Volume 45, 2020), 83–112.

<https://doi.org/10.1146/annurev-environ-012320-083019>

Doney, S. C., Fabry, V. J., Feely, R. A., & Kleypas, J. A. (2009). Ocean Acidification: The Other CO₂ Problem. *Annual Review of Marine Science*, 1(Volume 1, 2009), 169–192. <https://doi.org/10.1146/annurev.marine.010908.163834>

Dong, L., & Fan, R. (2023). Dynamic analysis of the optimal guiding mechanism for second emission trading market in China. *Journal of Cleaner Production*, 418, 138145. <https://doi.org/10.1016/j.jclepro.2023.138145>

Drake, H. F., Rivest, R. L., Edelman, A., & Deutch, J. (2021). A simple model for assessing climate control trade-offs and responding to unanticipated climate outcomes. *Environmental Research Letters*, 16(10), 104012.

<https://doi.org/10.1088/1748-9326/ac243e>

Easterling, D. R., Meehl, G. A., Parmesan, C., Changnon, S. A., Karl, T. R., & Mearns, L. O. (2000). Climate Extremes: Observations, Modeling, and Impacts. *Science*, 289(5487), 2068–2074. <https://doi.org/10.1126/science.289.5487.2068>

Ebi, K. L., Vanos, J., Baldwin, J. W., Bell, J. E., Hondula, D. M., Errett, N. A., Hayes, K., Reid, C. E., Saha, S., Spector, J., & Berry, P. (2021). Extreme Weather and Climate Change: Population Health and Health System Implications. *Annual*

Review of Public Health, 42(Volume 42, 2021), 293–315.

<https://doi.org/10.1146/annurev-publhealth-012420-105026>

Eekhout, J. P. C., Hunink, J. E., Terink, W., & de Vente, J. (2018). Why increased extreme precipitation under climate change negatively affects water security.

Hydrology and Earth System Sciences, 22(11), 5935–5946.

<https://doi.org/10.5194/hess-22-5935-2018>

Engler, N., & Krarti, M. (2021). Review of energy efficiency in controlled environment agriculture. *Renewable and Sustainable Energy Reviews*, 141, 110786.

<https://doi.org/10.1016/j.rser.2021.110786>

Etminan, M., Myhre, G., Highwood, E. J., & Shine, K. P. (2016). Radiative forcing of carbon dioxide, methane, and nitrous oxide: A significant revision of the methane radiative forcing. *Geophysical Research Letters*, 43(24), 12,614–12,623.

<https://doi.org/10.1002/2016GL071930>

Fawzy, S., Osman, A. I., Doran, J., & Rooney, D. W. (2020). Strategies for mitigation of climate change: A review. *Environmental Chemistry Letters*, 18(6), 2069–2094.

<https://doi.org/10.1007/s10311-020-01059-w>

Foote, E. (1856). Circumstances affecting the heat of the sun's rays. *Am. J. Sci. Arts*, 22(66), 383–384.

Forster, J., Vaughan, N. E., Gough, C., Lorenzoni, I., & Chilvers, J. (2020). Mapping feasibilities of greenhouse gas removal: Key issues, gaps and opening up assessments. *Global Environmental Change*, 63, 102073.

<https://doi.org/10.1016/j.gloenvcha.2020.102073>

- Forster, P. M., Maycock, A. C., McKenna, C. M., & Smith, C. J. (2020). Latest climate models confirm need for urgent mitigation. *Nature Climate Change*, *10*(1), 7–10. <https://doi.org/10.1038/s41558-019-0660-0>
- Forzieri, G., Bianchi, A., Silva, F. B. E., Marin Herrera, M. A., Leblois, A., Lavallo, C., Aerts, J. C. J. H., & Feyen, L. (2018). Escalating impacts of climate extremes on critical infrastructures in Europe. *Global Environmental Change*, *48*, 97–107. <https://doi.org/10.1016/j.gloenvcha.2017.11.007>
- Fyfe, J., Fox-Kemper, B., Kopp, R., & Garner, G. (2021). *Summary for Policymakers of the Working Group I Contribution to the IPCC Sixth Assessment Report—Data for Figure SPM.8 (v20210809)* [Application/xml]. NERC EDS Centre for Environmental Data Analysis. <https://doi.org/10.5285/98AF2184E13E4B91893AB72F301790DB>
- Gallagher, K. S., Grübler, A., Kuhl, L., Nemet, G., & Wilson, C. (2012). The Energy Technology Innovation System. *Annual Review of Environment and Resources*, *37*(1), 137–162. <https://doi.org/10.1146/annurev-environ-060311-133915>
- Geoffroy, O., Saint-martin, D., Olivié, D. J. L., Voldoire, A., Bellon, G., & Tytéca, S. (2013). Transient climate response in a two-layer energy-balance model. Part I: Analytical solution and parameter calibration using CMIP5 AOGCM experiments. *Journal of Climate*, *26*(6), 1841–1857. <https://doi.org/10.1175/JCLI-D-12-00195.1>
- Gingerich, D., Bielicki, J., Gardner, J., Masciola, M., & Chien, C. (2023). *2022 Ohio Sewer and Water Rate Survey*.

https://dam.assets.ohio.gov/image/upload/epa.ohio.gov/Portals/43/Rate%20Reports/Ohio_EPA_2022_Sewer_and_Water_Rate_Survey.pdf

- Golabi, K., & Scherer, C. R. (1981). Extraction timing and economic incentives for geothermal reservoir management. *Journal of Environmental Economics and Management*, 8(2), 156–174. [https://doi.org/10.1016/0095-0696\(81\)90005-X](https://doi.org/10.1016/0095-0696(81)90005-X)
- Golabi, K., Scherer, C. R., Tsang, C. F., & Mozumder, S. (1981). Optimal energy extraction from a hot water geothermal reservoir. *Water Resources Research*, 17(1), 1–10. <https://doi.org/10.1029/WR017i001p00001>
- Harmsen, J. H. M., van Vuuren, D. P., Nayak, D. R., Hof, A. F., Höglund-Isaksson, L., Lucas, P. L., Nielsen, J. B., Smith, P., & Stehfest, E. (2019). Long-term marginal abatement cost curves of non-CO2 greenhouse gases. *Environmental Science & Policy*, 99, 136–149. <https://doi.org/10.1016/j.envsci.2019.05.013>
- Held, I. M., Winton, M., Takahashi, K., Delworth, T., Zeng, F., & Vallis, G. K. (2010). Probing the fast and slow components of global warming by returning abruptly to preindustrial forcing. *Journal of Climate*, 23(9), 2418–2427. <https://doi.org/10.1175/2009JCLI3466.1>
- Höglund-Isaksson, L., Gómez-Sanabria, A., Klimont, Z., Rafaj, P., & Schöpp, W. (2020). Technical potentials and costs for reducing global anthropogenic methane emissions in the 2050 timeframe –results from the GAINS model. *Environmental Research Communications*, 2(2), 025004. <https://doi.org/10.1088/2515-7620/ab7457>

- Hu, G., May, E. F., & Li, K. G. (2022). We commercialized a methane capture technology in ten years—Here’s how. *Nature*, *604*(7905), 242–245.
<https://doi.org/10.1038/d41586-022-00999-3>
- Hu, G., Zhao, Q., Manning, M., Chen, L., Yu, L., May, E. F., & Li, K. G. (2022). Pilot scale assessment of methane capture from low concentration sources to town gas specification by pressure vacuum swing adsorption (PVSA). *Chemical Engineering Journal*, *427*(June 2021), 130810.
<https://doi.org/10.1016/j.cej.2021.130810>
- IEA. (2020). *Energy Technology Perspectives 2020—Special Report on Carbon Capture Utilisation and Storage*. IEA. <https://doi.org/10.1787/208b66f4-en>
- IEA. (2023). *Heating*. <https://www.iea.org/energy-system/buildings/heating>
- IEMA. (2020). *Pathways to Net Zero: Using the IEMA GHG Management Hierarchy*.
<https://www.iema.net/resources/reading-room/2020/11/26/pathways-to-net-zero-using-the-iema-ghg-management-hierarchy-november-2020>
- IPCC. (2022). *Global Warming of 1.5°C: IPCC Special Report on Impacts of Global Warming of 1.5°C above Pre-industrial Levels in Context of Strengthening Response to Climate Change, Sustainable Development, and Efforts to Eradicate Poverty* (1st ed.). Cambridge University Press.
<https://doi.org/10.1017/9781009157940>
- IPCC. (2023a). Annex III: Tables of Historical and Projected Well-mixed Greenhouse Gas Mixing Ratios and Effective Radiative Forcing of All Climate Forcers. In *Climate Change 2021 – The Physical Science Basis: Working Group I*

Contribution to the Sixth Assessment Report of the Intergovernmental Panel on Climate Change (pp. 2139–2152). Cambridge University Press.

<https://doi.org/10.1017/9781009157896.017>

IPCC. (2023b). *Climate Change 2023: Synthesis Report. Contribution of Working Groups I, II and III to the Sixth Assessment Report of the Intergovernmental Panel on Climate Change [Core Writing Team, H. Lee and J. Romero (eds.)]. IPCC, Geneva, Switzerland.* (pp. 1–34). <https://doi.org/10.59327/IPCC/AR6-9789291691647>

IRENA. (2018). *Renewable capacity statistics 2018.*

<https://www.irena.org/Publications/2018/Mar/Renewable-Capacity-Statistics-2018>

IRENA. (2023a). *Global geothermal: Market and technology assessment.* International Renewable Energy Agency ; International Geothermal Association.

<https://www.irena.org/Publications/2023/Feb/Global-geothermal-market-and-technology-assessment>

IRENA. (2023b). *Renewable power generation costs in 2022.* International Renewable Energy Agency. <https://www.irena.org/Publications/2023/Aug/Renewable-Power-Generation-Costs-in-2022>

IRENA. (2024). *Renewable capacity statistics 2024.*

<https://www.irena.org/Publications/2024/Mar/Renewable-capacity-statistics-2024>

Jackson, R. B., Abernethy, S., Canadell, J. G., Cargnello, M., Davis, S. J., Féron, S.,

Fuss, S., Heyer, A. J., Hong, C., Jones, C. D., Damon Matthews, H., O'Connor, F.

M., Pisciotta, M., Rhoda, H. M., de Richter, R., Solomon, E. I., Wilcox, J. L., & Zickfeld, K. (2021). Atmospheric methane removal: A research agenda.

Philosophical Transactions of the Royal Society A: Mathematical, Physical and Engineering Sciences, 379(2210), 20200454.

<https://doi.org/10.1098/rsta.2020.0454>

Jackson, R. B., Solomon, E. I., Canadell, J. G., Cargnello, M., & Field, C. B. (2019).

Methane removal and atmospheric restoration. *Nature Sustainability*, 2(6), 436–438. <https://doi.org/10.1038/s41893-019-0299-x>

Jackson, R. B., Solomon, E. I., Canadell, J. G., Cargnello, M., Field, C. B., & Abernethy,

S. (2020). Reply to: Practical constraints on atmospheric methane removal.

Nature Sustainability, 3(5), 358–359. <https://doi.org/10.1038/s41893-020-0498-5>

Joos, F., Roth, R., Fuglestedt, J. S., Peters, G. P., Enting, I. G., Von Bloh, W., Brovkin, V., Burke, E. J., Eby, M., Edwards, N. R., Friedrich, T., Frölicher, T. L., Halloran, P. R., Holden, P. B., Jones, C., Kleinen, T., Mackenzie, F. T., Matsumoto, K.,

Meinshausen, M., ... Weaver, A. J. (2013). Carbon dioxide and climate impulse response functions for the computation of greenhouse gas metrics: A multi-model analysis. *Atmospheric Chemistry and Physics*, 13(5), 2793–2825.

<https://doi.org/10.5194/acp-13-2793-2013>

Júlíusson, E., & Axelsson, G. (2018). Stock models for geothermal resources.

Geothermics, 72(April 2017), 249–257.

<https://doi.org/10.1016/j.geothermics.2017.11.006>

- Juliusson, E., & Bjornsson, S. (2021). Optimizing production strategies for geothermal resources. *Geothermics*, *94*(January), 102091.
<https://doi.org/10.1016/j.geothermics.2021.102091>
- Kangur, A., Jager, W., Verbrugge, R., & Bockarjova, M. (2017). An agent-based model for diffusion of electric vehicles. *Journal of Environmental Psychology*, *52*, 166–182. <https://doi.org/10.1016/j.jenvp.2017.01.002>
- Keith, D. W., Ha-Duong, M., & Stolaroff, J. K. (2006). Climate Strategy with Co2 Capture from the Air. *Climatic Change*, *74*(1), 17–45.
<https://doi.org/10.1007/s10584-005-9026-x>
- Kriegler, E., Bauer, N., Popp, A., Humpenöder, F., Leimbach, M., Strefler, J., Baumstark, L., Bodirsky, B. L., Hilaire, J., Klein, D., Mouratiadou, I., Weindl, I., Bertram, C., Dietrich, J.-P., Luderer, G., Pehl, M., Pietzcker, R., Piontek, F., Lotze-Campen, H., ... Edenhofer, O. (2017). Fossil-fueled development (SSP5): An energy and resource intensive scenario for the 21st century. *Global Environmental Change*, *42*, 297–315. <https://doi.org/10.1016/j.gloenvcha.2016.05.015>
- Lackner, K. S. (2020). Practical constraints on atmospheric methane removal. *Nature Sustainability*, *3*(5), 357–357. <https://doi.org/10.1038/s41893-020-0496-7>
- Lackner, K. S., & Azarabadi, H. (2021). Buying down the Cost of Direct Air Capture. *Industrial & Engineering Chemistry Research*, *60*(22), 8196–8208.
<https://doi.org/10.1021/acs.iecr.0c04839>

- Lackner, K. S., Ziock, H.-J., & Grimes, P. (1999). *Carbon Dioxide Extraction from Air: Is It An Option?* (LA-UR-99-583). Los Alamos National Lab. (LANL), Los Alamos, NM (United States). <https://www.osti.gov/biblio/770509>
- Lan, X., Tans, P., Thoning, K., & NOAA Global Monitoring Laboratory. (2024). *Trends in globally-averaged CO2 determined from NOAA Global Monitoring Laboratory measurements*. [dataset]. NOAA GML. <https://doi.org/10.15138/9N0H-ZH07>
- Liang, X., Xu, T., Feng, B., & Jiang, Z. (2018). Optimization of heat extraction strategies in fault-controlled hydro-geothermal reservoirs. *Energy*, *164*, 853–870. <https://doi.org/10.1016/j.energy.2018.09.043>
- Lofberg, J. (2004). YALMIP : a toolbox for modeling and optimization in MATLAB. *2004 IEEE International Conference on Robotics and Automation (IEEE Cat. No.04CH37508)*, 284–289. <https://doi.org/10.1109/CACSD.2004.1393890>
- Lucas, P. L., van Vuuren, D. P., Olivier, J. G. J., & den Elzen, M. G. J. (2007). Long-term reduction potential of non-CO2 greenhouse gases. *Environmental Science & Policy*, *10*(2), 85–103. <https://doi.org/10.1016/j.envsci.2006.10.007>
- MacDonald, S., & Eyre, N. (2018). An international review of markets for voluntary green electricity tariffs. *Renewable and Sustainable Energy Reviews*, *91*, 180–192. <https://doi.org/10.1016/j.rser.2018.03.028>
- Majdinasab, A., & Yuan, Q. (2017). Performance of the biotic systems for reducing methane emissions from landfill sites: A review. *Ecological Engineering*, *104*, 116–130. <https://doi.org/10.1016/j.ecoleng.2017.04.015>

- Malafeh, S., & Sharp, B. (2015). Role of royalties in sustainable geothermal energy development. *Energy Policy*, *85*, 235–242.
<https://doi.org/10.1016/j.enpol.2015.06.023>
- Malinauskaite, J., Jouhara, H., Egilegor, B., Al-Mansour, F., Ahmad, L., & Pusnik, M. (2020). Energy efficiency in the industrial sector in the EU, Slovenia, and Spain. *Energy*, *208*, 118398. <https://doi.org/10.1016/j.energy.2020.118398>
- Marcott, S. A., Shakun, J. D., Clark, P. U., & Mix, A. C. (2013). A Reconstruction of Regional and Global Temperature for the Past 11,300 Years. *Science*, *339*(6124), 1198–1201. <https://doi.org/10.1126/science.1228026>
- Matthews, E., & Fung, I. (1987). Methane emission from natural wetlands: Global distribution, area, and environmental characteristics of sources. *Global Biogeochemical Cycles*, *1*(1), 61–86. <https://doi.org/10.1029/GB001i001p00061>
- Minx, J. C., Lamb, W. F., Callaghan, M. W., Fuss, S., Hilaire, J., Creutzig, F., Amann, T., Beringer, T., Garcia, W. de O., Hartmann, J., Khanna, T., Lenzi, D., Luderer, G., Nemet, G. F., Rogelj, J., Smith, P., Vicente, J. L. V., Wilcox, J., & Dominguez, M. del M. Z. (2018). Negative emissions—Part 1: Research landscape and synthesis. *Environmental Research Letters*, *13*(6), 063001.
<https://doi.org/10.1088/1748-9326/aabf9b>
- Moglia, M., Podkalicka, A., & McGregor, J. (2018). An agent-based model of residential energy efficiency adoption. *JASSS*, *21*(3). <https://doi.org/10.18564/jasss.3729>
- Mousavi, M. E., Irish, J. L., Frey, A. E., Olivera, F., & Edge, B. L. (2011). Global warming and hurricanes: The potential impact of hurricane intensification and sea

level rise on coastal flooding. *Climatic Change*, 104(3), 575–597.

<https://doi.org/10.1007/s10584-009-9790-0>

Mundim, K. C., Baraldi, S., Machado, H. G., & Vieira, F. M. C. (2020). Temperature coefficient (Q10) and its applications in biological systems: Beyond the Arrhenius theory. *Ecological Modelling*, 431, 109127.

<https://doi.org/10.1016/j.ecolmodel.2020.109127>

Myers, S. S., Smith, M. R., Guth, S., Golden, C. D., Vaitla, B., Mueller, N. D., Dangour, A. D., & Huybers, P. (2017). Climate Change and Global Food Systems: Potential Impacts on Food Security and Undernutrition. *Annual Review of Public Health*, 38(Volume 38, 2017), 259–277. <https://doi.org/10.1146/annurev-publhealth-031816-044356>

Myhre, G., Shindell, D., Bréon, F.-M., Collins, W., Fuglestvedt, J., Huang, J., Koch, D., Lamarque, J.-F., Lee, D., Mendoza, B., Nakajima, T., Robock, A., Stephens, G., Tak, T., & Zhang, H. (2013). Anthropogenic and Natural Radiative Forcing. In Intergovernmental Panel on Climate Change (Ed.), *Climate Change 2013—The Physical Science Basis* (pp. 659–740). Cambridge University Press.

<https://doi.org/10.1017/CBO9781107415324.018>

Niamir, L., Filatova, T., Voinov, A., & Bressers, H. (2018). Transition to low-carbon economy: Assessing cumulative impacts of individual behavioral changes. *Energy Policy*, 118(April), 325–345. <https://doi.org/10.1016/j.enpol.2018.03.045>

Nisbet-Jones, P. B. R., Fernandez, J. M., Fisher, R. E., France, J. L., Lowry, D., Waltham, D. A., Woolley Maisch, C. A., & Nisbet, E. G. (2022). Is the

destruction or removal of atmospheric methane a worthwhile option?

Philosophical Transactions of the Royal Society A: Mathematical, Physical and

Engineering Sciences, 380(2215). <https://doi.org/10.1098/rsta.2021.0108>

NOAA. (2016, January). *Monthly Global Climate Report for Annual 2015*.

<https://www.ncei.noaa.gov/access/monitoring/monthly-report/global/201513>

NOAA. (2023). *The NOAA Annual Greenhouse Gas Index (AGGI)*.

<https://gml.noaa.gov/aggi/aggi.html>

NREL. (2024). *Best Research-Cell Efficiency Chart*. [https://www.nrel.gov/pv/cell-](https://www.nrel.gov/pv/cell-efficiency.html)

[efficiency.html](https://www.nrel.gov/pv/cell-efficiency.html)

O'Neill, B. C., Carter, T. R., Ebi, K., Harrison, P. A., Kemp-Benedict, E., Kok, K.,

Kriegler, E., Preston, B. L., Riahi, K., Sillmann, J., van Ruijven, B. J., van

Vuuren, D., Carlisle, D., Conde, C., Fuglestvedt, J., Green, C., Hasegawa, T.,

Leininger, J., Monteith, S., & Pichs-Madruga, R. (2020). Achievements and

Needs for the Climate Change Scenario Framework. *Nature Climate Change*,

10(12), 1074–1084. <https://doi.org/10.1038/s41558-020-00952-0>

O'Neill, B. C., Kriegler, E., Ebi, K. L., Kemp-Benedict, E., Riahi, K., Rothman, D. S.,

van Ruijven, B. J., van Vuuren, D. P., Birkmann, J., Kok, K., Levy, M., &

Solecki, W. (2017). The roads ahead: Narratives for shared socioeconomic

pathways describing world futures in the 21st century. *Global Environmental*

Change, 42, 169–180. <https://doi.org/10.1016/j.gloenvcha.2015.01.004>

- Osička, J., & Černoč, F. (2022). European energy politics after Ukraine: The road ahead. *Energy Research & Social Science*, *91*, 102757.
<https://doi.org/10.1016/j.erss.2022.102757>
- Preston, C. J. (2017). Ethics and geoen지니어ing: Reviewing the moral issues raised by solar radiation management and carbon dioxide removal. In *The Ethics of Nanotechnology, Geoengineering, and Clean Energy*. Routledge.
- Pruess, K. (2006). Enhanced geothermal systems (EGS) using CO₂ as working fluid-A novel approach for generating renewable energy with simultaneous sequestration of carbon. *Geothermics*, *35*(4), 351–367.
<https://doi.org/10.1016/j.geothermics.2006.08.002>
- Ramos, A., Gago, A., Labandeira, X., & Linares, P. (2015). The role of information for energy efficiency in the residential sector. *Energy Economics*, *52*, S17–S29.
<https://doi.org/10.1016/j.eneco.2015.08.022>
- Randolph, J. B., & Saar, M. O. (2011). Combining geothermal energy capture with geologic carbon dioxide sequestration. *Geophysical Research Letters*, *38*(10).
<https://doi.org/10.1029/2011GL047265>
- Riahi, K., van Vuuren, D. P., Kriegler, E., Edmonds, J., O'Neill, B. C., Fujimori, S., Bauer, N., Calvin, K., Dellink, R., Fricko, O., Lutz, W., Popp, A., Cuaresma, J. C., KC, S., Leimbach, M., Jiang, L., Kram, T., Rao, S., Emmerling, J., ... Tavoni, M. (2017). The Shared Socioeconomic Pathways and their energy, land use, and greenhouse gas emissions implications: An overview. *Global Environmental Change*, *42*, 153–168. <https://doi.org/10.1016/j.gloenvcha.2016.05.009>

- Richstein, J. C., Chappin, E. J. L., & de Vries, L. J. (2014). Cross-border electricity market effects due to price caps in an emission trading system: An agent-based approach. *Energy Policy*, *71*, 139–158.
<https://doi.org/10.1016/j.enpol.2014.03.037>
- Ritchie, H., Rosado, P., & Roser, M. (2023a). Electricity Mix. *Our World in Data*.
<https://ourworldindata.org/electricity-mix>
- Ritchie, H., Rosado, P., & Roser, M. (2023b). Energy Mix. *Our World in Data*.
<https://ourworldindata.org/energy-mix>
- Ritchie, H., Rosado, P., & Roser, M. (2023c). Meat and Dairy Production. *Our World in Data*. <https://ourworldindata.org/meat-production>
- Rogers, E. M. (2003). *Diffusion of innovations* (Fifth edition, Free Press trade paperback edition). Free Press.
- Sanz-Pérez, E. S., Murdock, C. R., Didas, S. A., & Jones, C. W. (2016). Direct Capture of CO₂ from Ambient Air. *Chemical Reviews*, *116*(19), 11840–11876.
<https://doi.org/10.1021/acs.chemrev.6b00173>
- Saunio, M., Stavert, A. R., Poulter, B., Bousquet, P., Canadell, J. G., Jackson, R. B., Raymond, P. A., Dlugokencky, E. J., Houweling, S., Patra, P. K., Ciais, P., Arora, V. K., Bastviken, D., Bergamaschi, P., Blake, D. R., Brailsford, G., Bruhwiler, L., Carlson, K. M., Carrol, M., ... Zhuang, Q. (2020). The Global Methane Budget 2000–2017. *Earth System Science Data*, *12*(3), 1561–1623.
<https://doi.org/10.5194/essd-12-1561-2020>

- Sigurdardottir, S. R., Valfells, A., Palsson, H., & Stefansson, H. (2015). Mixed integer optimization model for utilizing a geothermal reservoir. *Geothermics*, 55, 171–181. <https://doi.org/10.1016/j.geothermics.2015.01.006>
- Smith, L. G., Williams, A. G., & Pearce, B. D. (2015). The energy efficiency of organic agriculture: A review. *Renewable Agriculture and Food Systems*, 30(3), 280–301. <https://doi.org/10.1017/S1742170513000471>
- Spittler, N., Shafiei, E., Davidsdottir, B., & Juliusson, E. (2020). Modelling geothermal resource utilization by incorporating resource dynamics, capacity expansion, and development costs. *Energy*, 190. <https://doi.org/10.1016/j.energy.2019.116407>
- Staniaszek, Z., Griffiths, P. T., Folberth, G. A., O'Connor, F. M., Abraham, N. L., & Archibald, A. T. (2022). The role of future anthropogenic methane emissions in air quality and climate. *Npj Climate and Atmospheric Science*, 5(1), 1–8. <https://doi.org/10.1038/s41612-022-00247-5>
- Svoboda, T., & Irvine, P. (2014). Ethical and Technical Challenges in Compensating for Harm Due to Solar Radiation Management Geoengineering. *Ethics, Policy & Environment*, 17(2), 157–174. <https://doi.org/10.1080/21550085.2014.927962>
- SWACO. (2024). *Franklin County Sanitary Landfill*. <https://www.swaco.org/286/Franklin-County-Sanitary-Landfill>
- Szabo, J. (2022). Energy transition or transformation? Power and politics in the European natural gas industry's trasformismo. *Energy Research & Social Science*, 84, 102391. <https://doi.org/10.1016/j.erss.2021.102391>

- Tang, L., Wu, J., Yu, L., & Bao, Q. (2015). Carbon emissions trading scheme exploration in China: A multi-agent-based model. *Energy Policy*, *81*(2015), 152–169.
<https://doi.org/10.1016/j.enpol.2015.02.032>
- Tang, L., Wu, J., Yu, L., & Bao, Q. (2017). Carbon allowance auction design of China's emissions trading scheme: A multi-agent-based approach. *Energy Policy*, *102*, 30–40. <https://doi.org/10.1016/j.enpol.2016.11.041>
- The White House. (2021). *U.S. Methane Emissions Reduction Action Plan* (Issue November).
- Thoning, K., Dlugokencky, E., Lan, X., & NOAA Global Monitoring Laboratory. (2024). *Trends in globally-averaged CH₄, N₂O, and SF₆* [dataset]. NOAA GML.
<https://doi.org/10.15138/P8XG-AA10>
- UNEP & CCAC. (2021). *Global Methane Assessment: Benefits and Costs of Mitigating Methane Emissions*. <https://www.unep.org/resources/report/global-methane-assessment-benefits-and-costs-mitigating-methane-emissions>
- UNFCCC. (1992). *United Nations Framework Convention on Climate Change*.
<https://unfccc.int/resource/docs/convkp/conveng.pdf>
- UNFCCC. (1998). *Kyoto Protocol to the United Nations Framework Convention on Climate Change*. <https://unfccc.int/resource/docs/convkp/kpeng.pdf>
- UNFCCC. (2015). *Paris Agreement*.
https://unfccc.int/sites/default/files/english_paris_agreement.pdf
- USEPA. (2019). Global Non-CO₂ Greenhouse Gas Emission Projections & Mitigation Potential: 2015-2050. In *U.S. Environmental Protection Agency (EPA)*.

<https://www.epa.gov/global-mitigation-non-co2-greenhouse-gases/global-non-co2-greenhouse-gas-emission-projections>

USEPA. (2021). *Climate Change Indicators: Atmospheric Concentrations of Greenhouse Gases*. <https://www.epa.gov/climate-indicators/climate-change-indicators-atmospheric-concentrations-greenhouse-gases>

USEPA. (2022a). *Methane Emissions*. <https://www.epa.gov/ghgemissions/overview-greenhouse-gases#methane>

USEPA. (2022b). *U.S. State-level Non-CO₂ Greenhouse Gas Mitigation Potential: 2025-2050*. <https://cfpub.epa.gov/ghgdata/nonco2/usreports/#page1>

USEPA. (2023, December 15). *Biden-Harris Administration Announces \$350 Million to 14 States to Reduce Methane Emissions from Oil and Gas Sector as Part of Investing in America Agenda* (United States) [News Release]. <https://www.epa.gov/newsreleases/biden-harris-administration-announces-350-million-14-states-reduce-methane-emissions>

USEPA. (2024, January 12). *Biden-Harris Administration Announces Proposed Rule to Reduce Wasteful Methane Emissions from the Oil and Gas Sector to Drive Innovation and Protect Communities* [News Release]. <https://www.epa.gov/newsreleases/biden-harris-administration-announces-proposed-rule-reduce-wasteful-methane-emissions>

van der Kam, M. J., Meelen, A. A. H., van Sark, W. G. J. H. M., & Alkemade, F. (2018). Diffusion of solar photovoltaic systems and electric vehicles among Dutch

- consumers: Implications for the energy transition. *Energy Research & Social Science*, 46, 68–85. <https://doi.org/10.1016/j.erss.2018.06.003>
- van der Zwaan, B., & Rabl, A. (2003). Prospects for PV: A learning curve analysis. *Solar Energy*, 74(1), 19–31. [https://doi.org/10.1016/S0038-092X\(03\)00112-9](https://doi.org/10.1016/S0038-092X(03)00112-9)
- Van Dyk, S., Su, J., Ebadian, M., & Saddler, J. (2022). Production of lower carbon-intensity fuels by co-processing biogenic feedstocks: Potential and challenges for refineries. *Fuel*, 324, 124636. <https://doi.org/10.1016/j.fuel.2022.124636>
- Van Dyke Parunak, H., Savit, R., & Riolo, R. L. (1998). Agent-Based Modeling vs. Equation-Based Modeling: A Case Study and Users' Guide. In J. S. Sichman, R. Conte, & N. Gilbert (Eds.), *Multi-Agent Systems and Agent-Based Simulation* (pp. 10–25). Springer. https://doi.org/10.1007/10692956_2
- Velenturf, A. P. M., & Purnell, P. (2021). Principles for a sustainable circular economy. *Sustainable Production and Consumption*, 27, 1437–1457. <https://doi.org/10.1016/j.spc.2021.02.018>
- Wächter, A., & Biegler, L. T. (2006). On the implementation of an interior-point filter line-search algorithm for large-scale nonlinear programming. *Mathematical Programming*, 106(1), 25–57. <https://doi.org/10.1007/s10107-004-0559-y>
- Waller, L., Rayner, T., Chilvers, J., Gough, C. A., Lorenzoni, I., Jordan, A., & Vaughan, N. (2020). Contested framings of greenhouse gas removal and its feasibility: Social and political dimensions. *WIREs Climate Change*, 11(4), e649. <https://doi.org/10.1002/wcc.649>

- Wei, Y., Liang, X., Xu, L., Kou, G., & Chevallier, J. (2023). Trading, storage, or penalty? Uncovering firms' decision-making behavior in the Shanghai emissions trading scheme: Insights from agent-based modeling. *Energy Economics*, *117*(December 2022), 106463. <https://doi.org/10.1016/j.eneco.2022.106463>
- Weitzman, M. L. (2003). *Income, wealth, and the maximum principle*. Harvard University Press.
- Weller, Z. D., Hamburg, S. P., & von Fischer, J. C. (2020). A National Estimate of Methane Leakage from Pipeline Mains in Natural Gas Local Distribution Systems. *Environmental Science & Technology*, *54*(14), 8958–8967. <https://doi.org/10.1021/acs.est.0c00437>
- Wilson, T. J. B., Cooley, S. R., Tai, T. C., Cheung, W. W. L., & Tyedmers, P. H. (2020). Potential socioeconomic impacts from ocean acidification and climate change effects on Atlantic Canadian fisheries. *PLOS ONE*, *15*(1), e0226544. <https://doi.org/10.1371/journal.pone.0226544>
- Zhang, H., Cao, L., & Zhang, B. (2017). Emissions trading and technology adoption: An adaptive agent-based analysis of thermal power plants in China. *Resources, Conservation and Recycling*, *121*, 23–32. <https://doi.org/10.1016/j.resconrec.2016.05.001>
- Zhang, K., Douglas, B. C., & Leatherman, S. P. (2004). Global Warming and Coastal Erosion. *Climatic Change*, *64*(1), 41–58. <https://doi.org/10.1023/B:CLIM.0000024690.32682.48>

- Zhu, L., Chen, L., Yu, X., & Fan, Y. (2018). Buying green or producing green? Heterogeneous emitters' strategic choices under a phased emission-trading scheme. *Resources, Conservation and Recycling*, 136(May), 223–237.
<https://doi.org/10.1016/j.resconrec.2018.04.017>
- Zuberi, M. J. S., Santoro, M., Eberle, A., Bhadbhade, N., Sulzer, S., Wellig, B., & Patel, M. K. (2020). A detailed review on current status of energy efficiency improvement in the Swiss industry sector. *Energy Policy*, 137, 111162.
<https://doi.org/10.1016/j.enpol.2019.111162>

Appendix A

A.1. Climate Model Calibration

The calibration of the *MOMENTUM* considers historical CH₄ emissions (Crippa et al., 2023) and total historical radiative forcing (IPCC, 2023a). Historical CO₂ emissions are not considered in the calibration, since this study focuses on the change of CH₄ emissions and resulting influences on the radiative forcing and temperature. The calibration results are shown in Figure A-1.

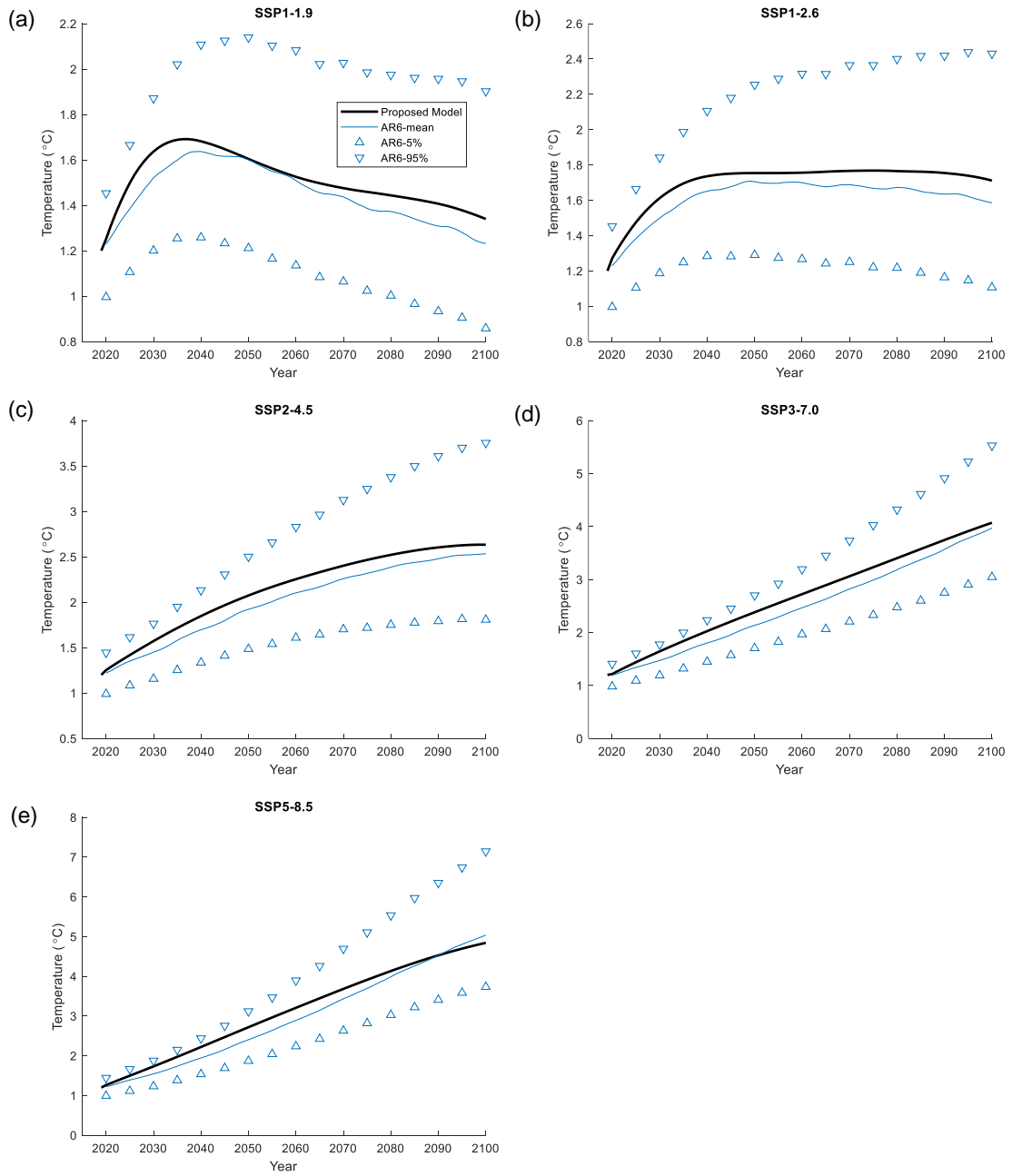


Figure A-1: Climate Model Calibration Results for Five Representative SSPs.

A.2. Methane Mitigation Technology Model

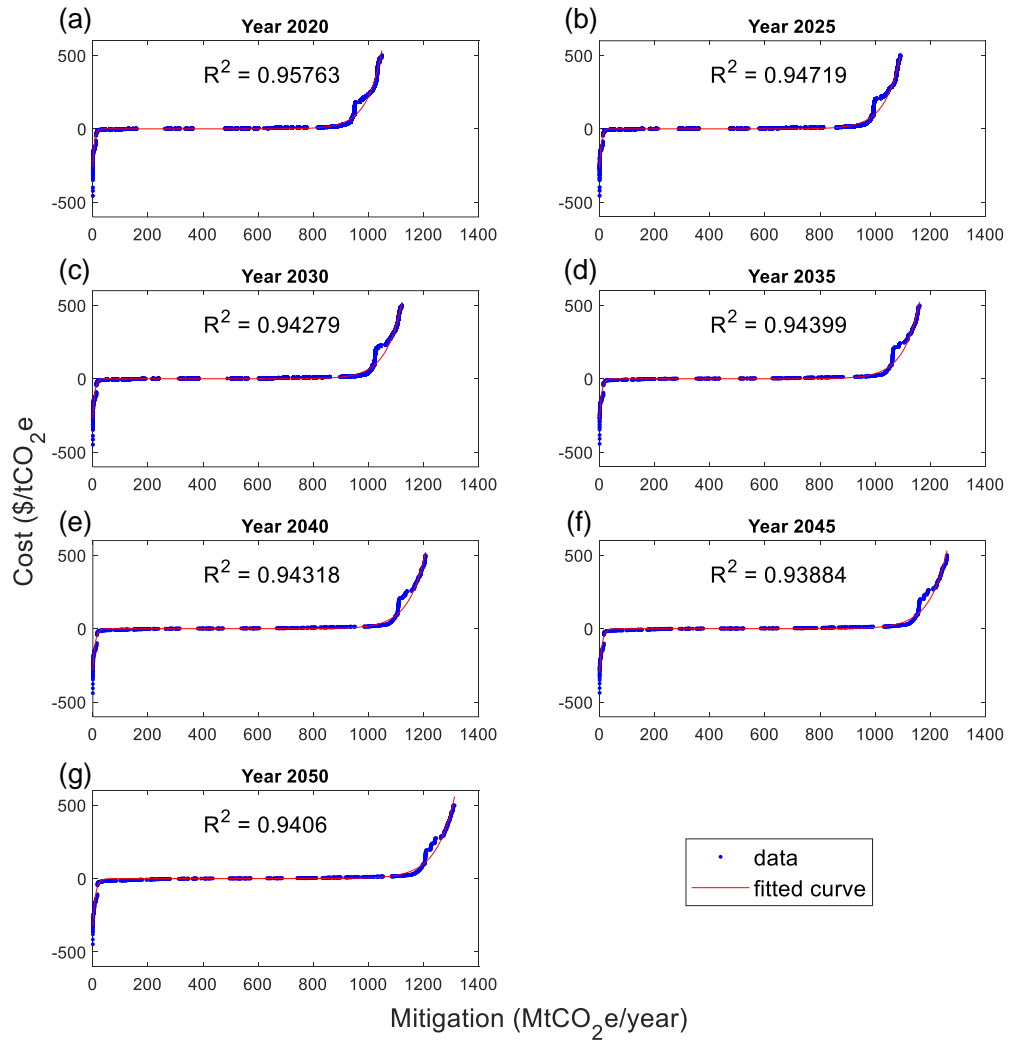


Figure A-2: Fitting Curves of USEPA Marginal Cost Data for CH₄ Mitigation Technologies in the Energy Sector

A.3. Methane Removal Technology Model

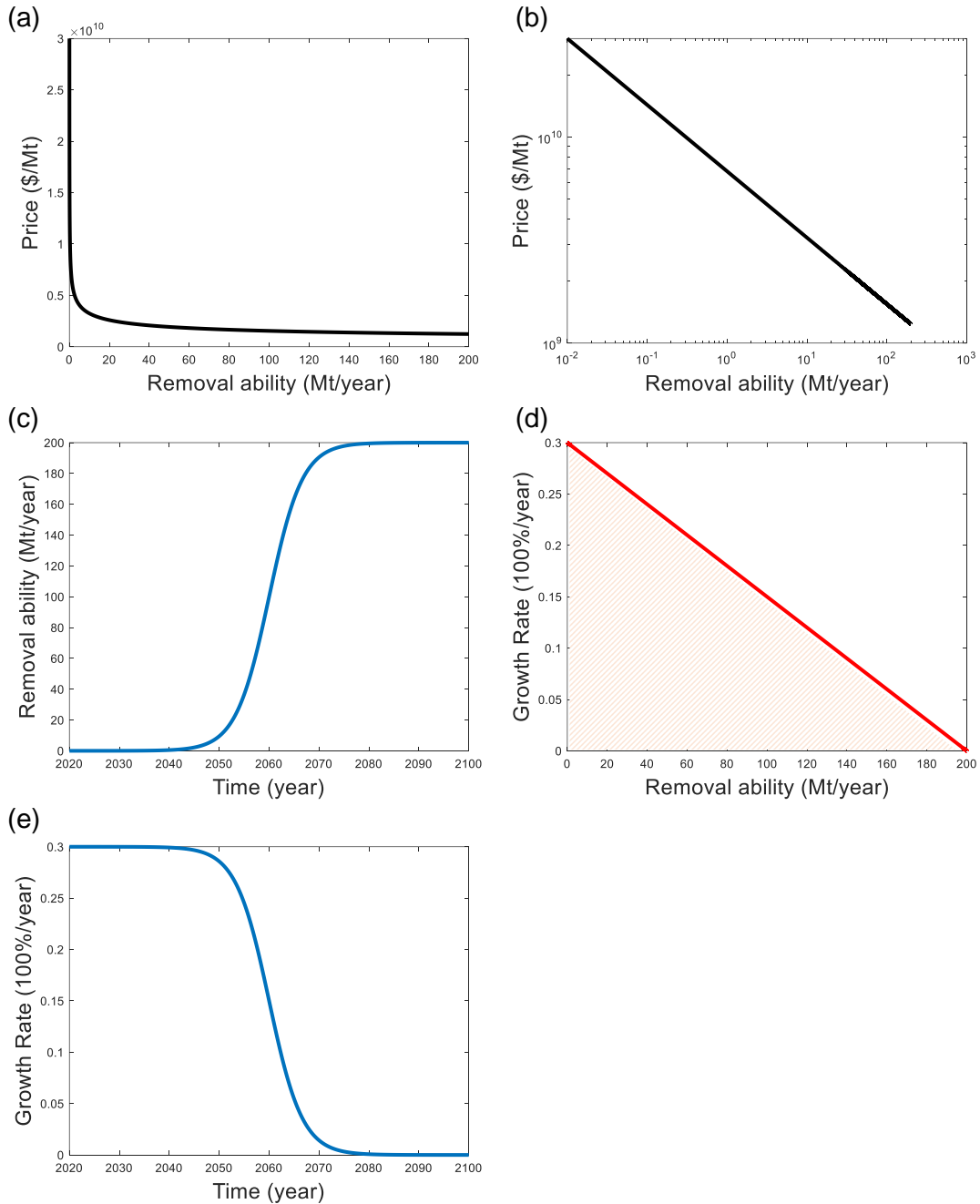


Figure A-3: Methane removal technology model. Parameters used for illustration: $R_0 = 10\text{kt}$, $P_{R_0} = \$30\text{k/t}$, $l_R = 20\%$, $R_{max} = 200\text{Mt/year}$, $g_{max} = 30\%$, $t_{mid} = 2060$. (a) learning curve (normal axes). (b) learning curve (log-log axes). (c) growth curve (removal ability vs. time). (d) growth curve (Growth rate vs. removal ability), where the shadow represents the feasible region of corresponding constraint in the optimization model. (e) growth curve (Growth rate vs. time).

A.4. Other Results

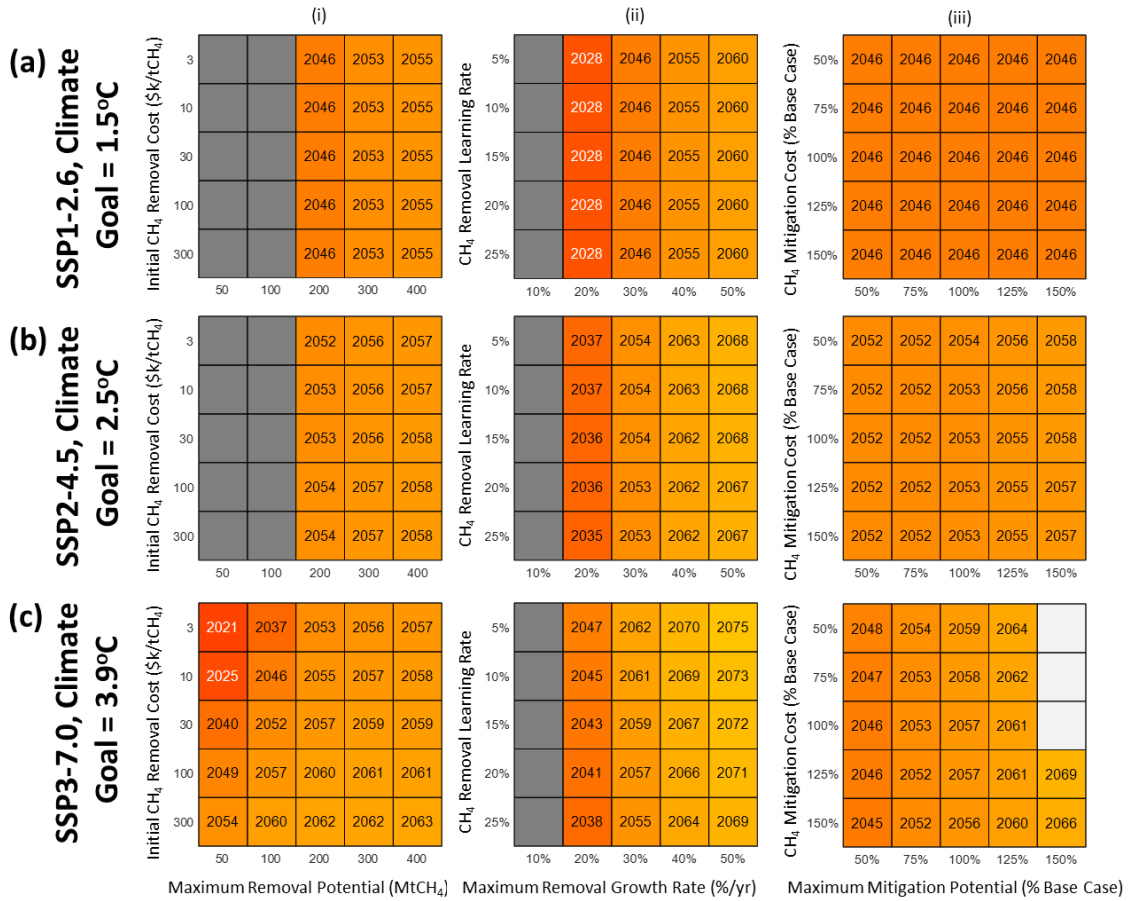


Figure A-4: Full Results of Sensitivity Analysis of the Year that CH₄ Removal Starts to Important Parameters

Dark Grey = no feasible solution; Light Grey = CH₄ removal never starts.

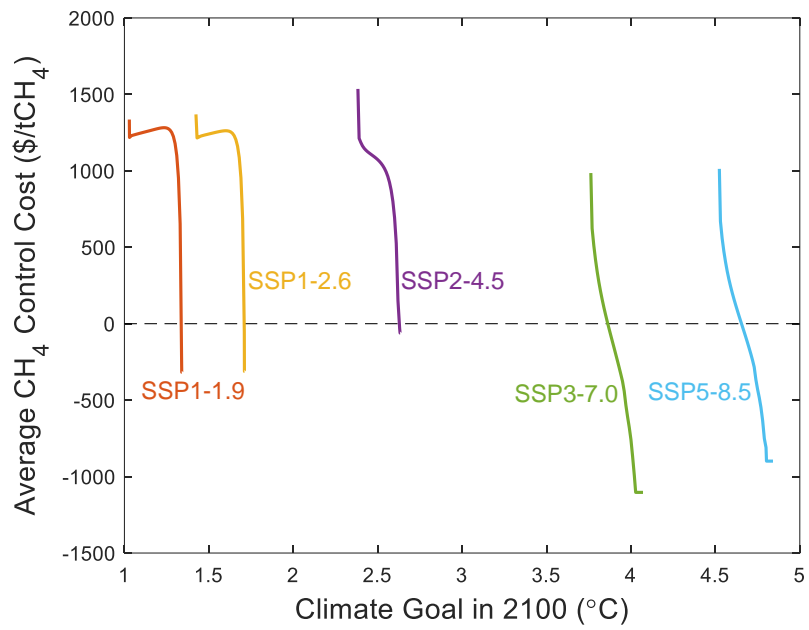


Figure A-5: Estimated Average Cost for CH₄ Control for Relevant Climate Goals in Different Scenarios

Appendix B

B.1. Stable Market Shares

The stable market shares in subzone s is solved through iterations as follows.

Based on Equation (4-13), the iteration equation is

$$\mathbf{M}_s^{(i+1)} = \sum_{i \in \mathcal{S}} \mathbb{X}_i^{stable} \mathbf{M}_s^{(i)} \quad (\text{B-1})$$

where the superscript i represents the iteration index.

Choose two initial values for the market share vector, i.e., $\mathbf{M}_s^{(0)}$, as $(1, 0, 0, \dots, 0)^T$ and $(0, 0, 0, \dots, 1)^T$. In other words, it is assumed that initially the first or the last supplier has all the market. Put the two initial market share vectors into Equation (B-1), respectively, and continue the iteration in parallel. The stopping criteria is that the maximum difference between the elements in the two market share vectors is less than a given tolerance (i.e., 10^{-8}). Take the average of the two market share vectors when the iteration stops as the stable market shares in subzone s , i.e., \mathbf{M}_s^{stable} .

B.2. Commodity/Service Prices Under the Nash Equilibrium

The commodity/service prices under the Nash equilibrium in zone z is solved through iterations as follows.

Based on Equation (4-16), the iteration equation is

$$x_j^{price(i+1)} = \operatorname{argmax}_{x_j^{price(i)}} F_j^{stable,(i)} = \operatorname{argmax}_{x_j^{price(i)}} \left[M_{zj}^{stable,(i)} (x_j^{price,(i)} - c_j) \right], \quad (\text{B-2})$$
$$\forall j \in \text{zone } z$$

Set all heterogeneous parameters (except for the price) for all suppliers in zone z , and set the initial values of prices, i.e., $x_j^{price,(0)}$ based on the costs and the average profit rate in the sector. For each supplier, put the initial price value into Equation (B-2), respectively, and continue the iteration in parallel. The stopping criteria is that the maximum difference between $x_j^{price,(i)}$ and $x_j^{price,(i+1)}$ is less than a given tolerance (i.e., 10^{-5}). The price of commodity/service j under the Nash equilibrium, i.e., $x_j^{price,nash}$, is then the value in the $(i+1)^{\text{th}}$ iteration.